X-ray Emission and Absorption in Massive Star Winds

Constraints on shock heating and wind mass-loss rates

David Cohen
Swarthmore College

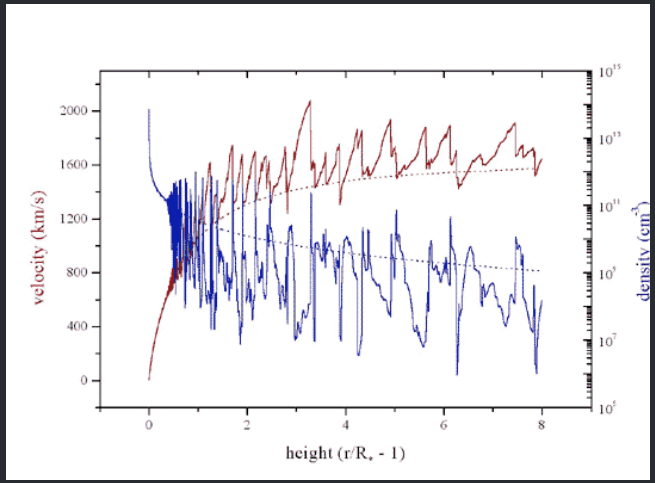

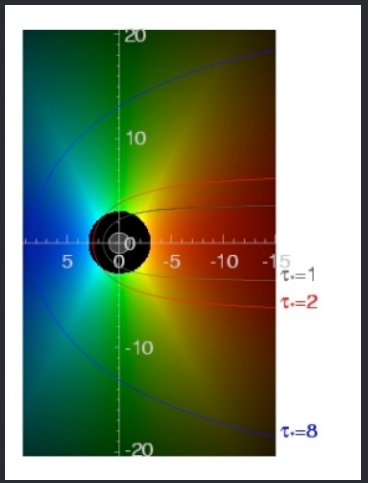

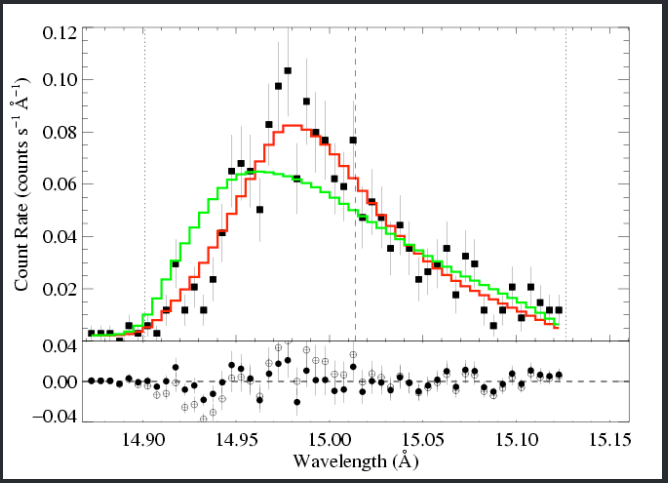

What we know about X-rays from single O stars

via high-resolution spectroscopy

David Cohen
Swarthmore College

Outline

Morphology of X-ray spectra

Embedded Wind Shocks: X-ray diagnostics of kinematics and spatial distribution

Line profiles and mass-loss rates

Broadband absorption

Morphology

ζ Pup (O4 If)

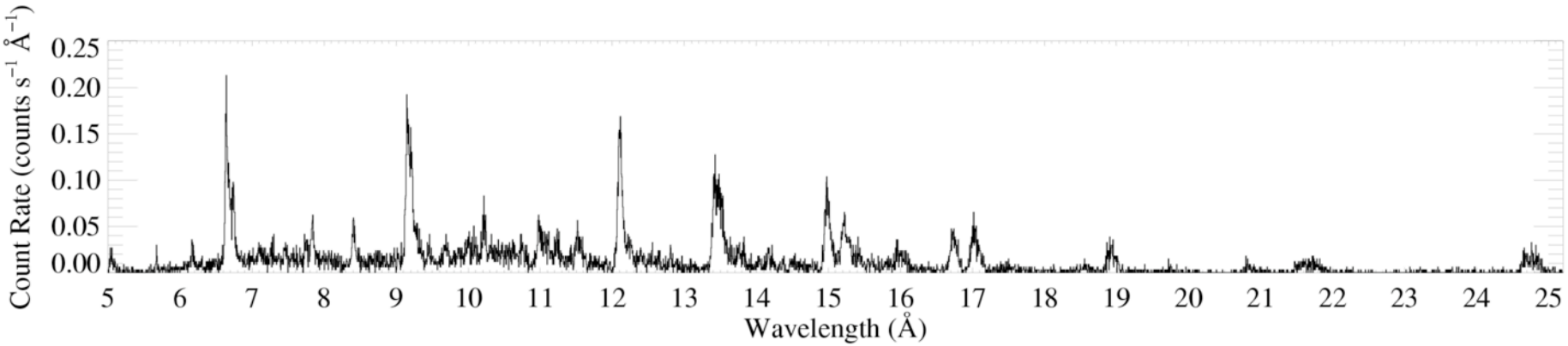

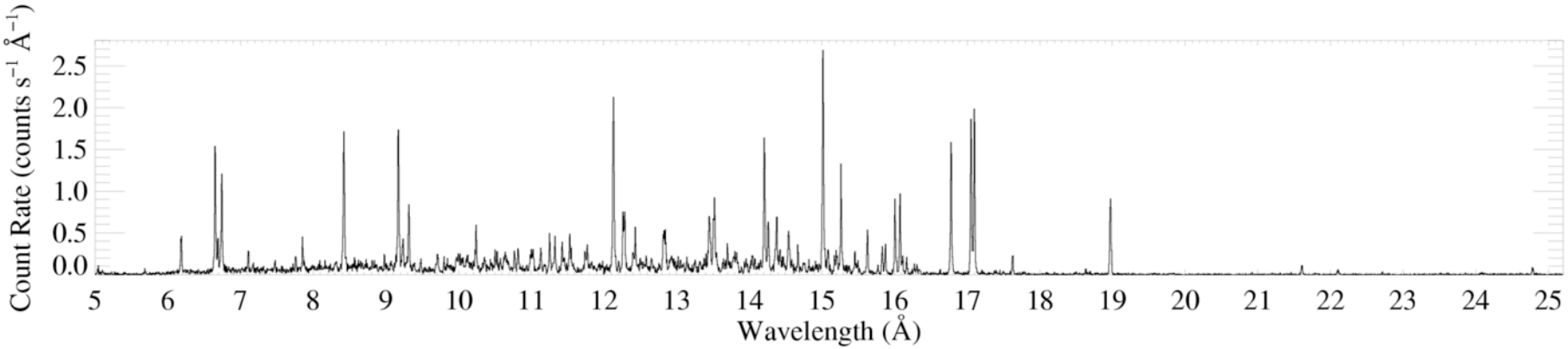

Capella (G5 III) – coronal source
– for comparison

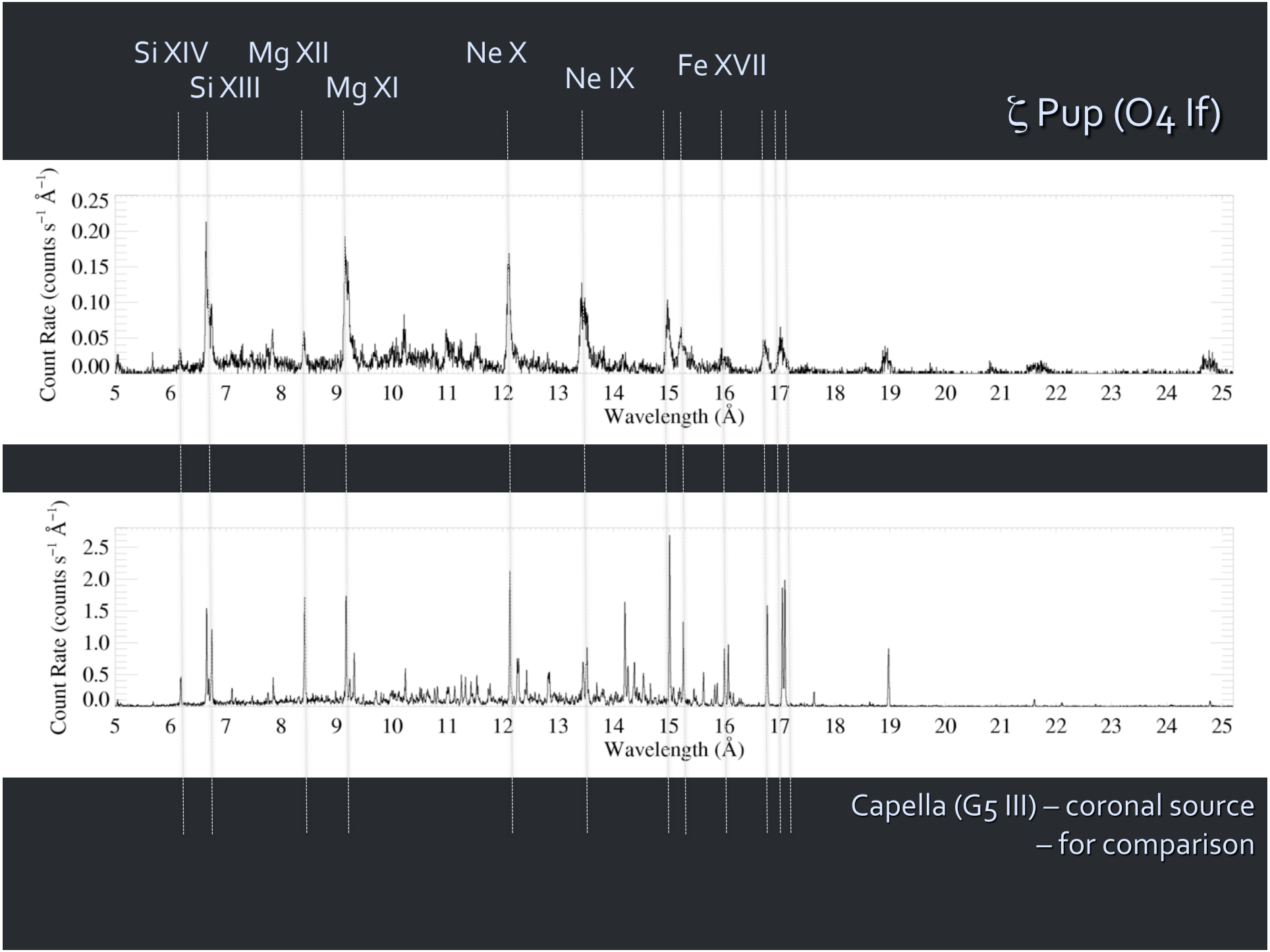
Si XIV
Si XIII
Mg XII
Mg XI
Ne X
Ne IX
Fe XVII
ζ Pup (O4 If)
Count Rate (counts s⁻¹ Å⁻¹)
Wavelength (Å)
Capella (G5 III) – coronal source
– for comparison

Si XIV
Si XIII
Mg XII
Mg XI
Ne X
Ne IX

H-like vs. He-like

ζ Pup (O4 If)

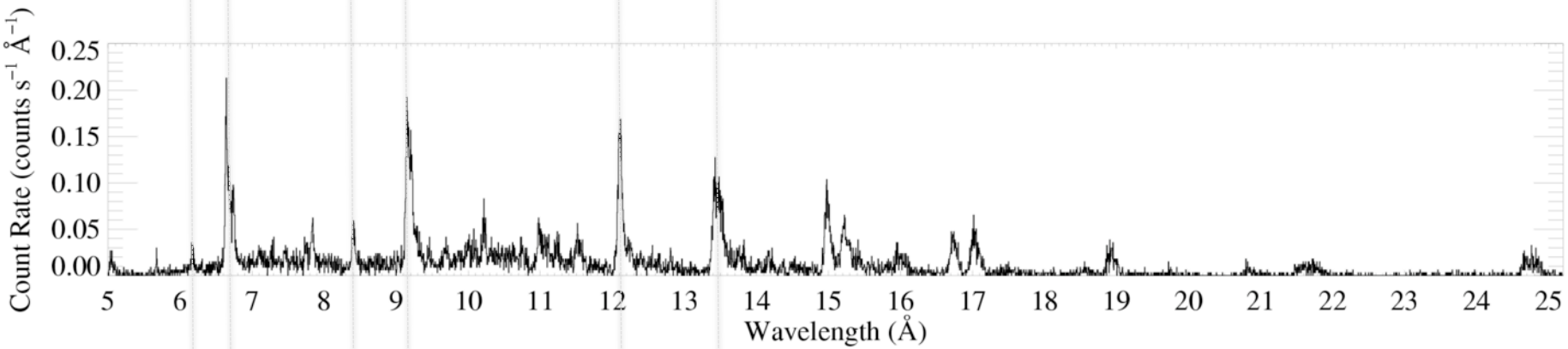

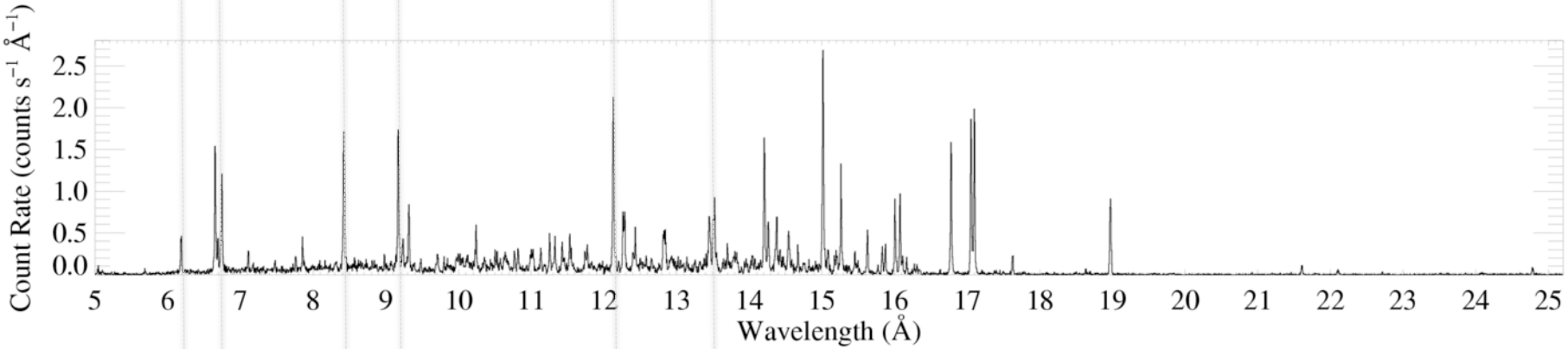

Capella (G5 III) – coronal source
– for comparison

Mg XII

Mg XI

H-like vs. He-like

ζ Pup (O4 If)

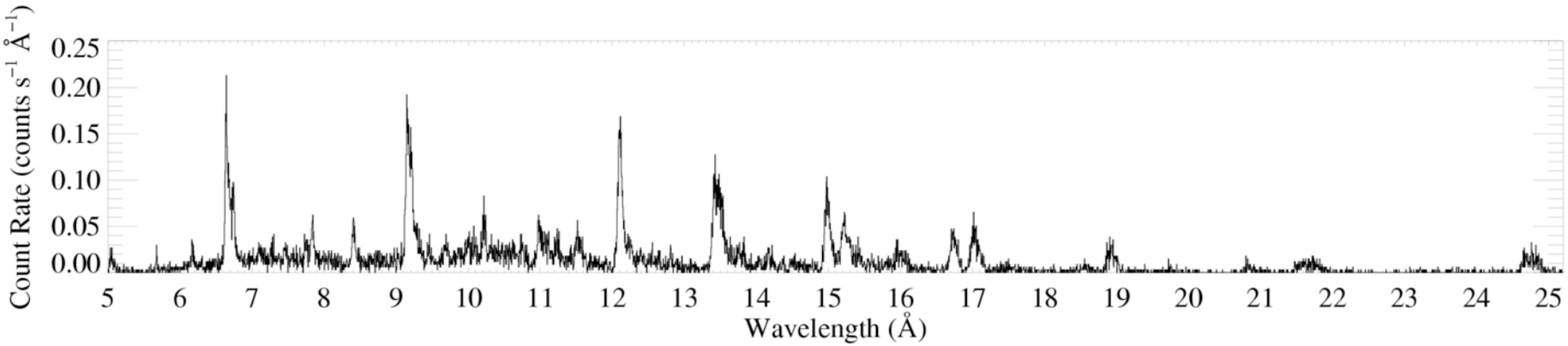

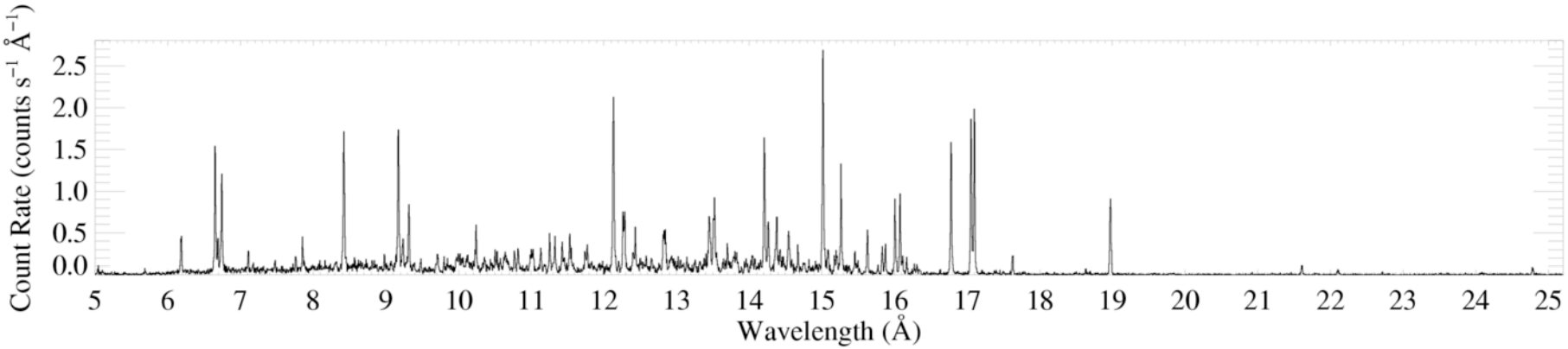

Capella (G5 III) – coronal source – for comparison

Mg XII

Mg XI

H-like vs. He-like

ζ Pup (O4 If)

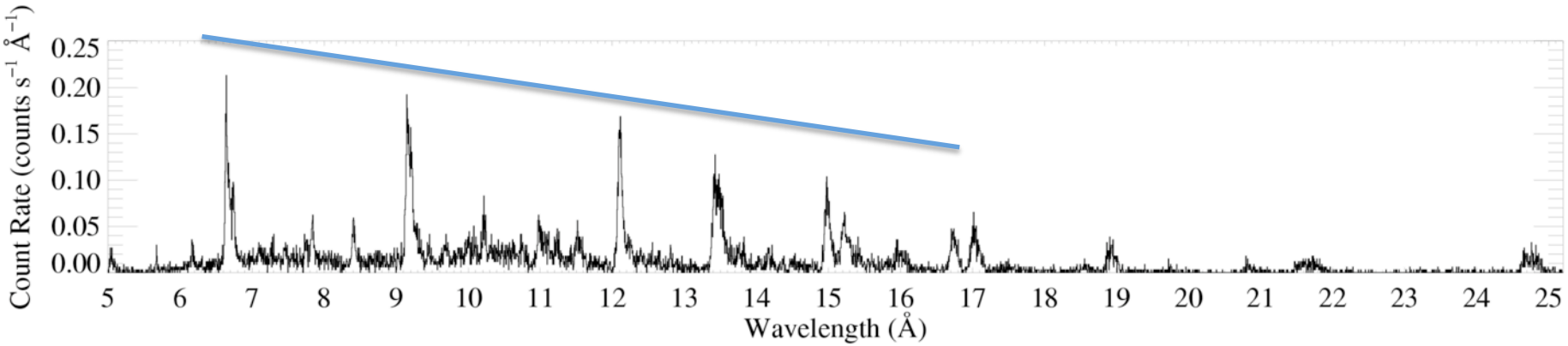

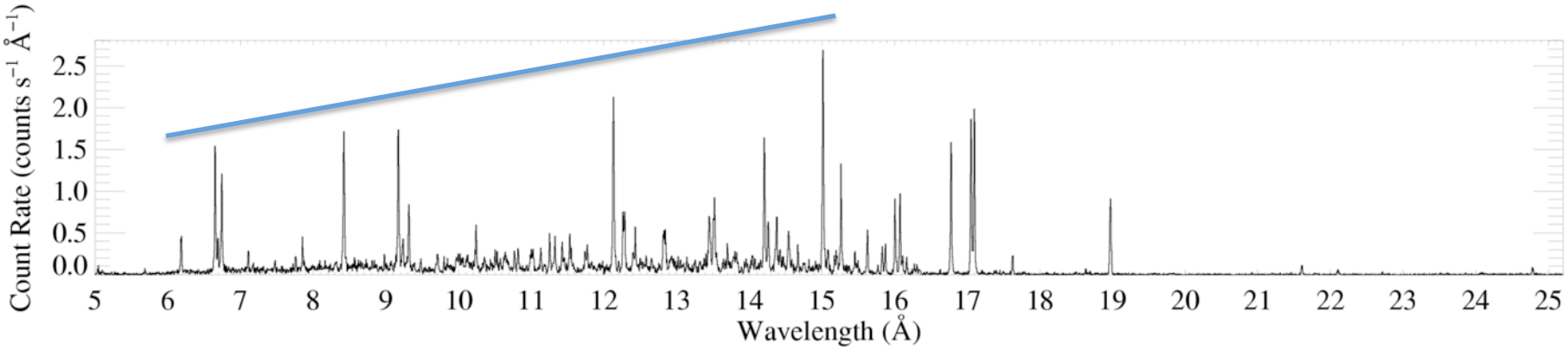

Capella (G5 III) – coronal source – for comparison

Spectral energy distribution trends

The O star has a *harder spectrum*, but apparently *cooler plasma*

*We'll see later on that soft X-ray **absorption** by the **winds** of O stars explains this*

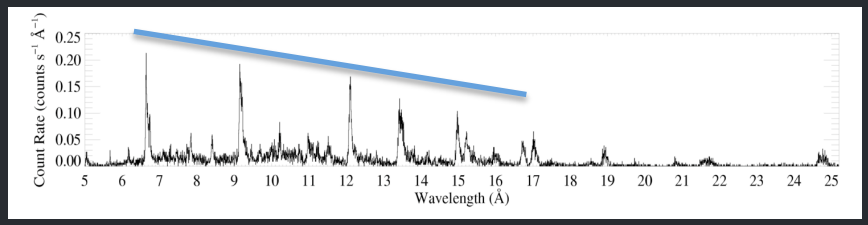

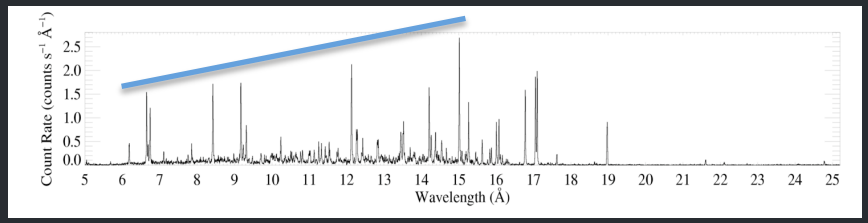

Next

First, we'll look at what can be learned about the **kinematics** and **location** of the X-ray emitting plasma from the **emission lines**

After that, we'll look at the issues of wind absorption and its effects on line shapes and on the broadband hardness trend

Embedded wind shocks

Numerical simulations of the line-driven instability (LDI) predict:

1. Distribution of shock-heated plasma
2. Above an onset radius of $r \sim 1.5\ R_*$

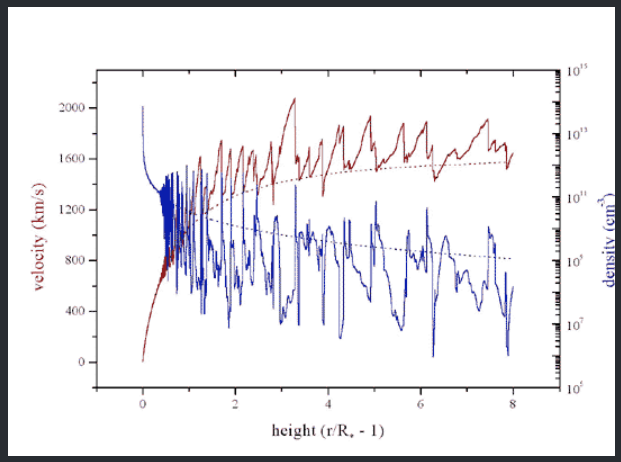

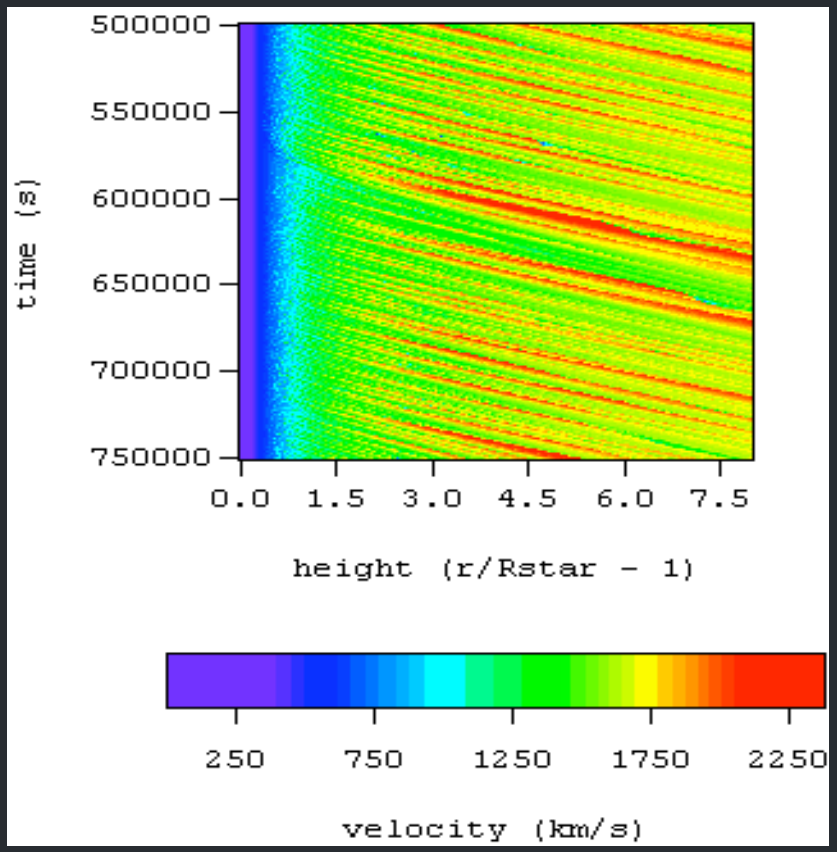

1-D rad-hydro simulations

Self-excited instability (smooth initial conditions)

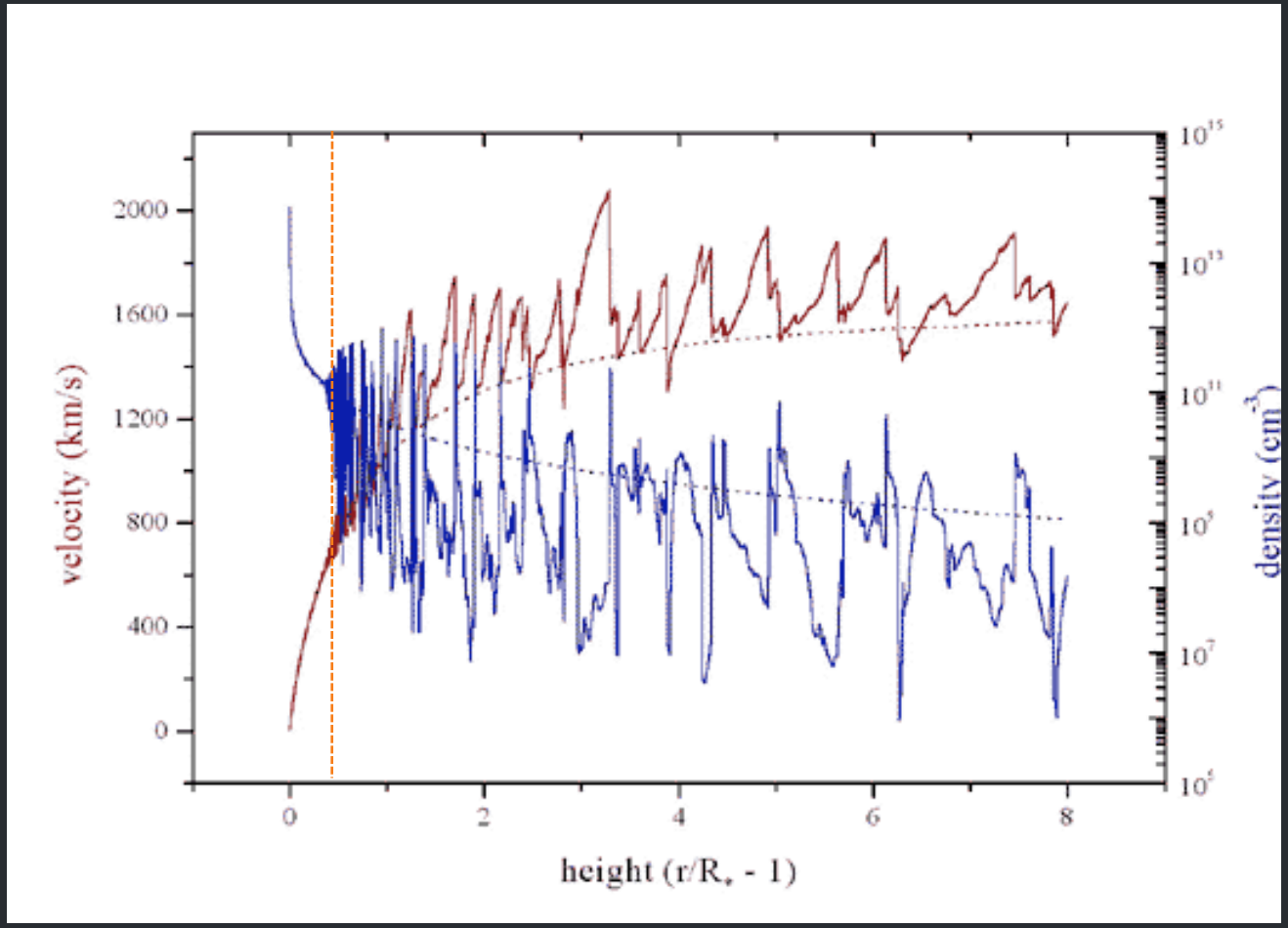

shock onset at r ~ 1.5 R_{star}

V_{shock} ~ 300 km/s :
T ~ 10^6 K

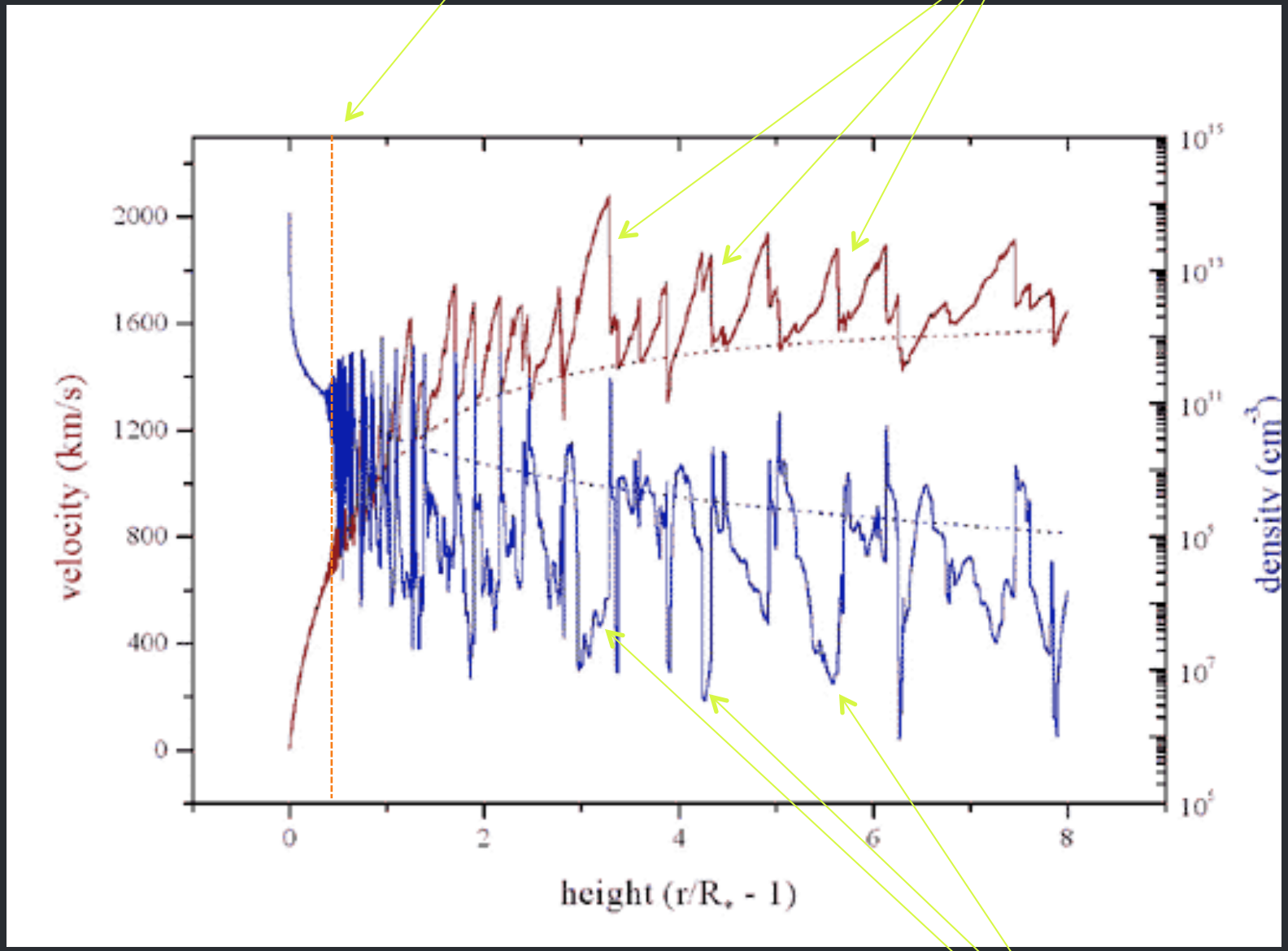

pre-shock wind plasma has low density

shock onset at r ~ 1.5 R_{star}

V_{shock} ~ 300 km/s :
T ~ 10^6 K

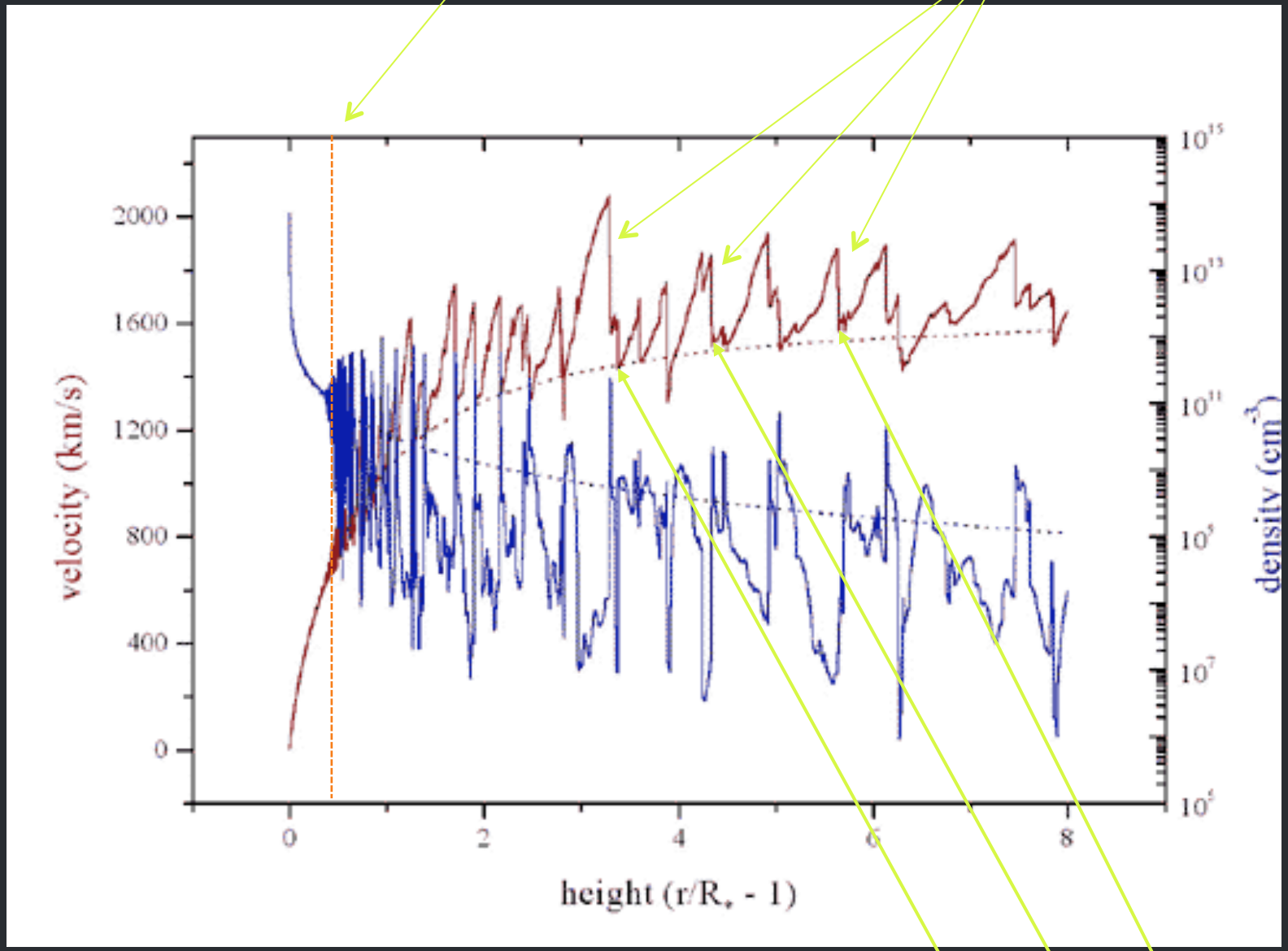

Shocked wind plasma is decelerated back down to the local CAK wind velocity

Morphology

ζ Pup (O4 If)

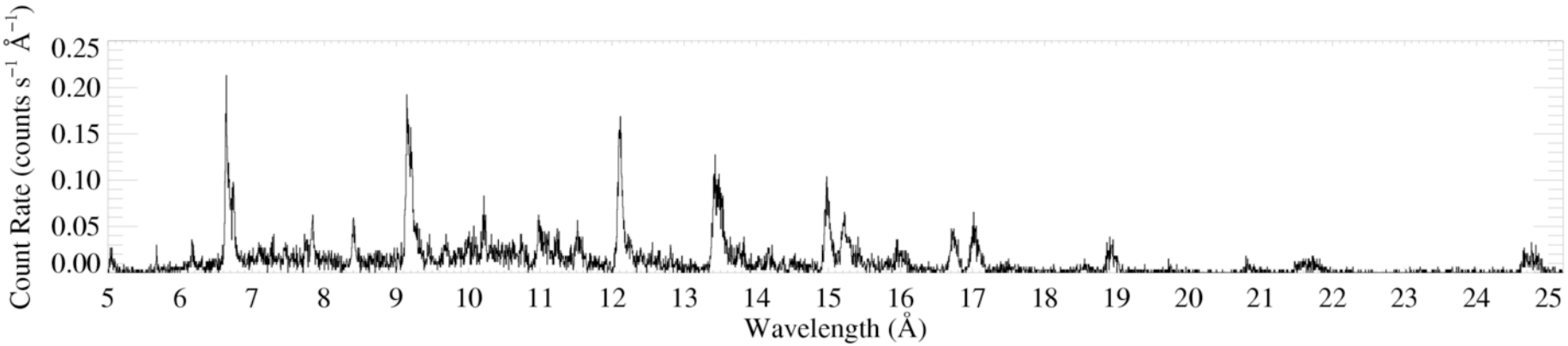

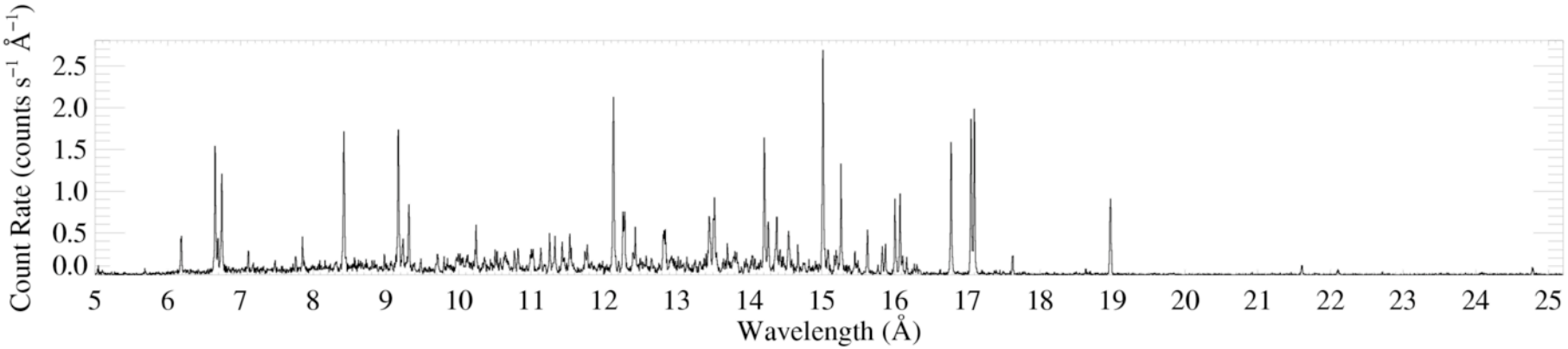

Capella (G5 III) – coronal source
– for comparison

Morphology – line widths

ζ Pup (O4 If)

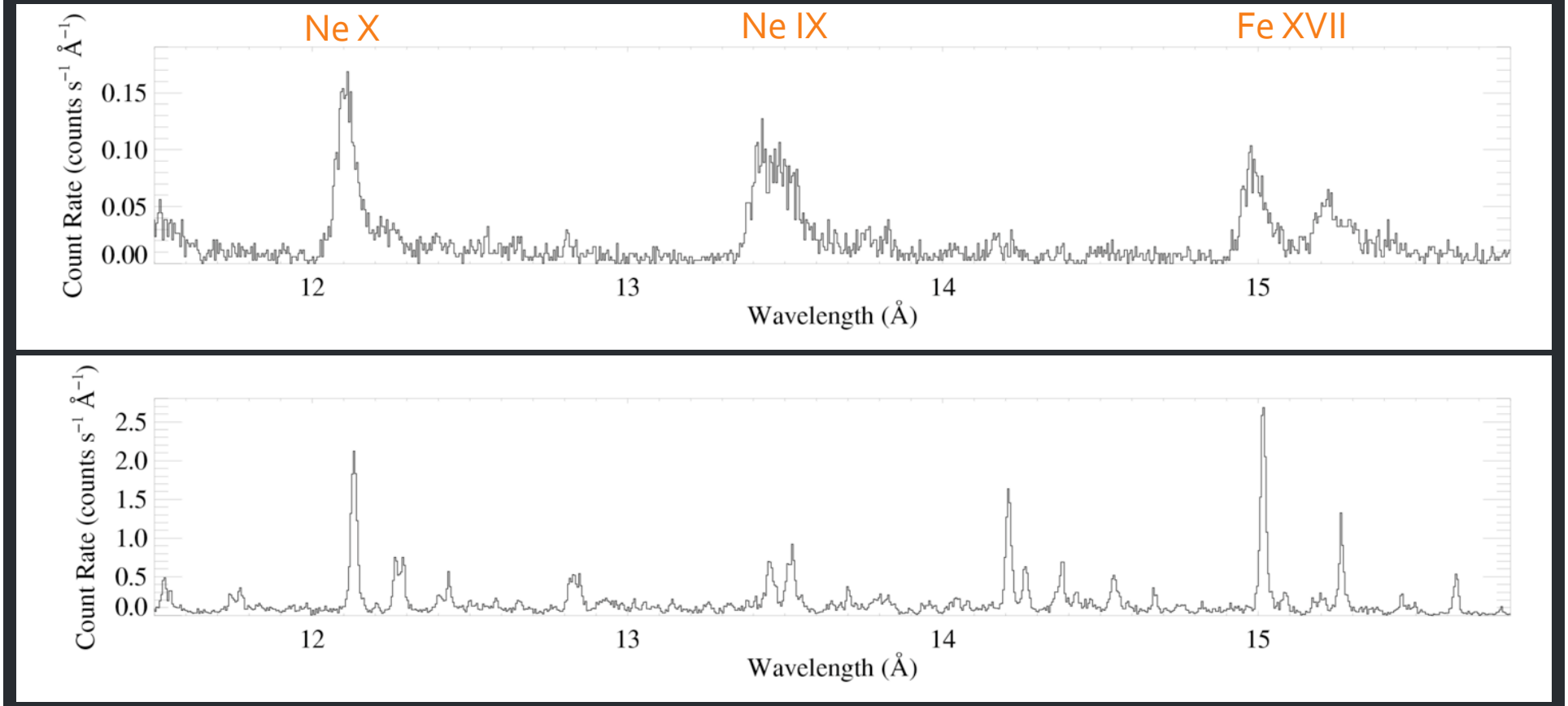

Capella (G5 III) – coronal source
– for comparison

Morphology – line widths

ζ Pup (O4 If)

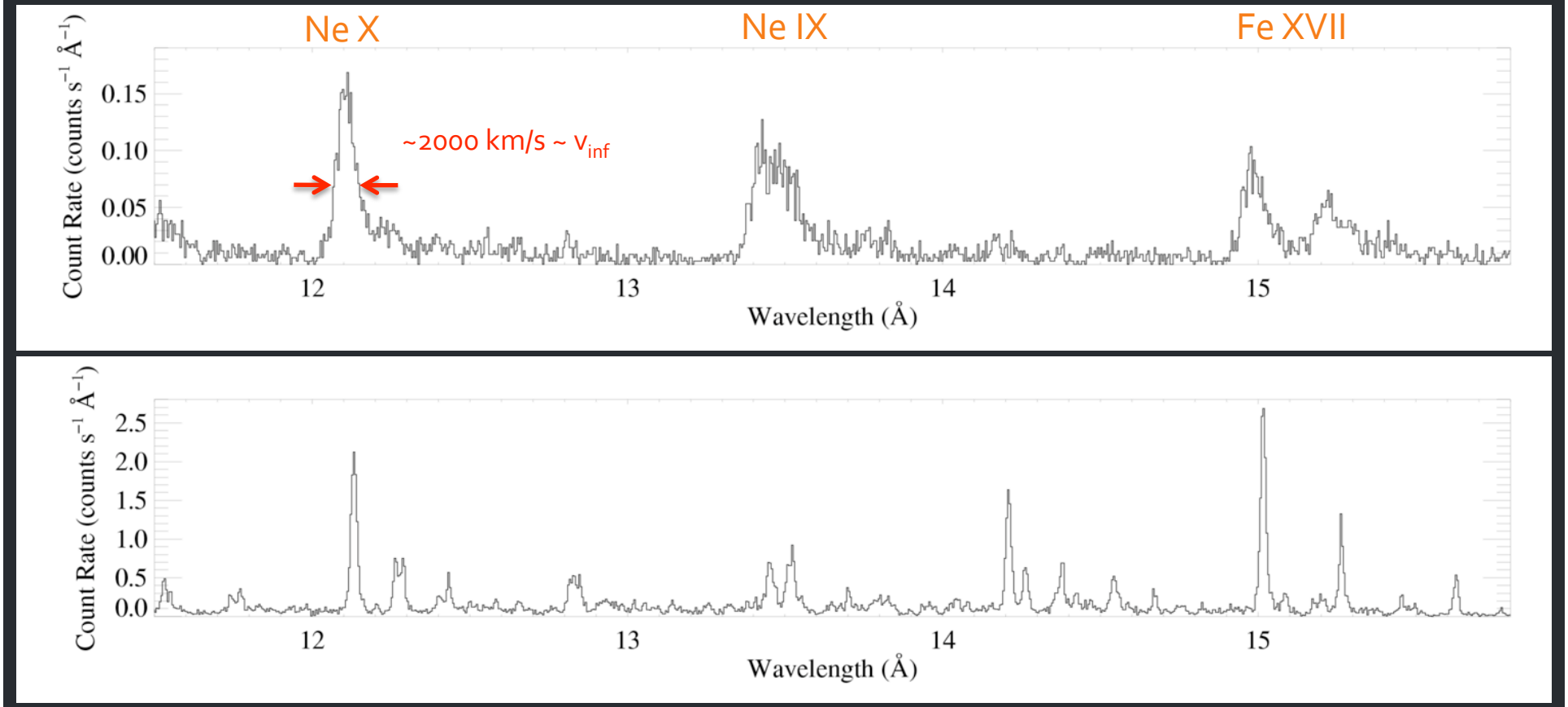

Capella (G5 III) – coronal source
– for comparison

Shock heated wind plasma is moving at >1000 km/s : broad X-ray emission lines

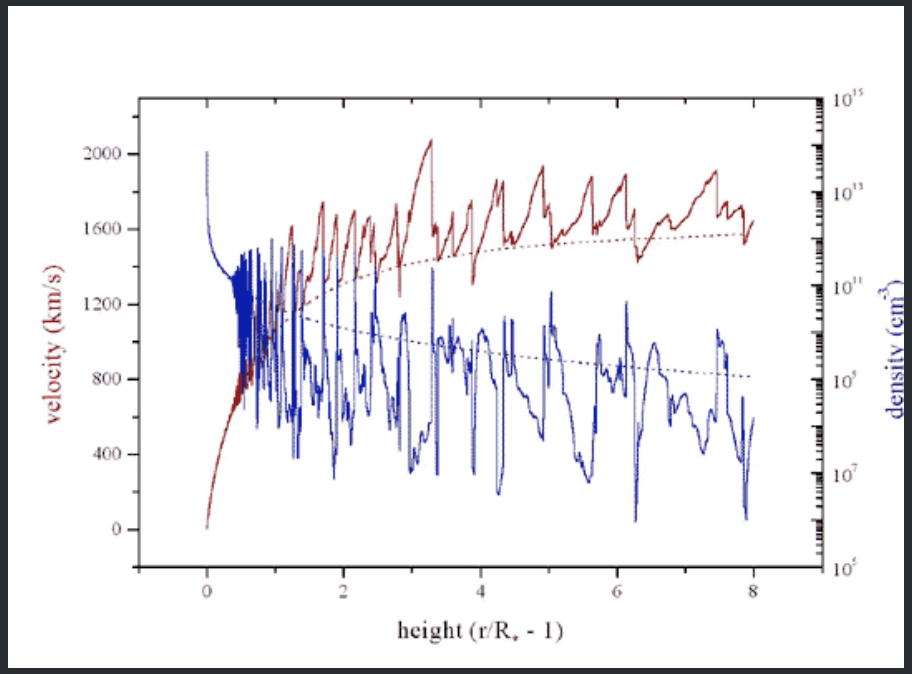

99% of the wind mass is cold*, partially ionized… x-ray **absorbing**

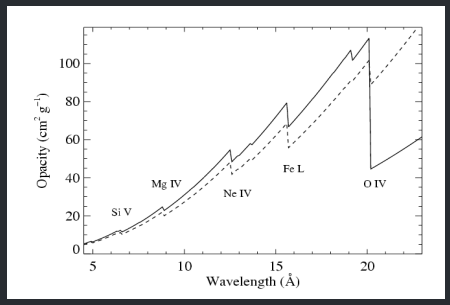

opacity

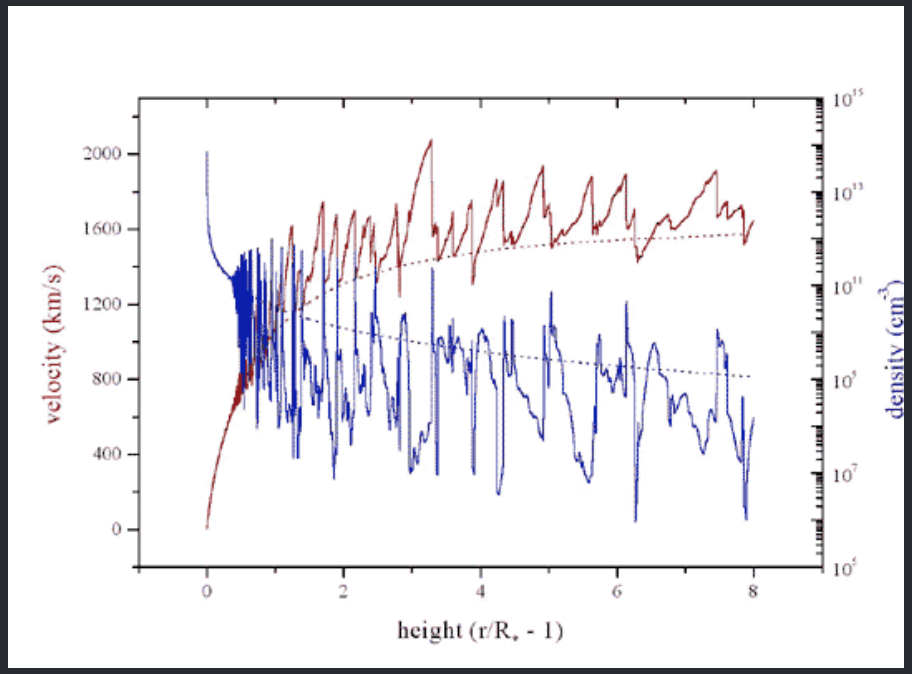

*typically 20,000 – 30,000 K; maybe better described as "warm"

x-ray absorption is due to bound-free opacity of metals

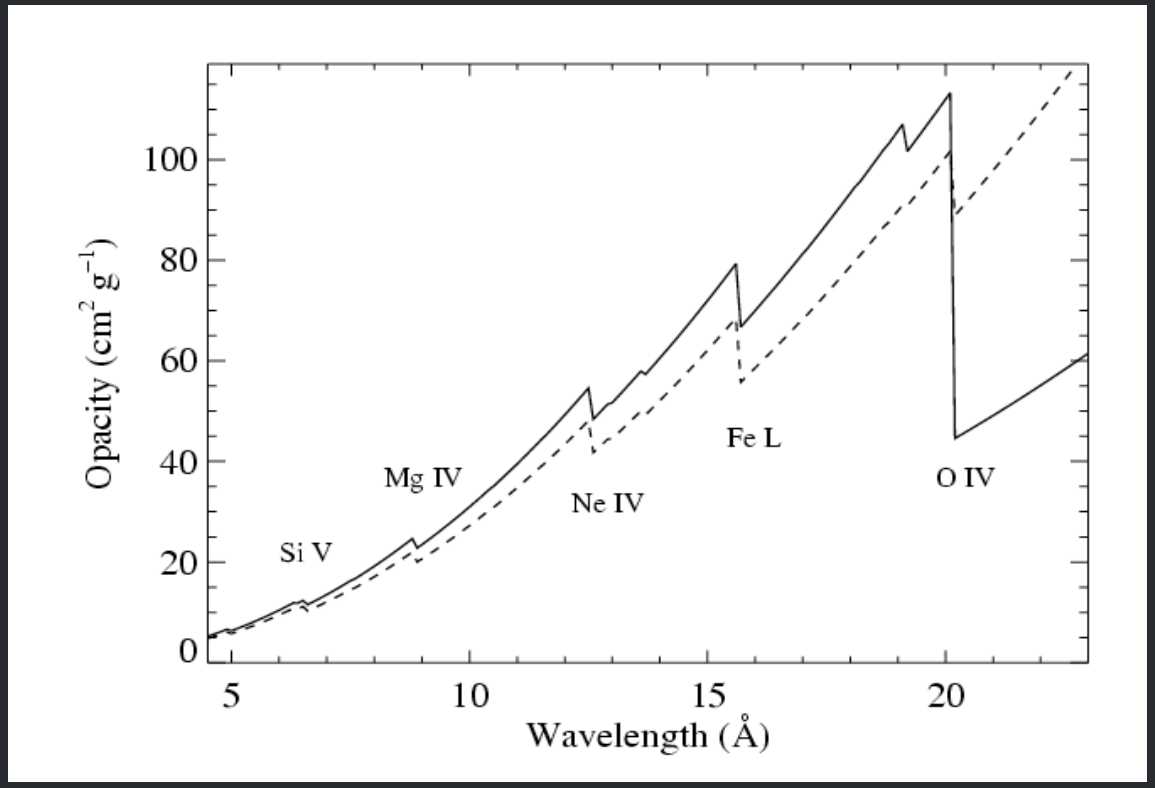

opacity

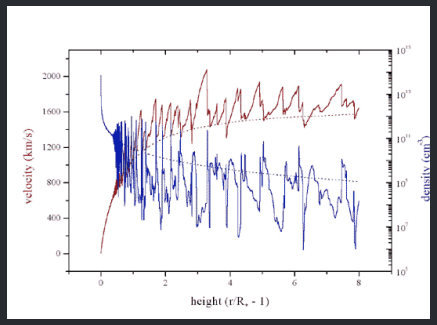

...and it takes place in the 99% of the wind that is **unshocked**

Emission + absorption = profile model

The kinematics of the emitting material dictates the line **width** and overall profile

Absorption affects line **shapes**

isovelocity contours

Onset radius of X-ray emission, R_o

observer on left

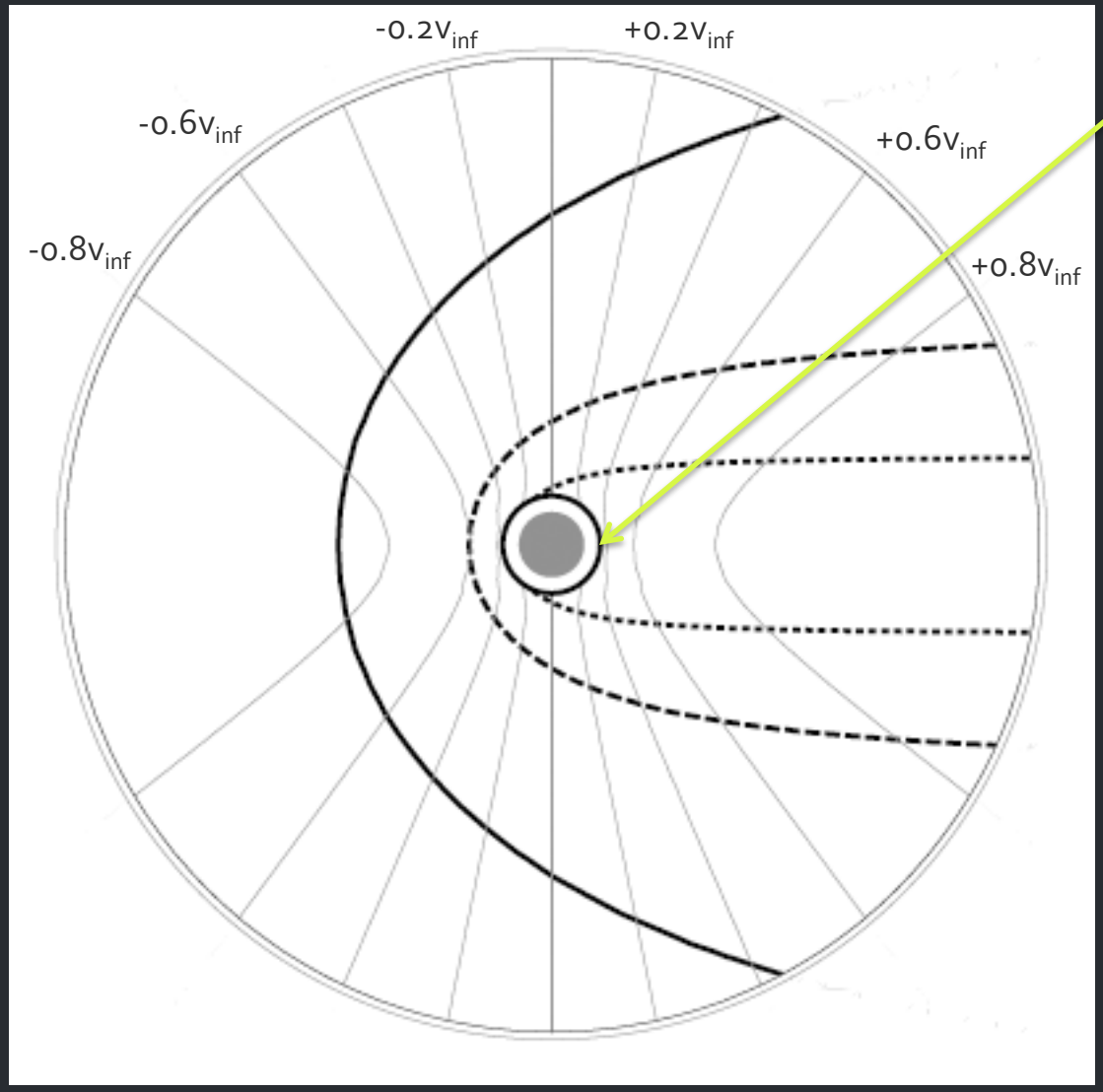

isovelocity contours

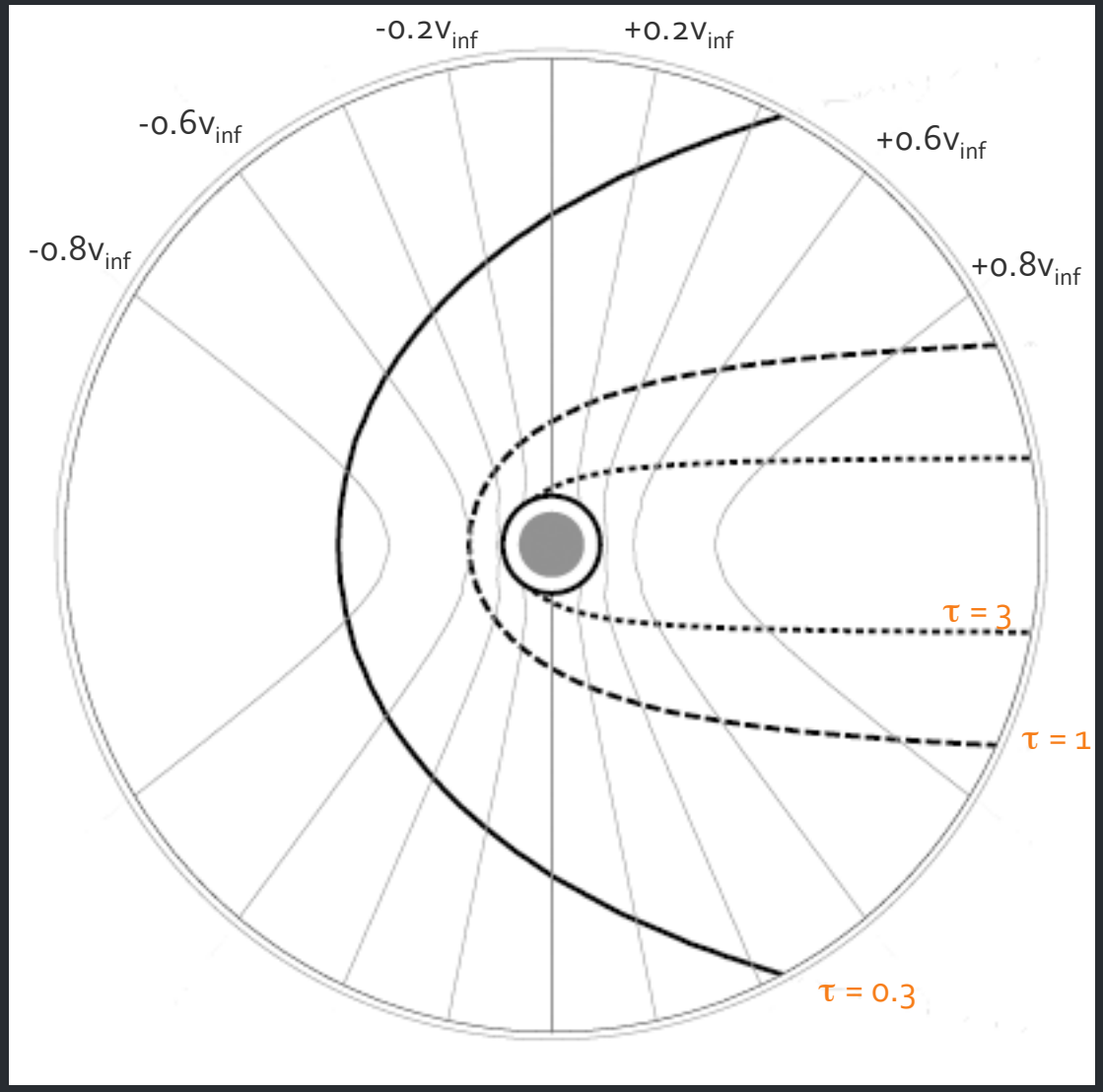

observer
on left

optical depth
contours

Line Asymmetry

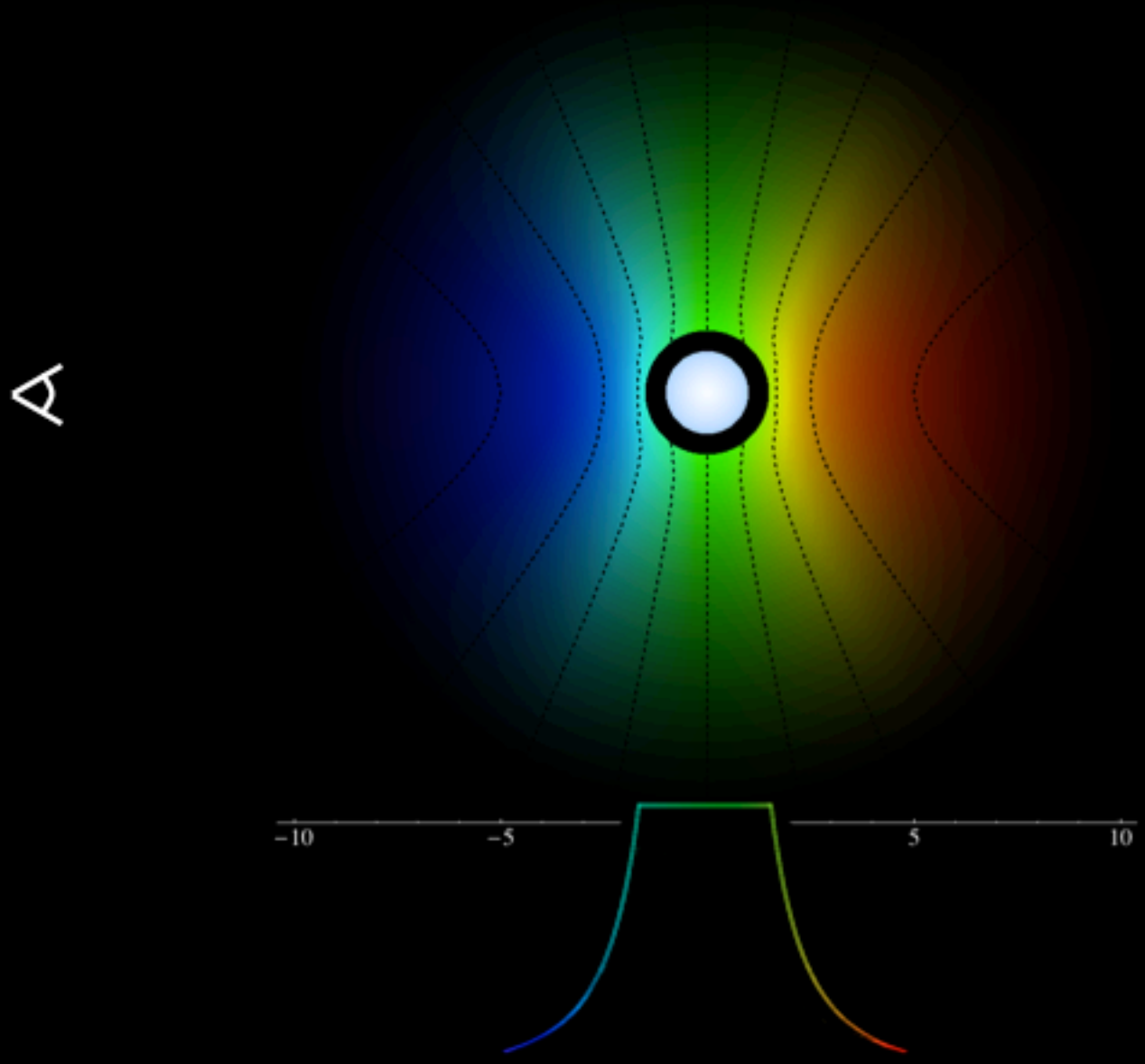

Line Asymmetry

A

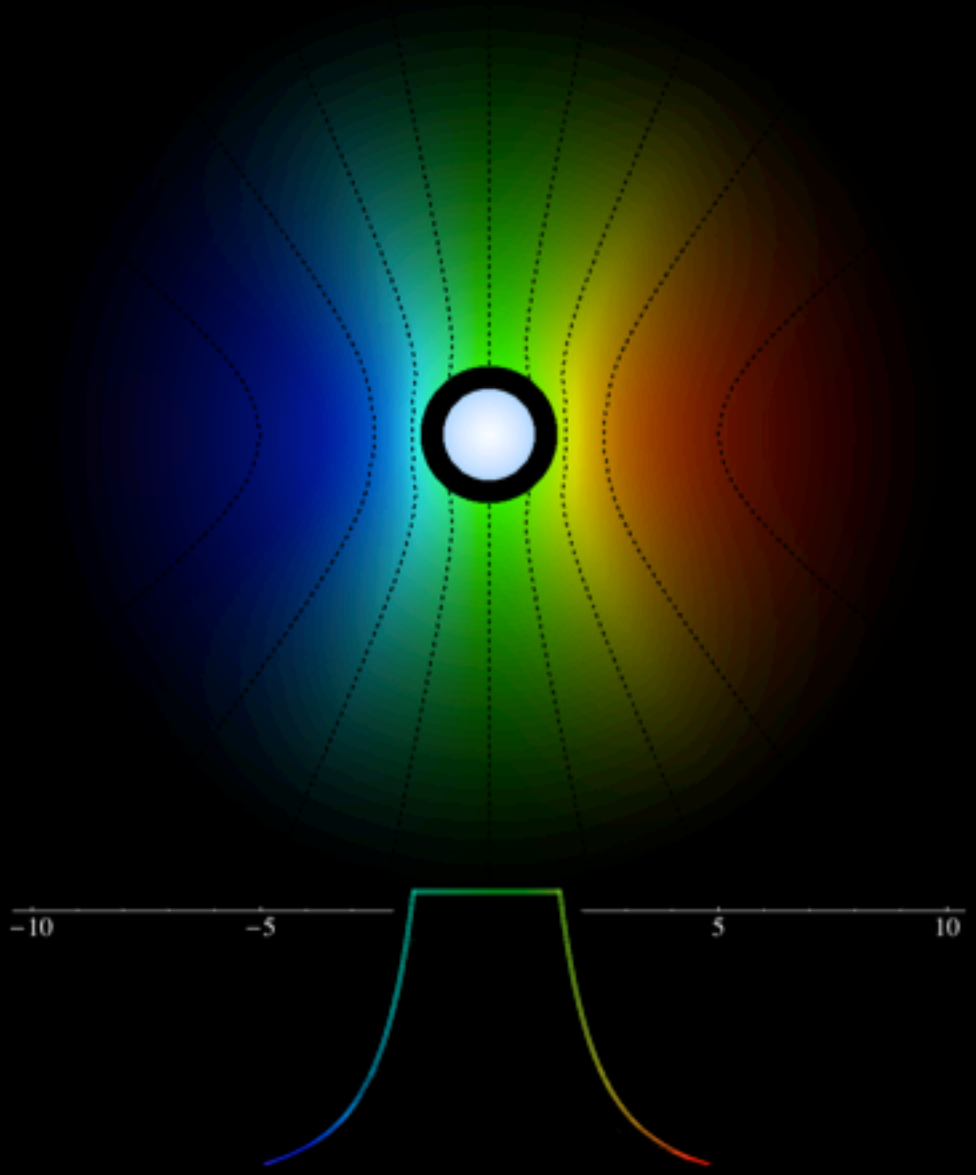

Profile shape assumes beta velocity law and onset radius, R_o

Line Asymmetry

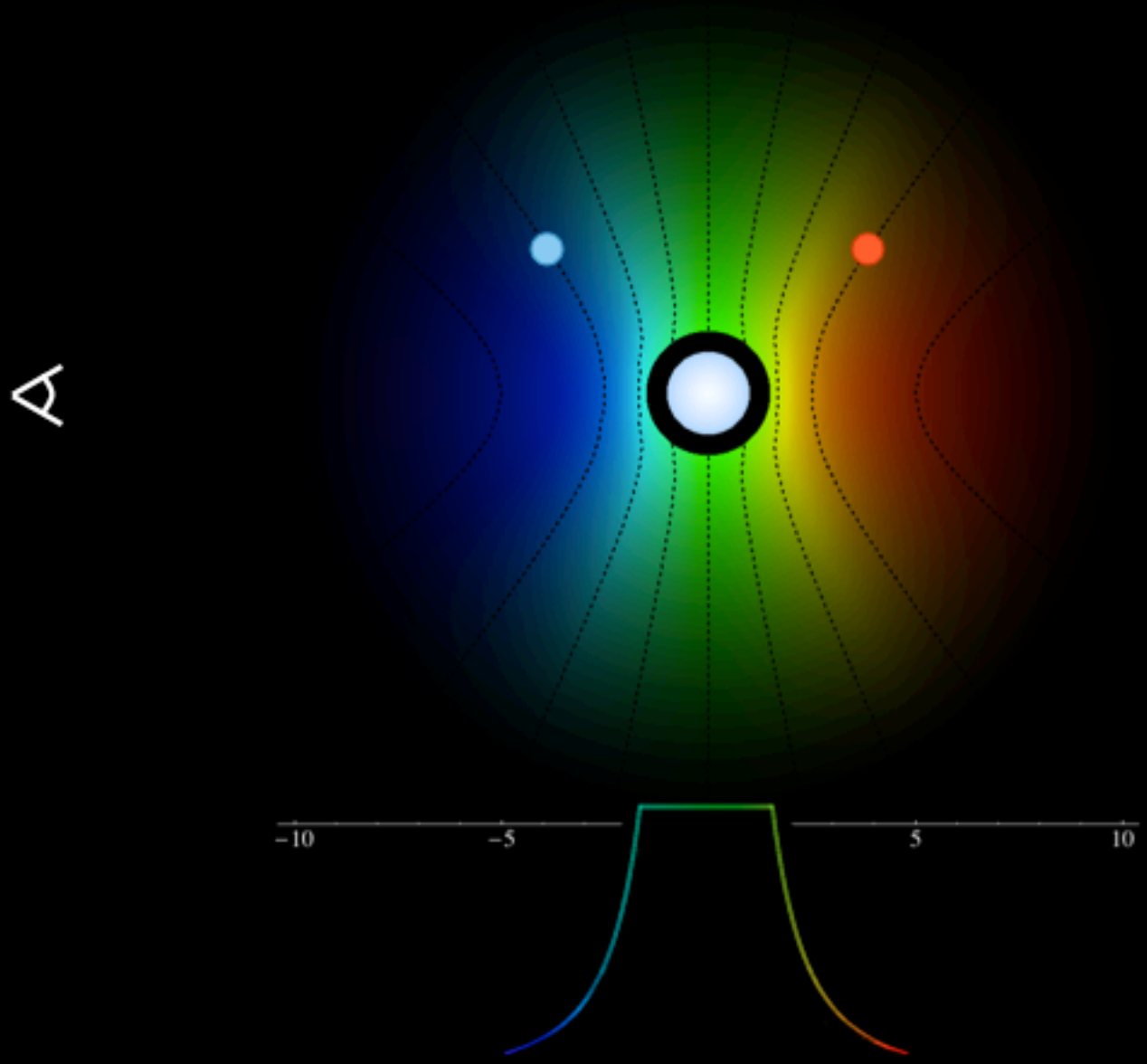

Line Asymmetry

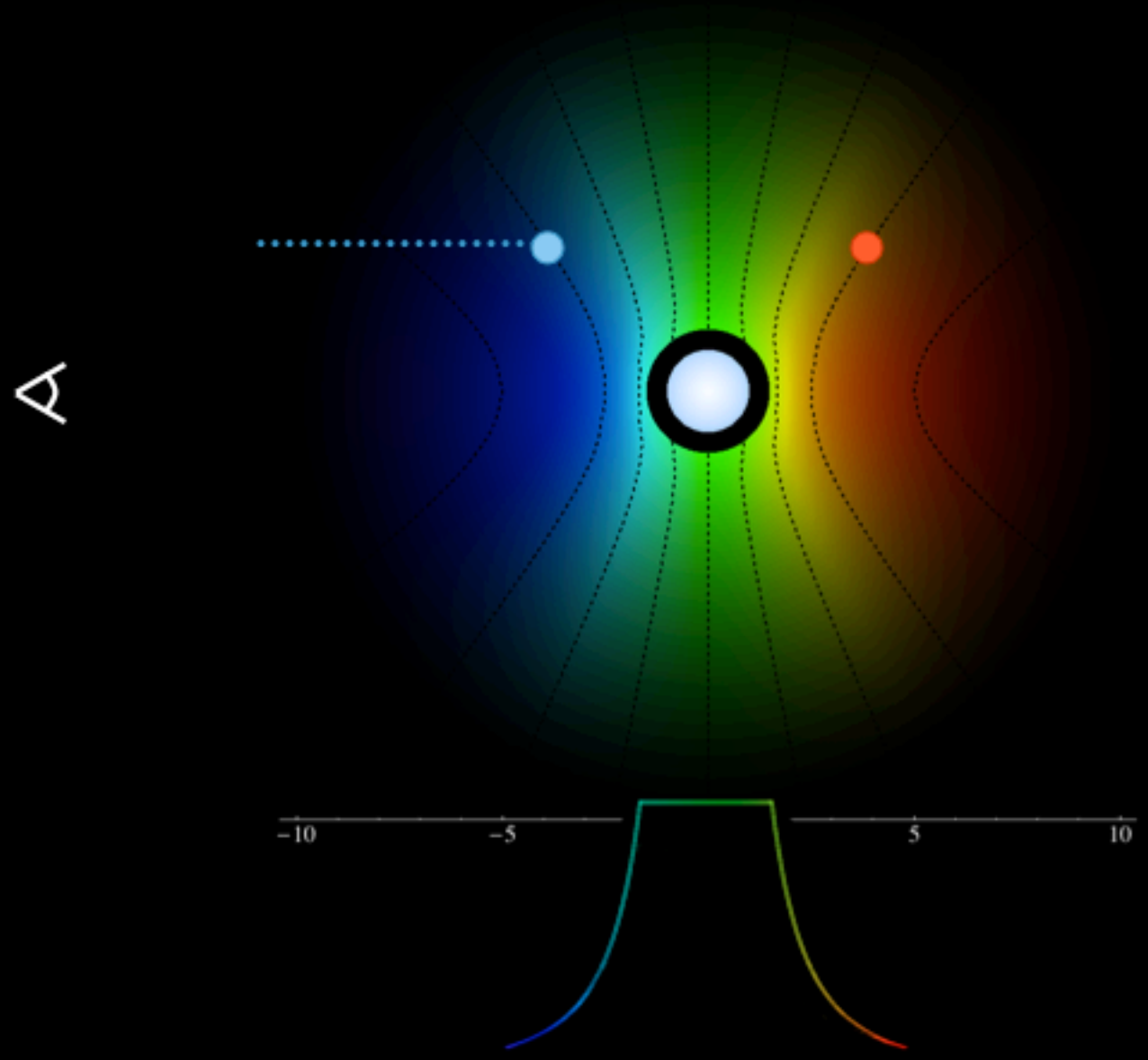

Line Asymmetry

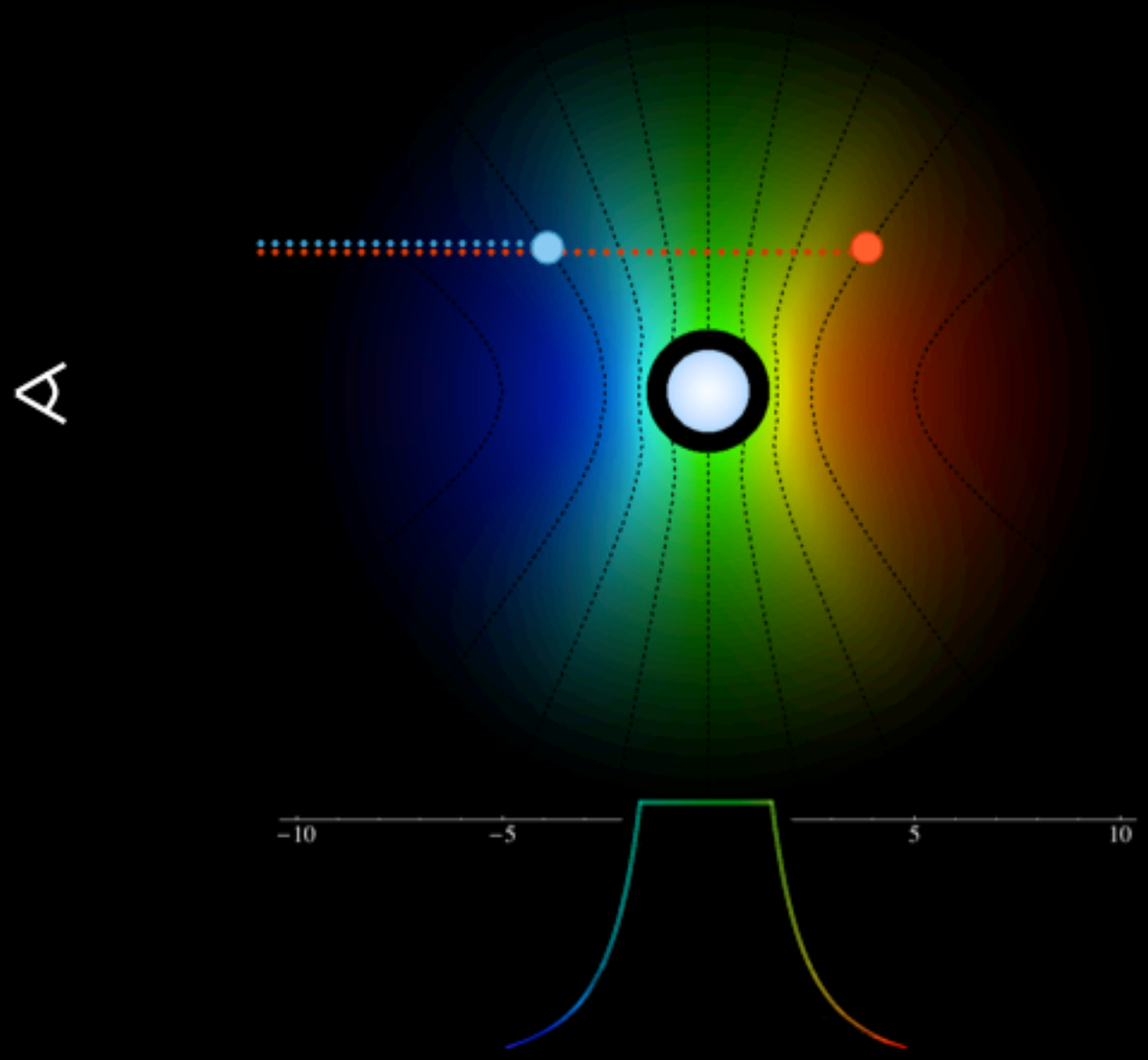

Line Asymmetry

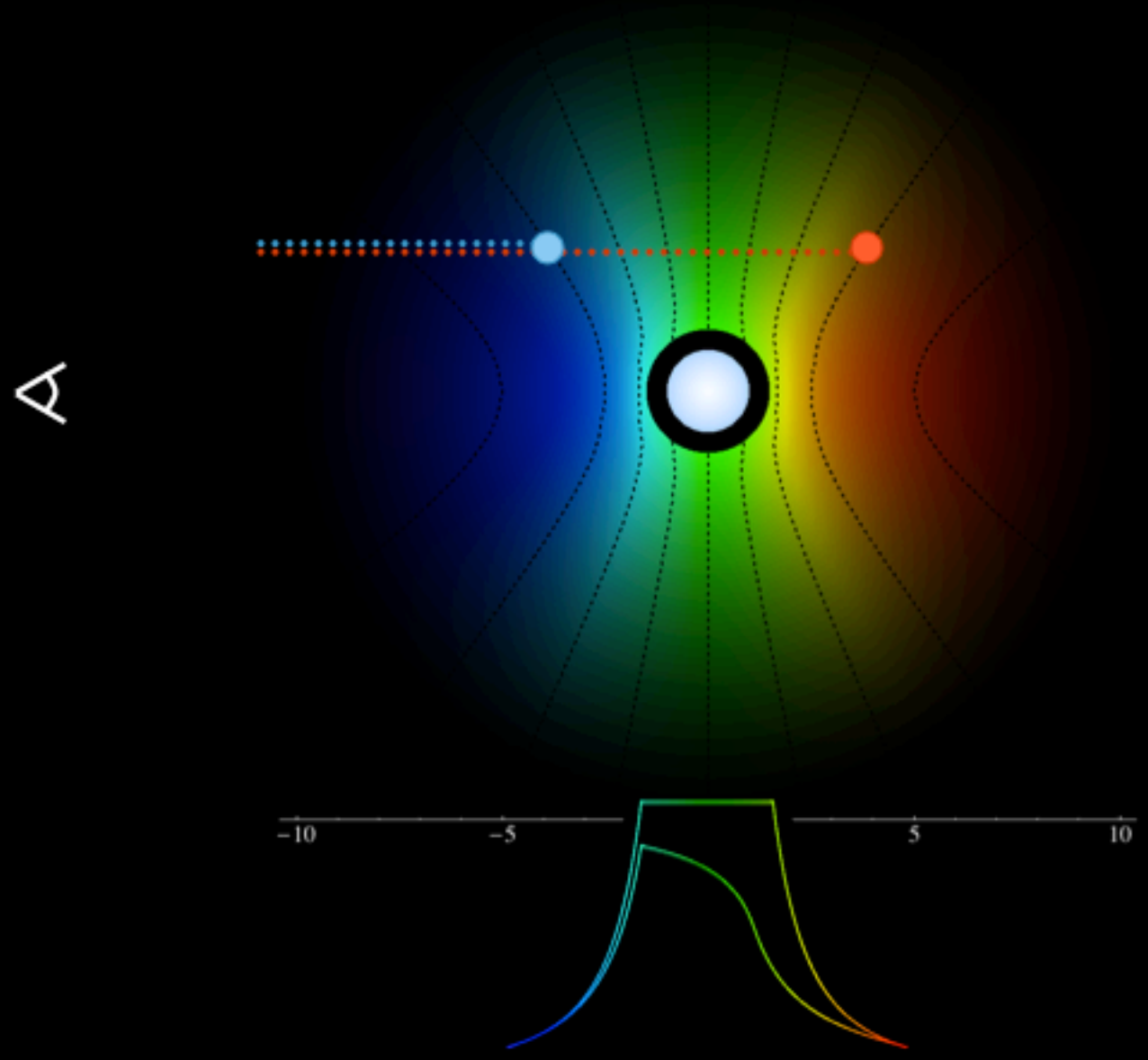

Line Asymmetry

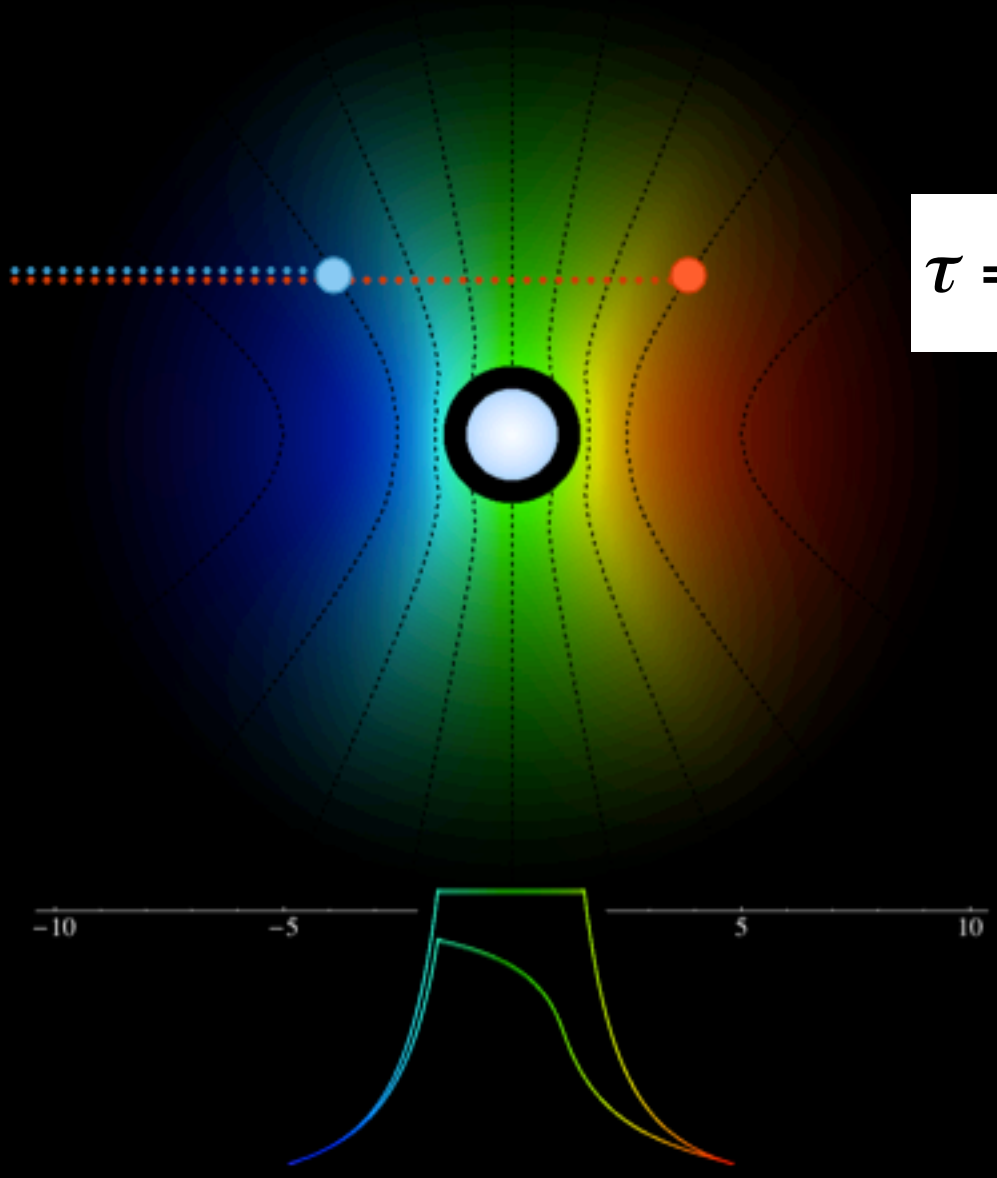

$$\tau = \tau_* \int_z^\infty \frac{R_* dz'}{r'^2 (1 - R_*/r')^\beta}$$

Line Asymmetry

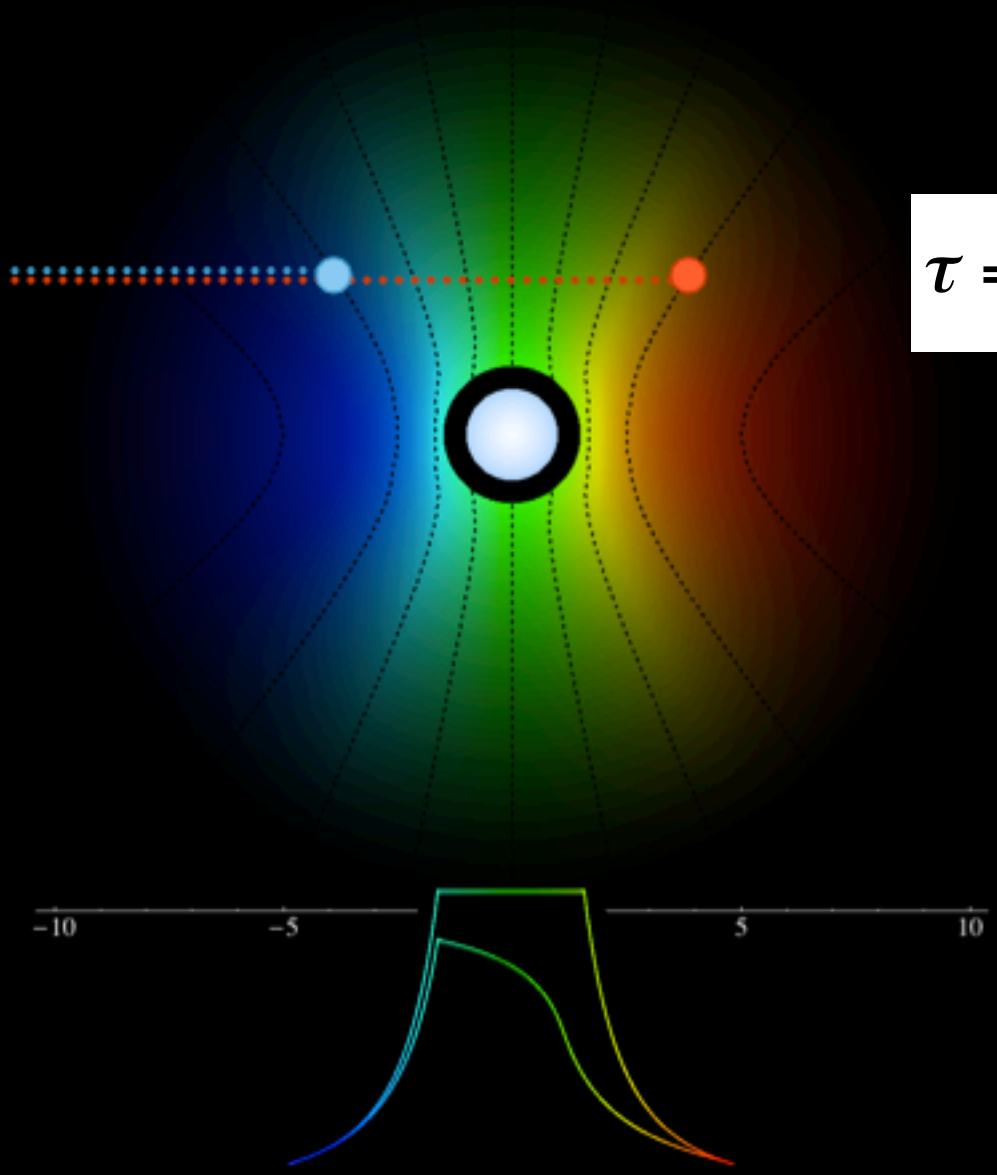

Universal property of the wind

$$\tau = \tau_* \int_z^\infty \frac{R_* dz'}{r'^2 (1 - R_*/r')^\beta}$$

z different for each point

Wind Profile Model

$$\tau_* = \frac{\kappa \dot{M}}{4\pi R_* v_\infty}$$

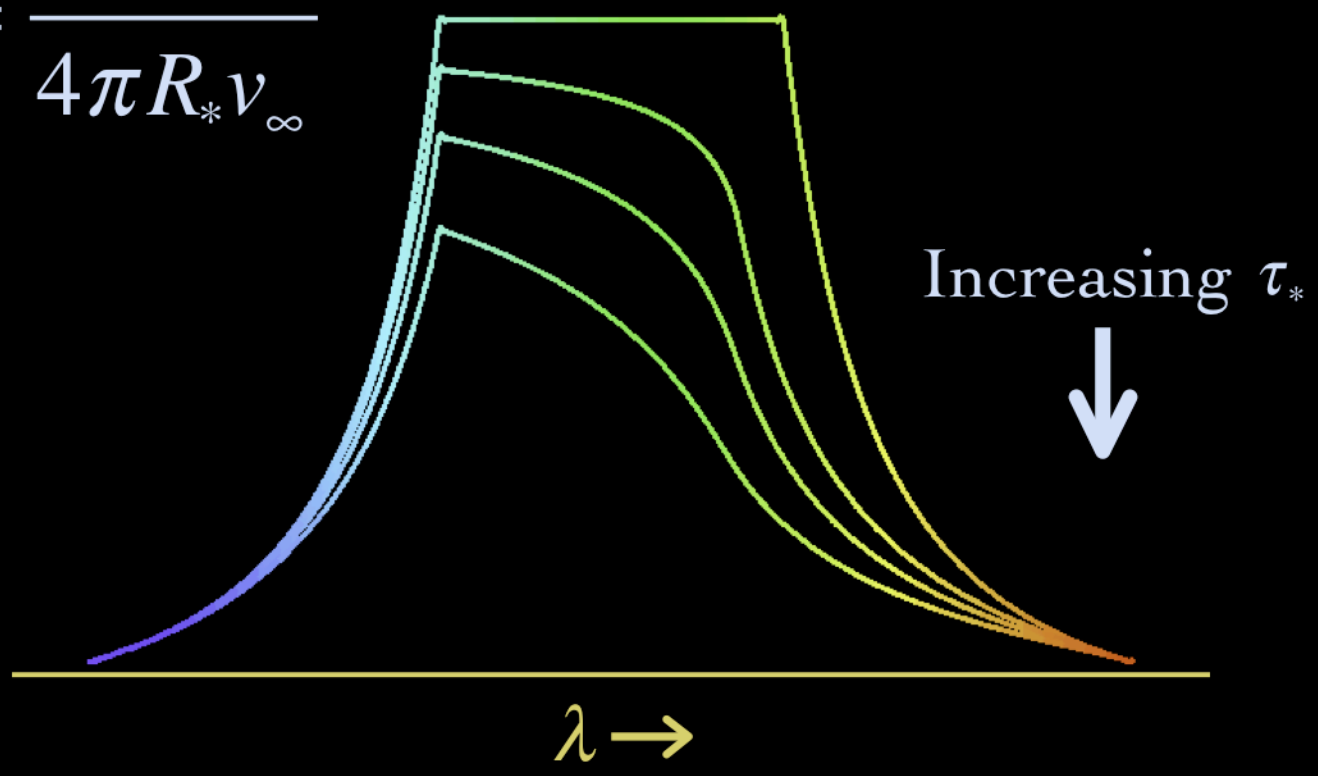

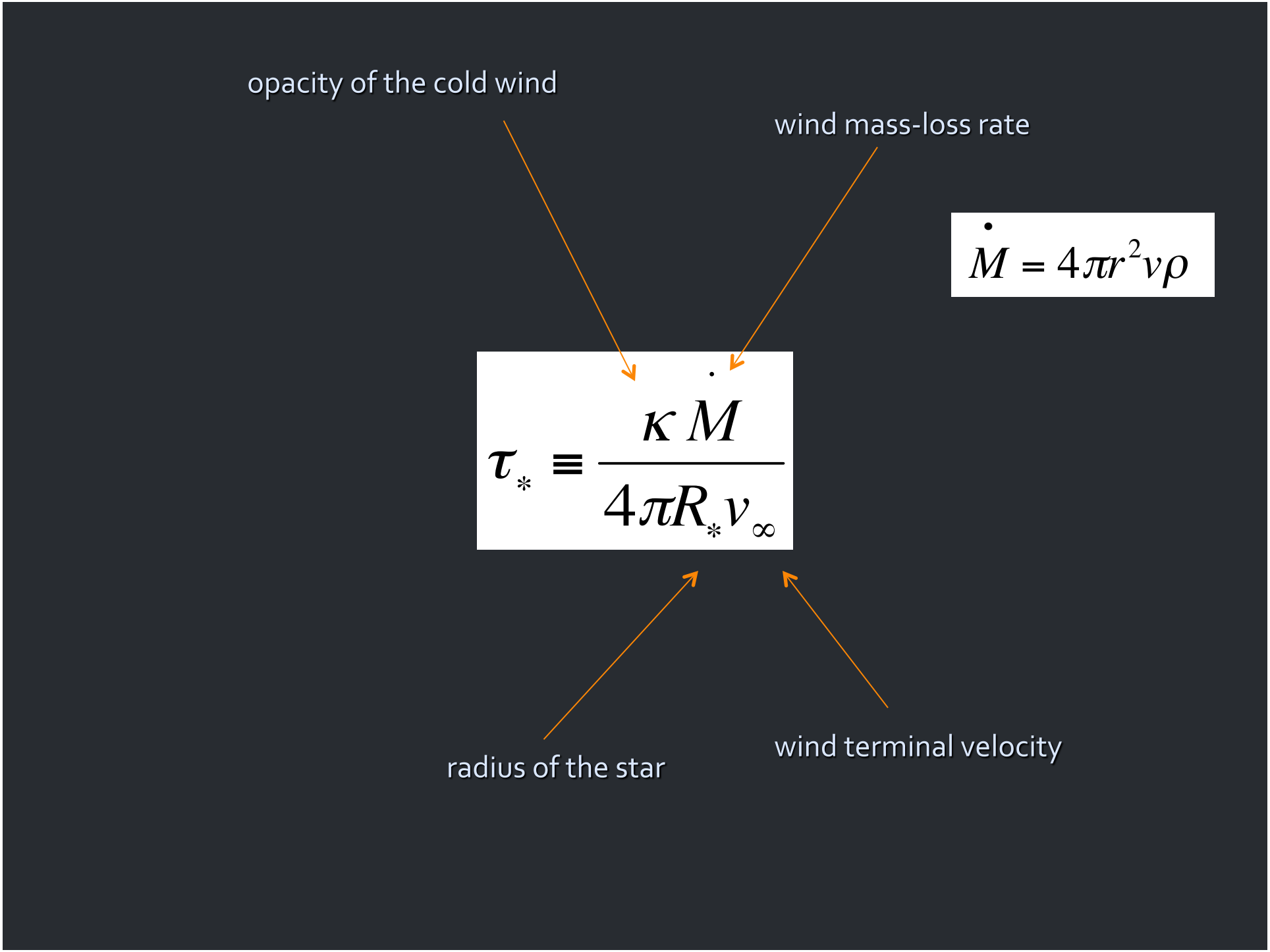
opacity of the cold wind
wind mass-loss rate
$\dot{M} = 4\pi r^2 v \rho$
$\tau_* \equiv \frac{\kappa \dot{M}}{4\pi R_* v_\infty}$
radius of the star
wind terminal velocity

τ = 1 contours

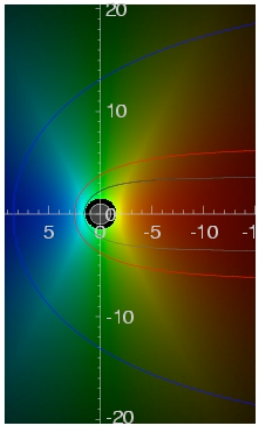

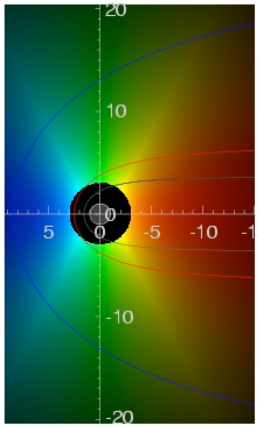

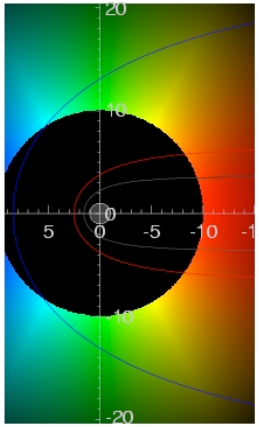

τ_*=1, 2, 8

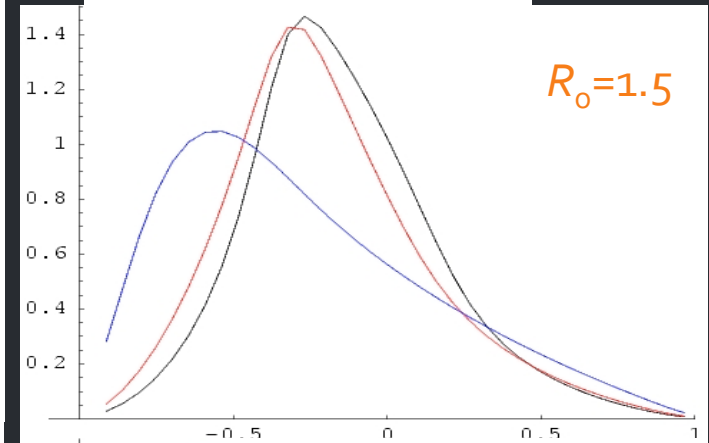

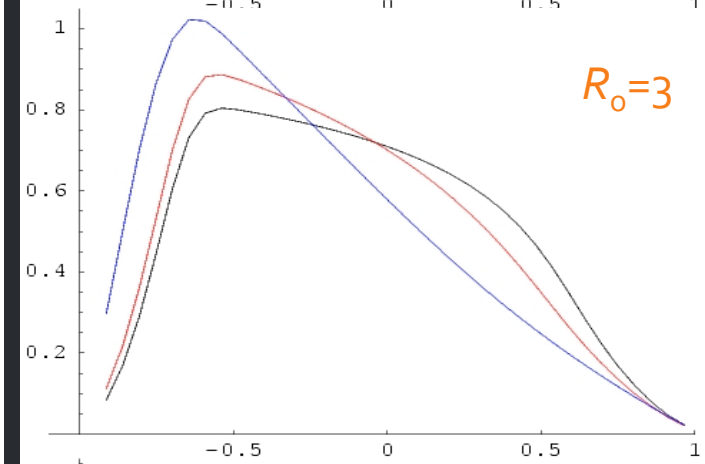

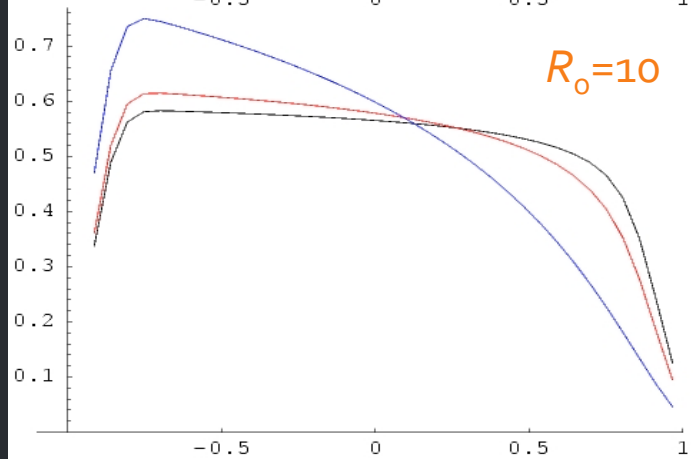

key parameters: R_o & τ_*

$j \sim \rho^2$ for $r/R_* > R_o$

$= 0$ otherwise

$$\tau = \tau_* \int_z^\infty \frac{R_* dz'}{r'^2 (1 - R_*/r')^\beta}$$

$$\tau_* \equiv \frac{\kappa \dot{M}}{4\pi R_* v_\infty}$$

We fit these x-ray line profile models to each line in the *Chandra* data

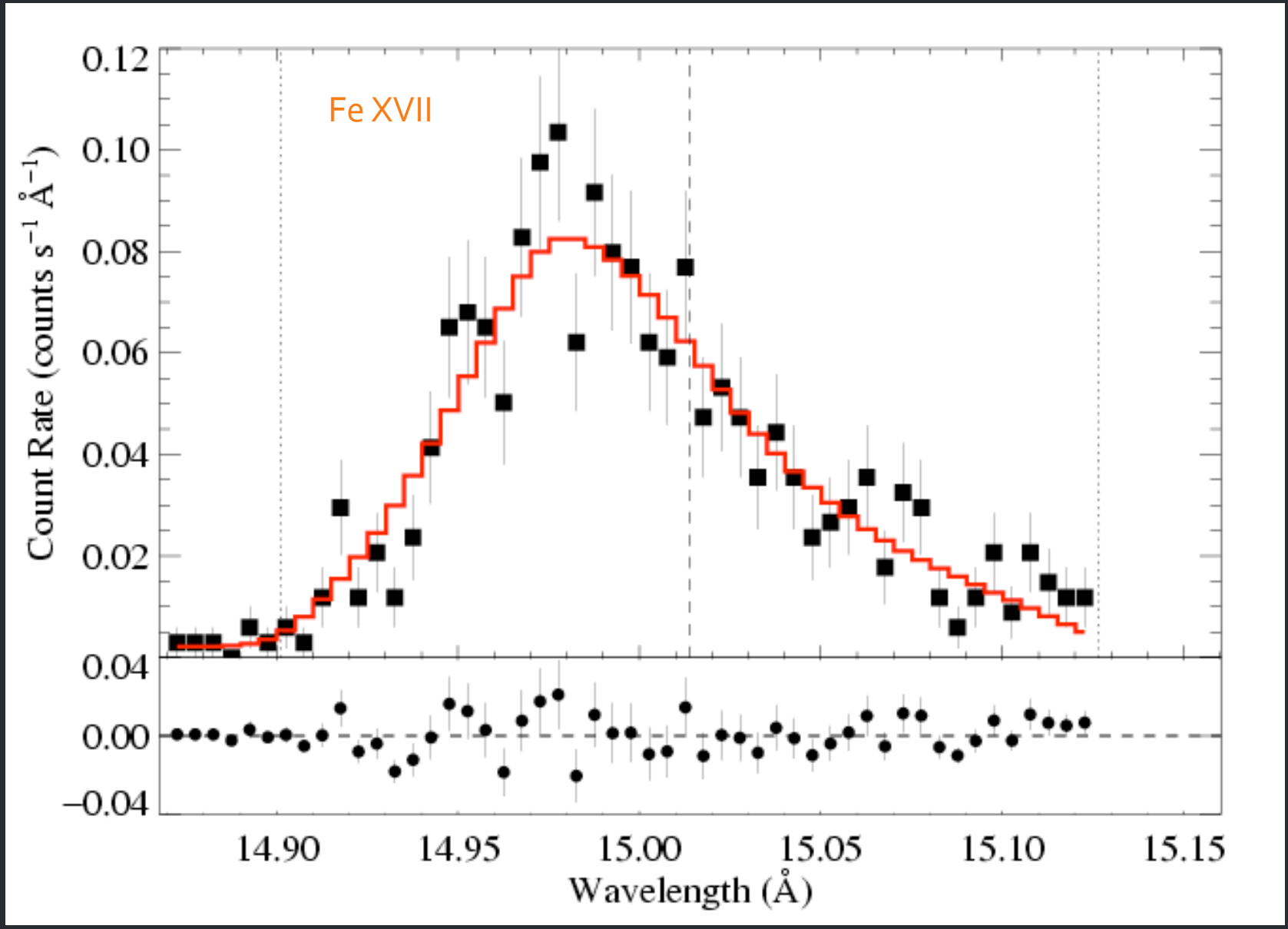

And find a best-fit τ_* and R_o...

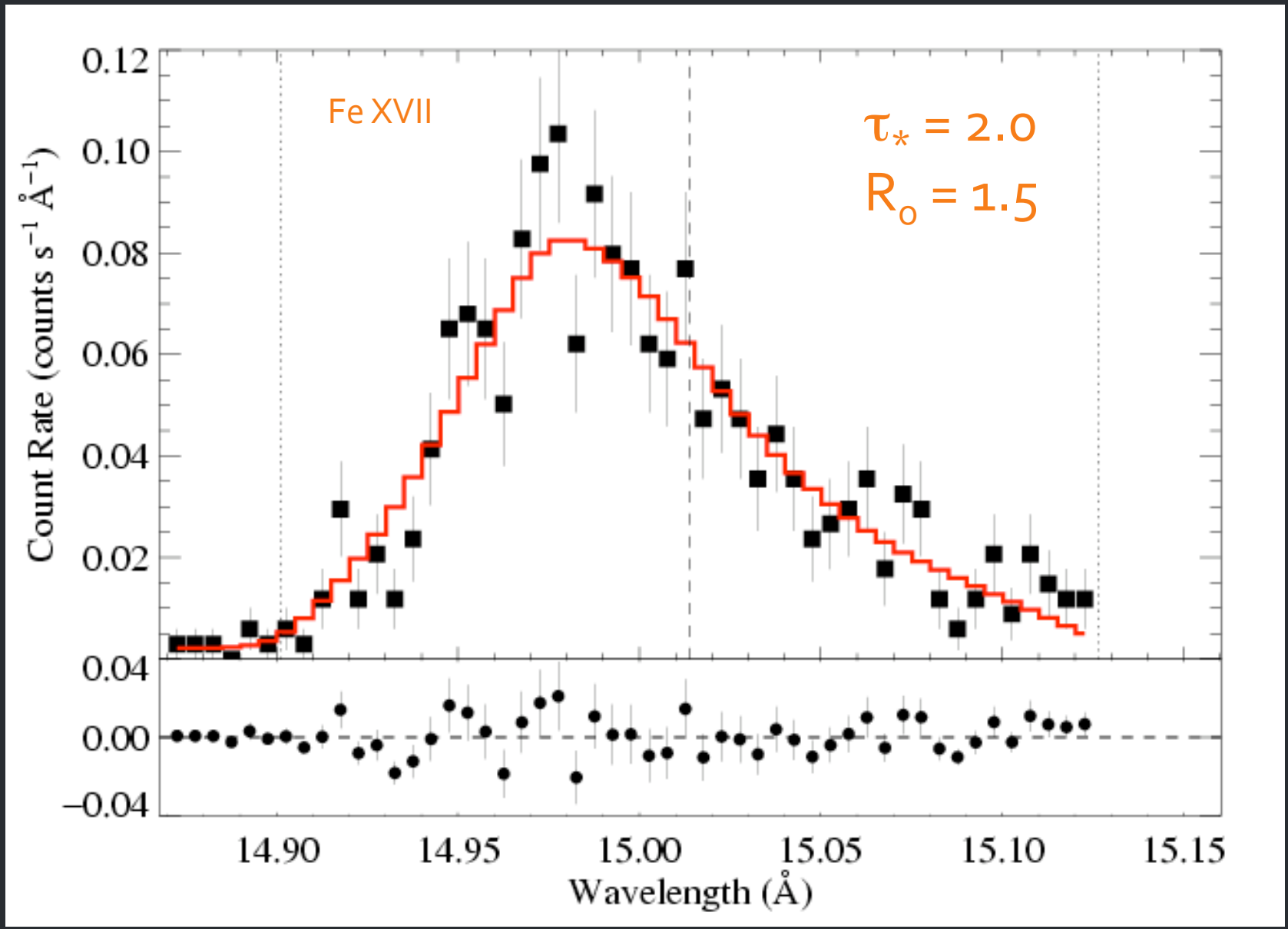

…and place confidence limits on these fitted parameter values

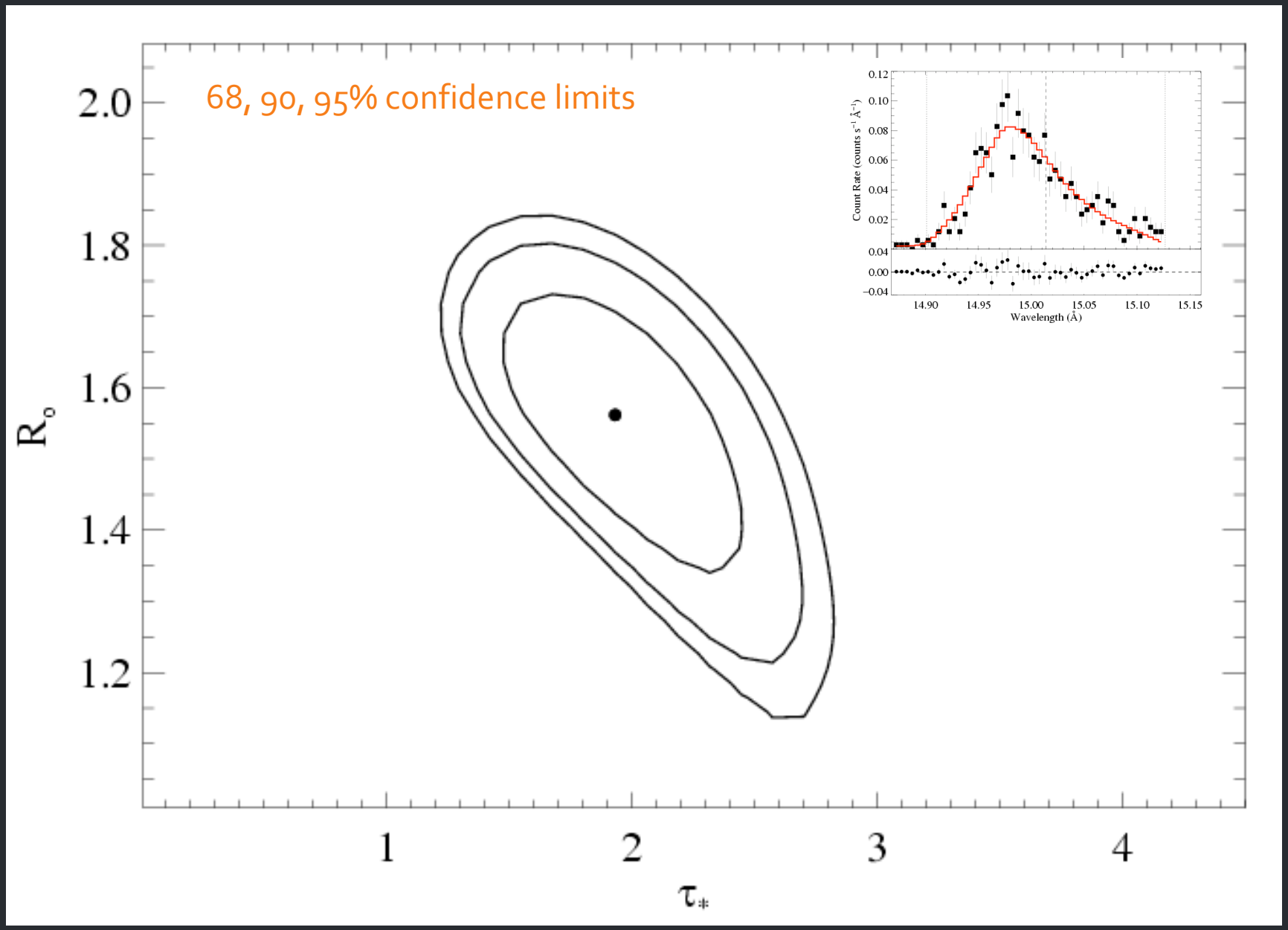

Let's focus on the R_o parameter first

Note that for $\beta = 1$, $v = 1/3\ v_{inf}$ at 1.5 R_* and $1/2\ v_{inf}$ at 2 R_*

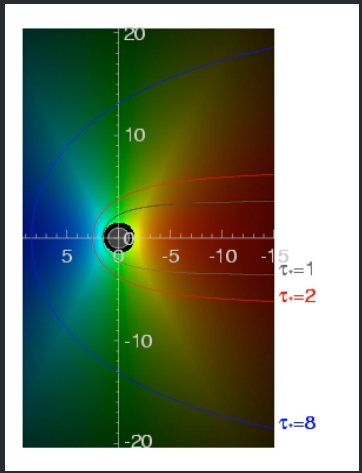

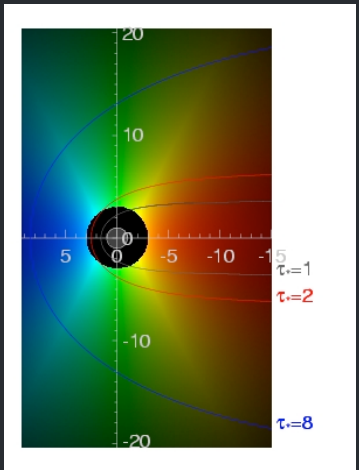

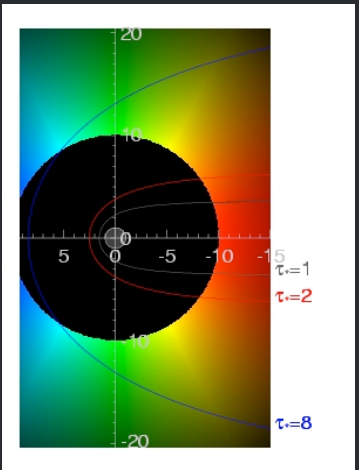

Distribution of R_o values in the Chandra spectrum of ζ Pup

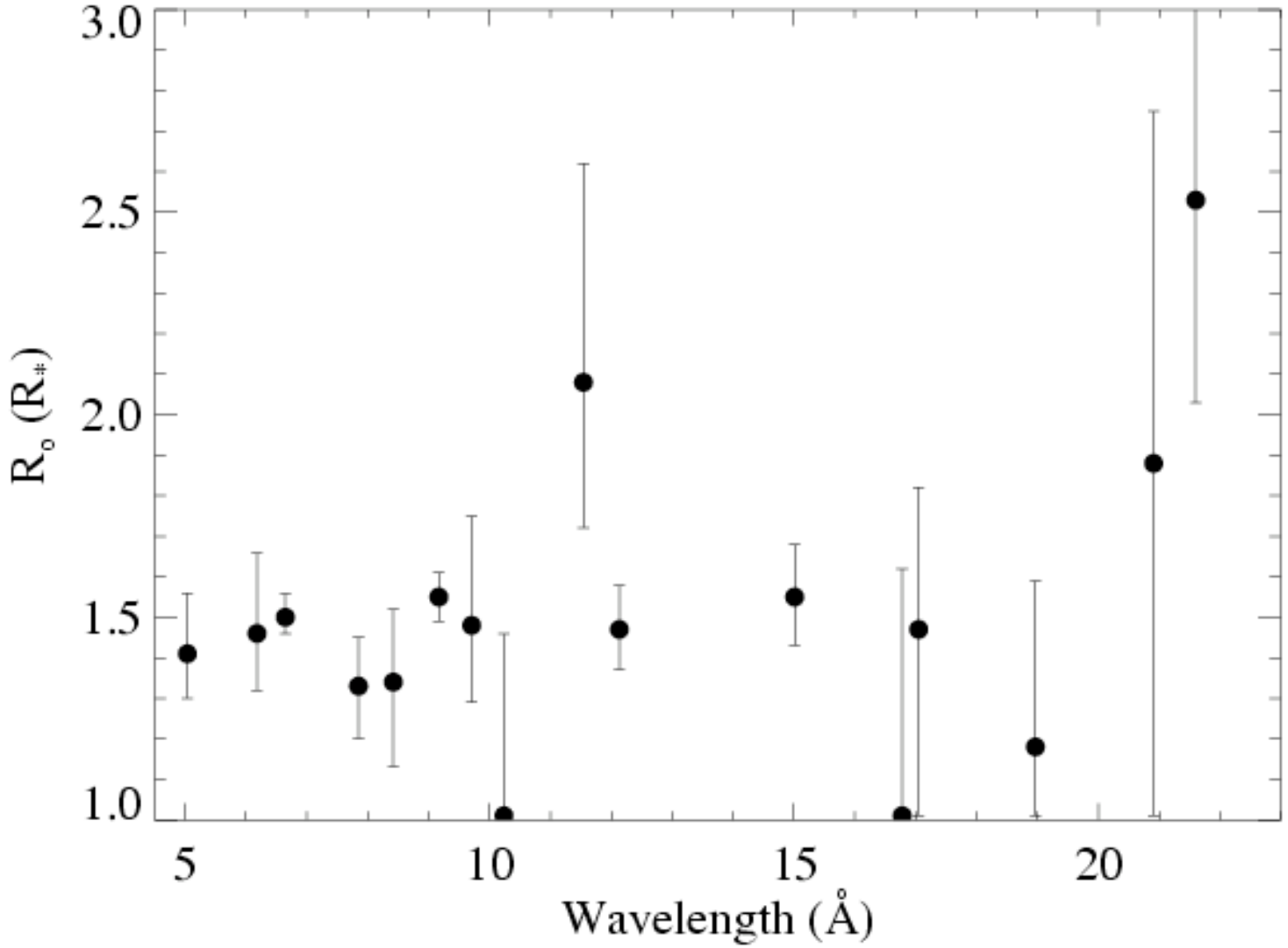

V_{inf} can be constrained by the line fitting too

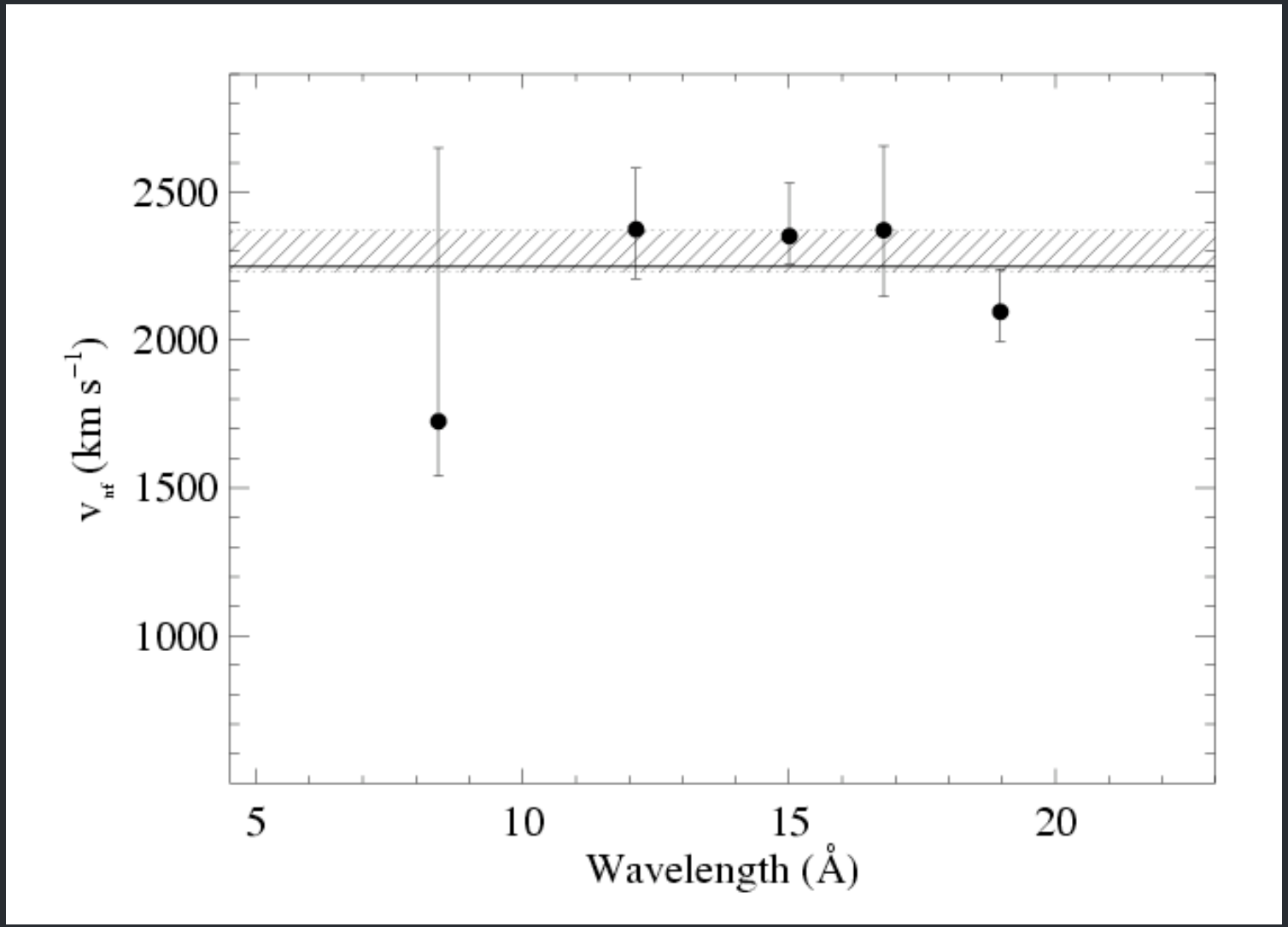

Wind Absorption

Next, we see how absorption in the bulk, cool, partially ionized wind component affects the observed X-rays

opacity ⟶

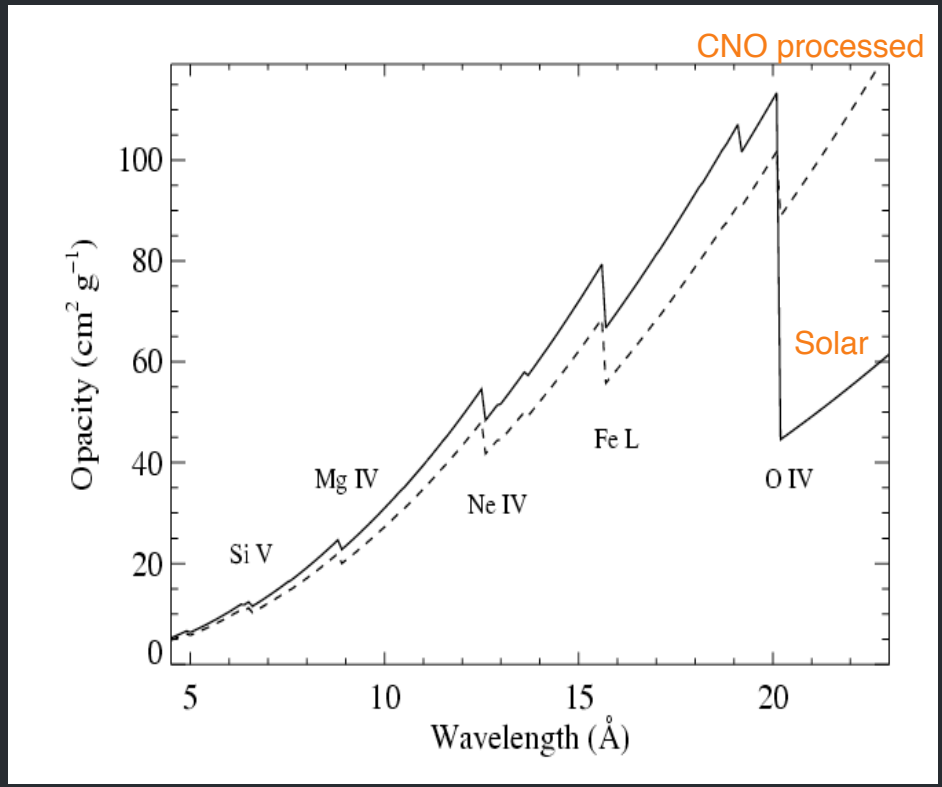

Morphology

ζ Pup (O4 If)

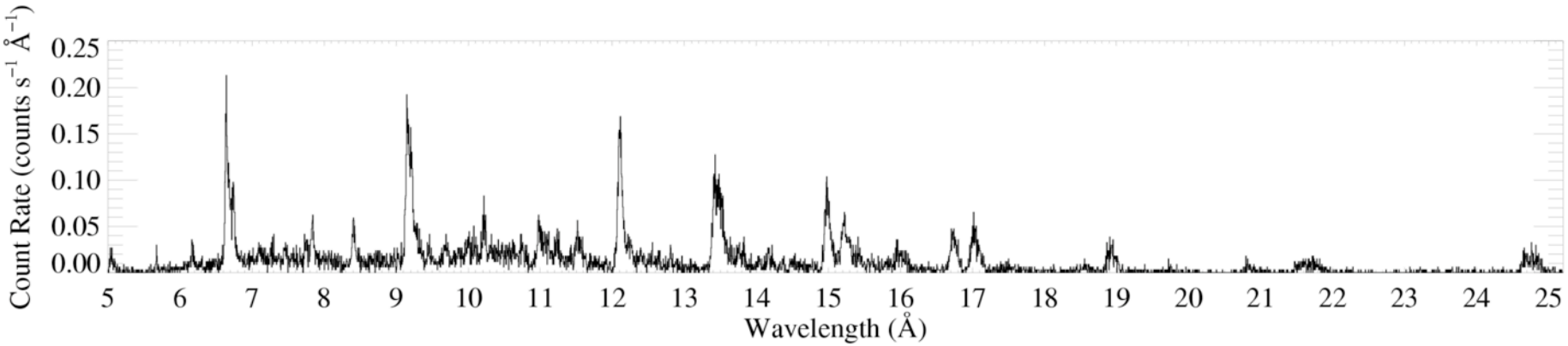

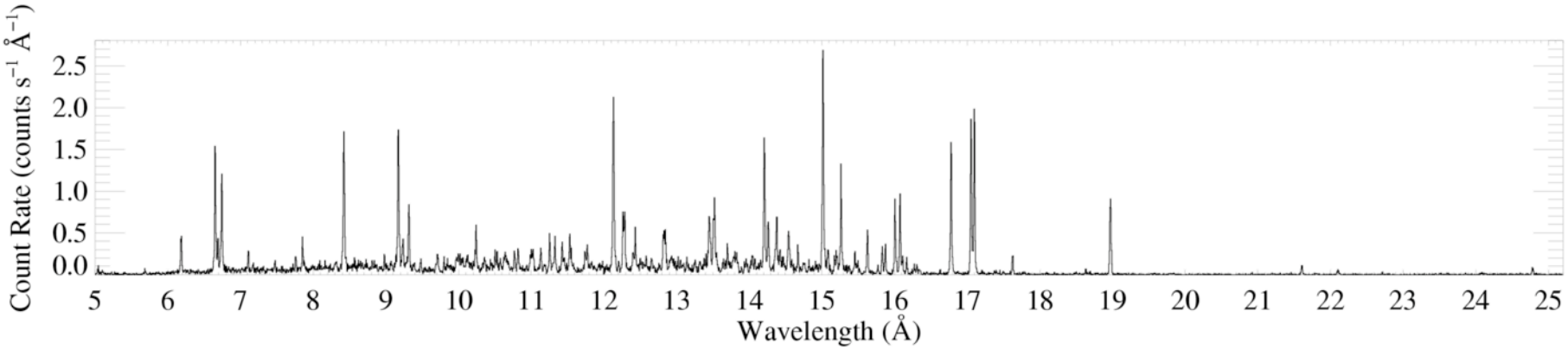

Capella (G5 III) – coronal source
– for comparison

Morphology – line widths

ζ Pup (O4 If)

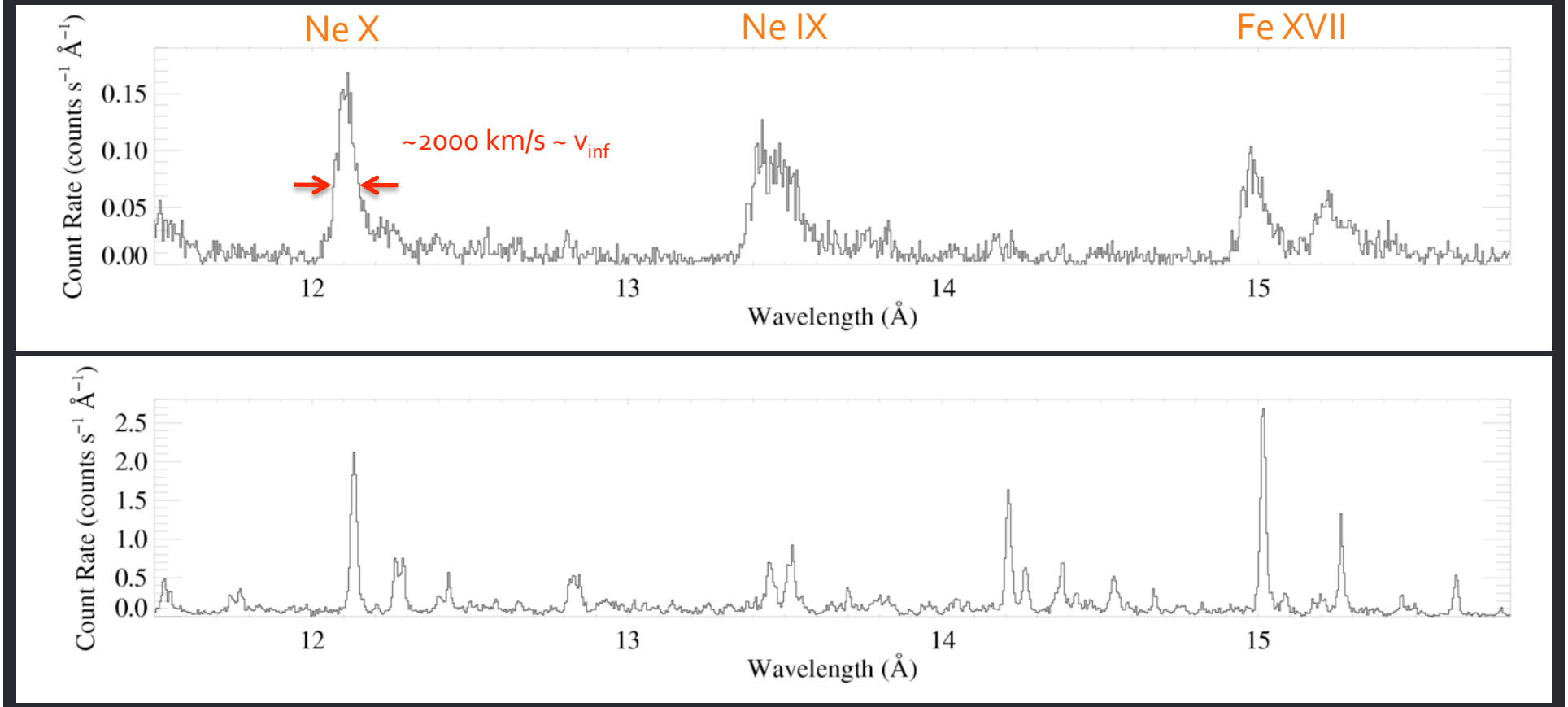

Capella (G5 III) – coronal source
– for comparison

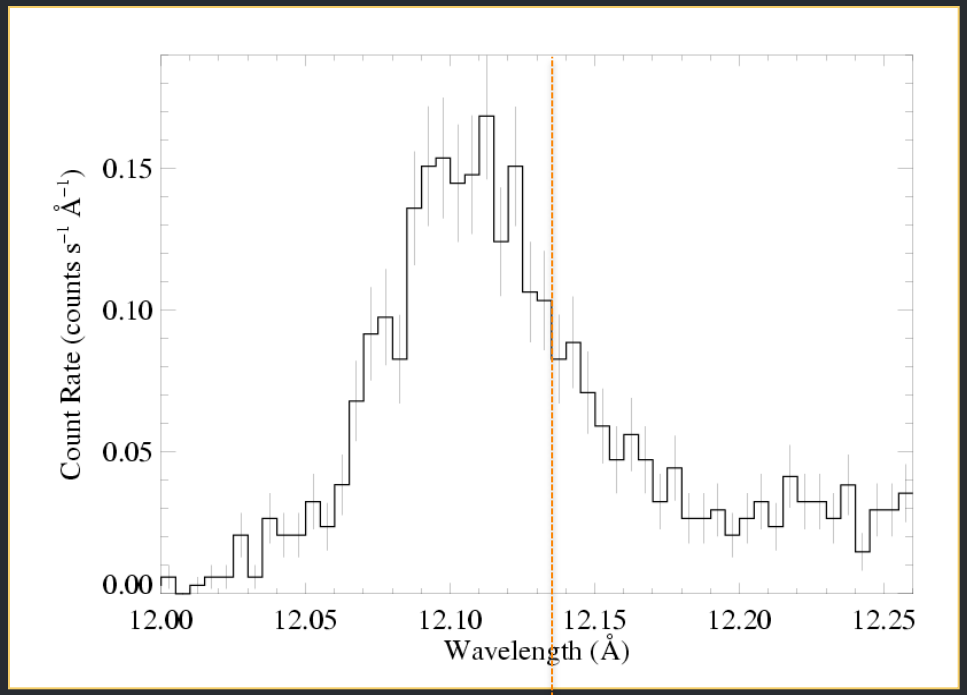

ζ Pup (O4 If)

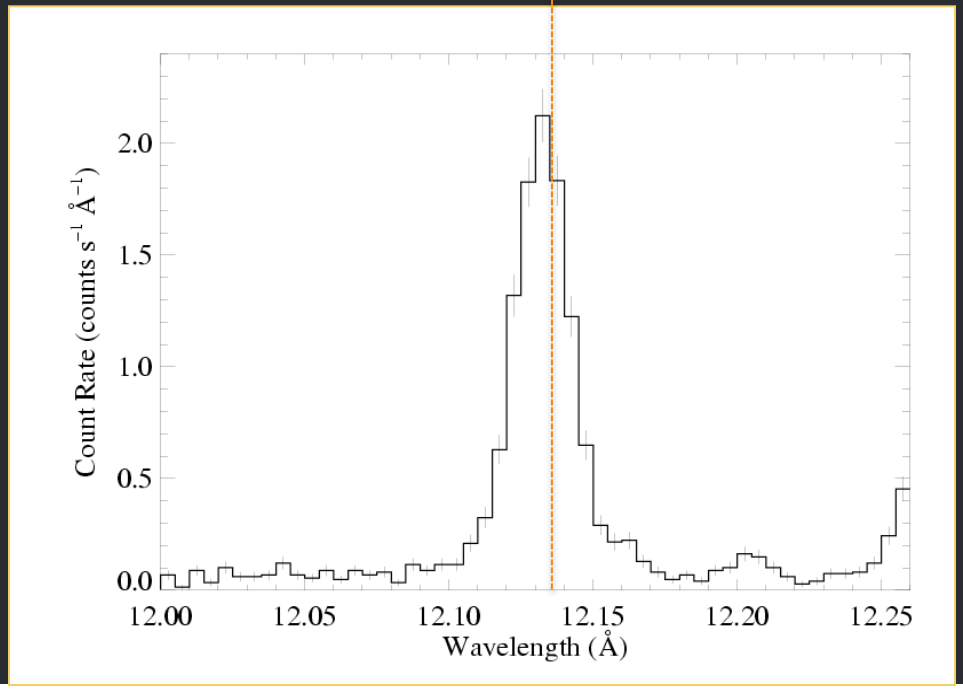

Capella (G5 III) – *unresolved*

opacity of the cold wind

wind mass-loss rate

$$\dot{M} = 4\pi r^2 v \rho$$

τ_* is the key parameter describing the absorption

$$\tau_* \equiv \frac{\kappa \dot{M}}{4\pi R_* v_\infty}$$

radius of the star

wind terminal velocity

$\tau_* = 2$ in this wind

observer on left

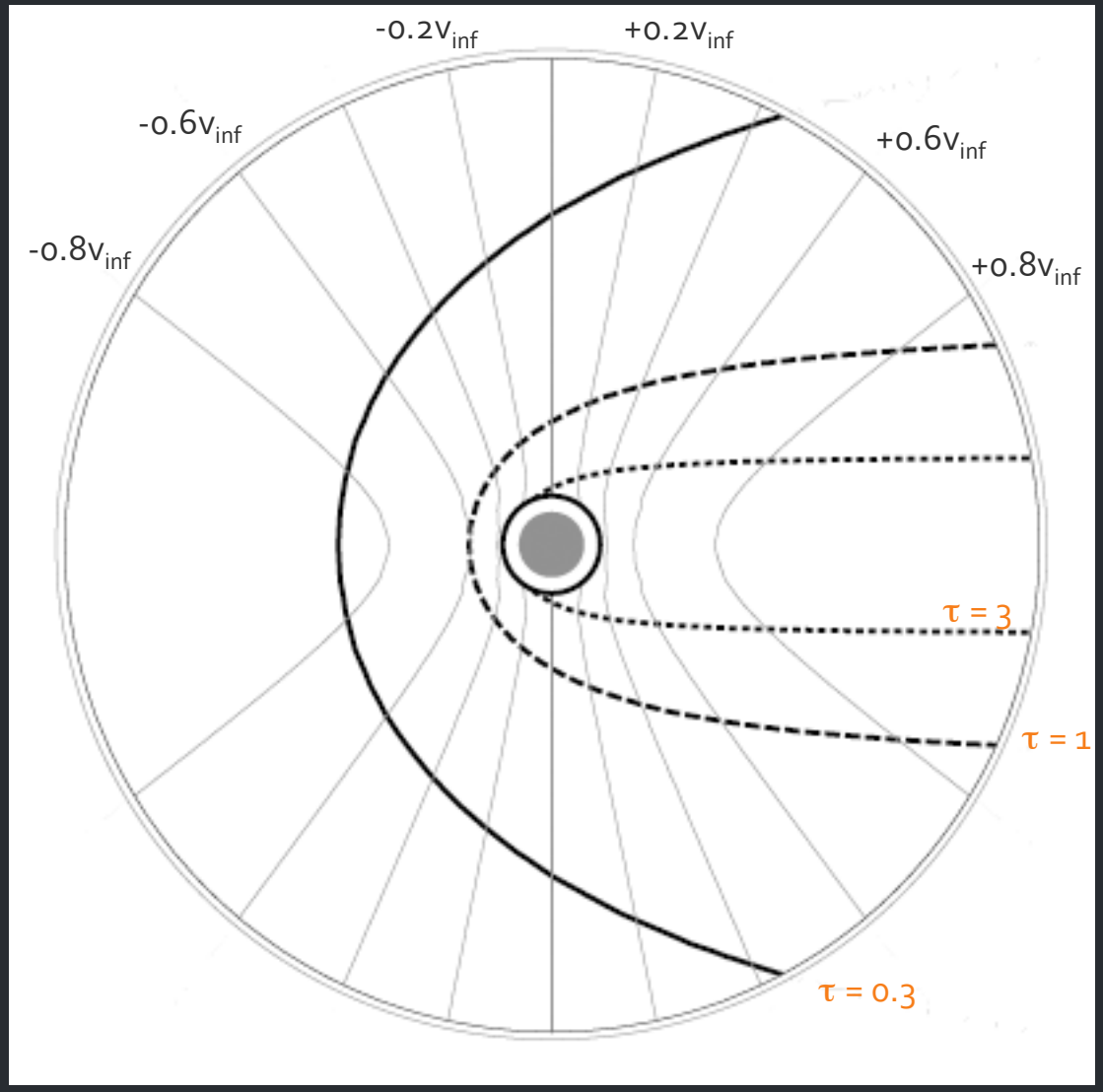

optical depth contours

Wind opacity

X-ray bandpass

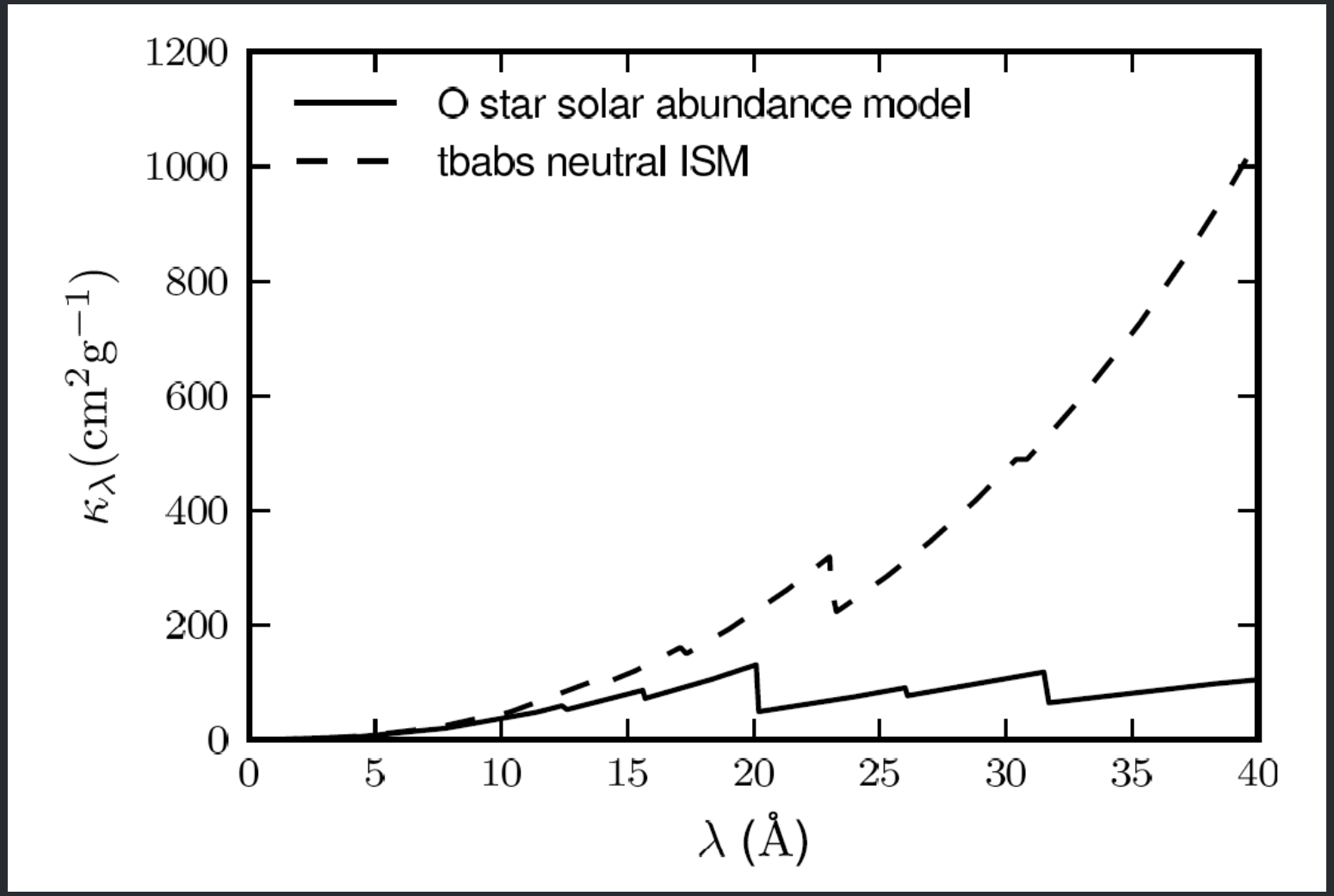

Wind opacity

X-ray bandpass

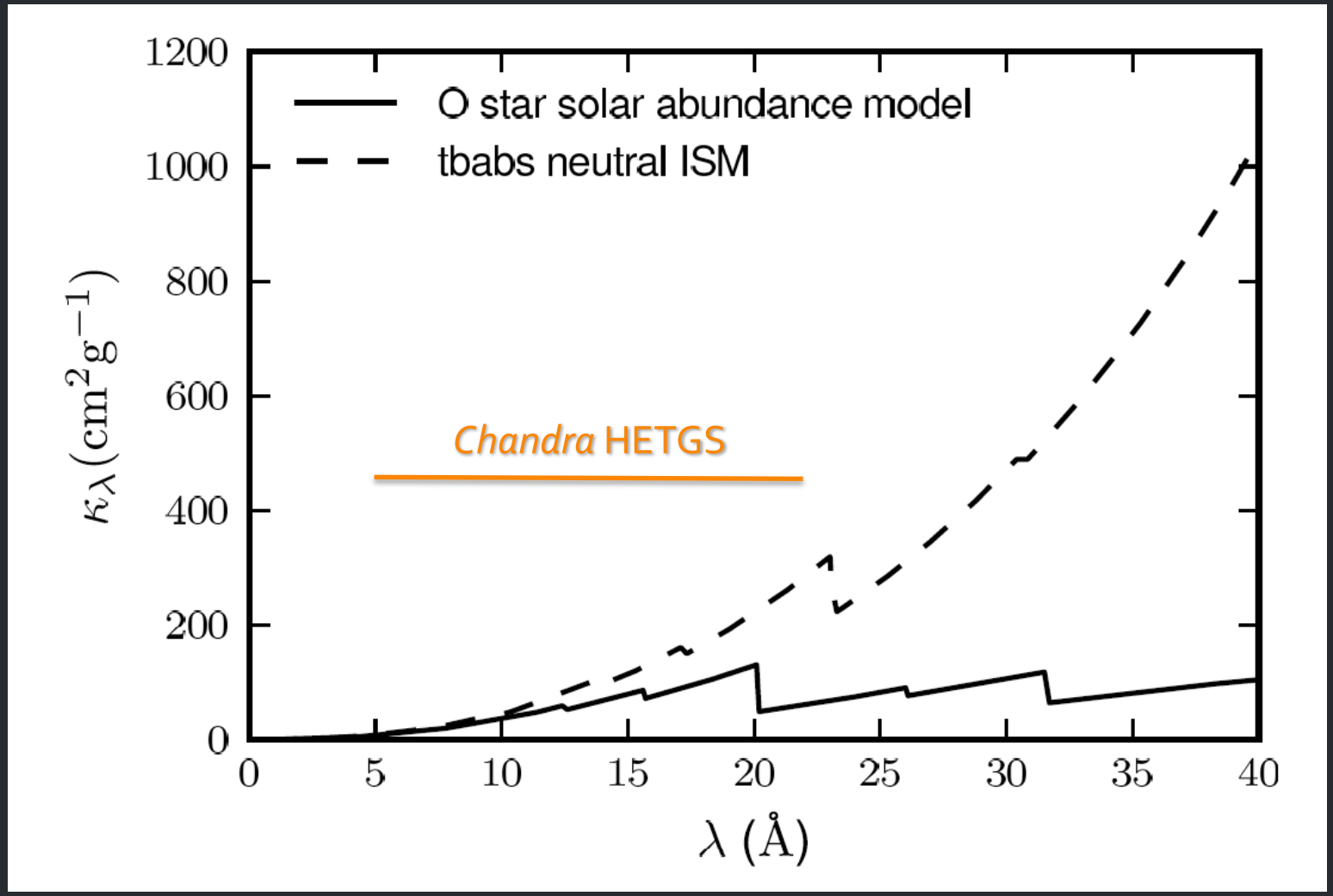

X-ray opacity

Zoom in

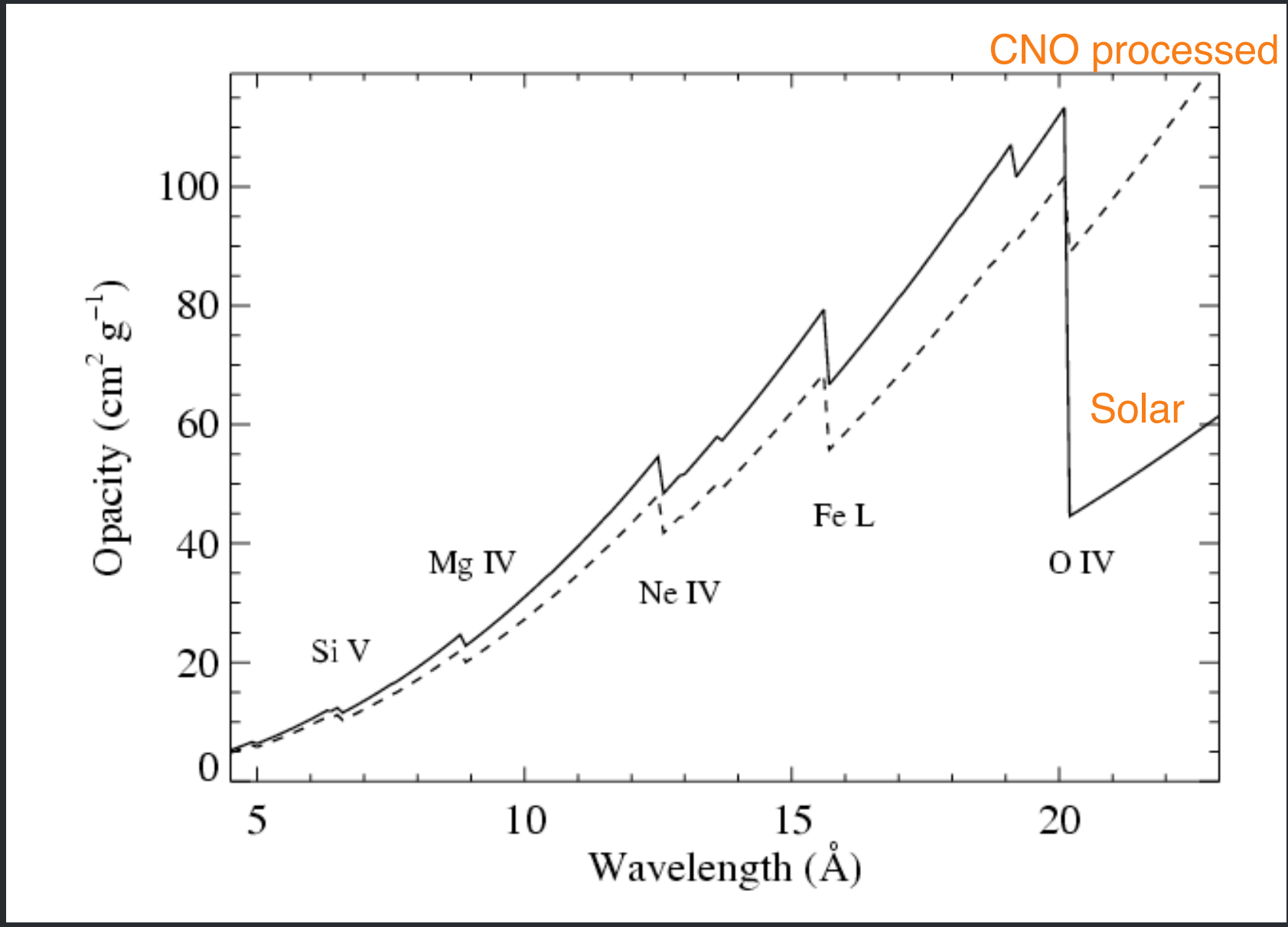

We fit these x-ray line profile models to each line in the *Chandra* data

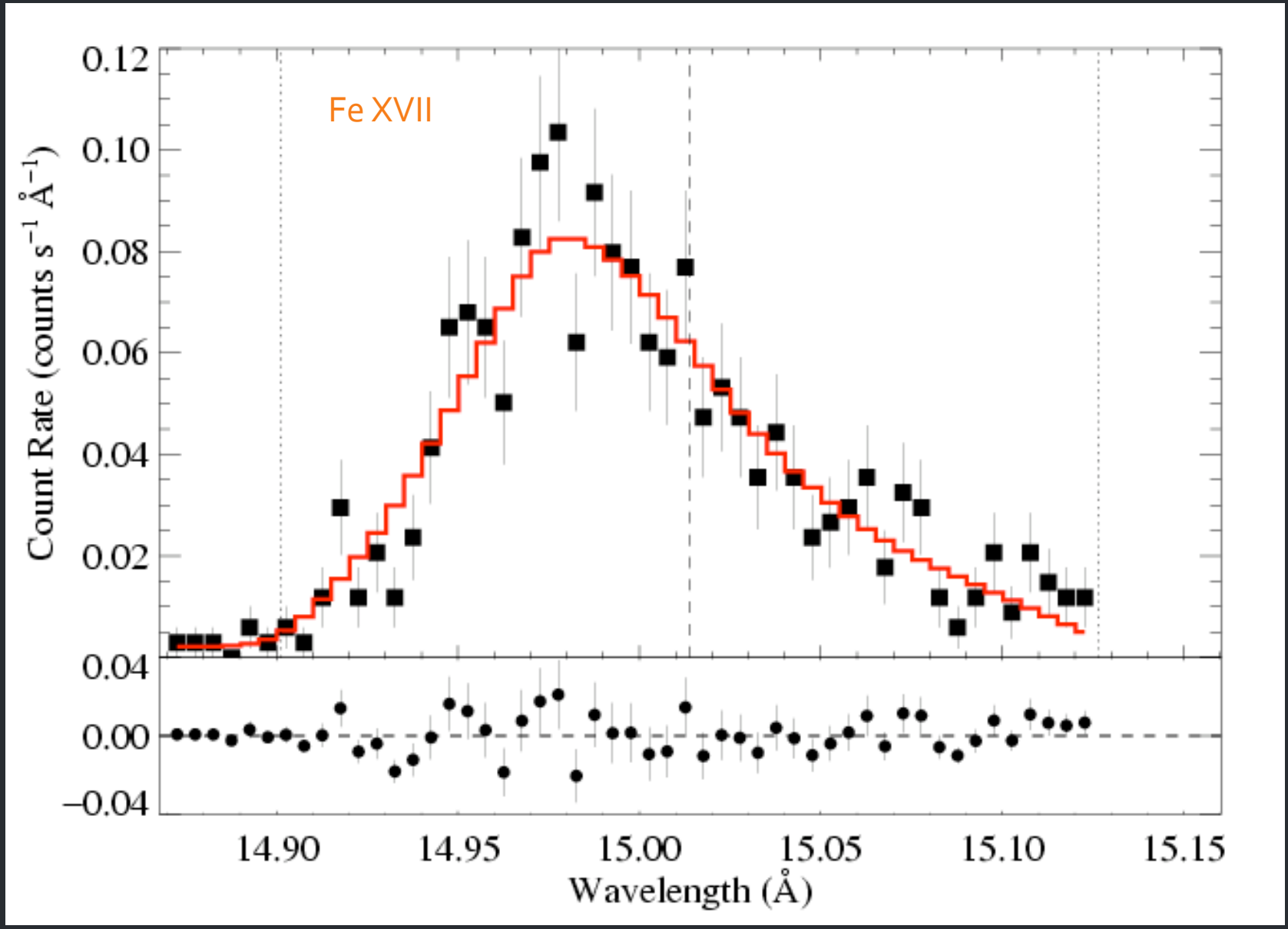

And find a best-fit τ_* and R_o...

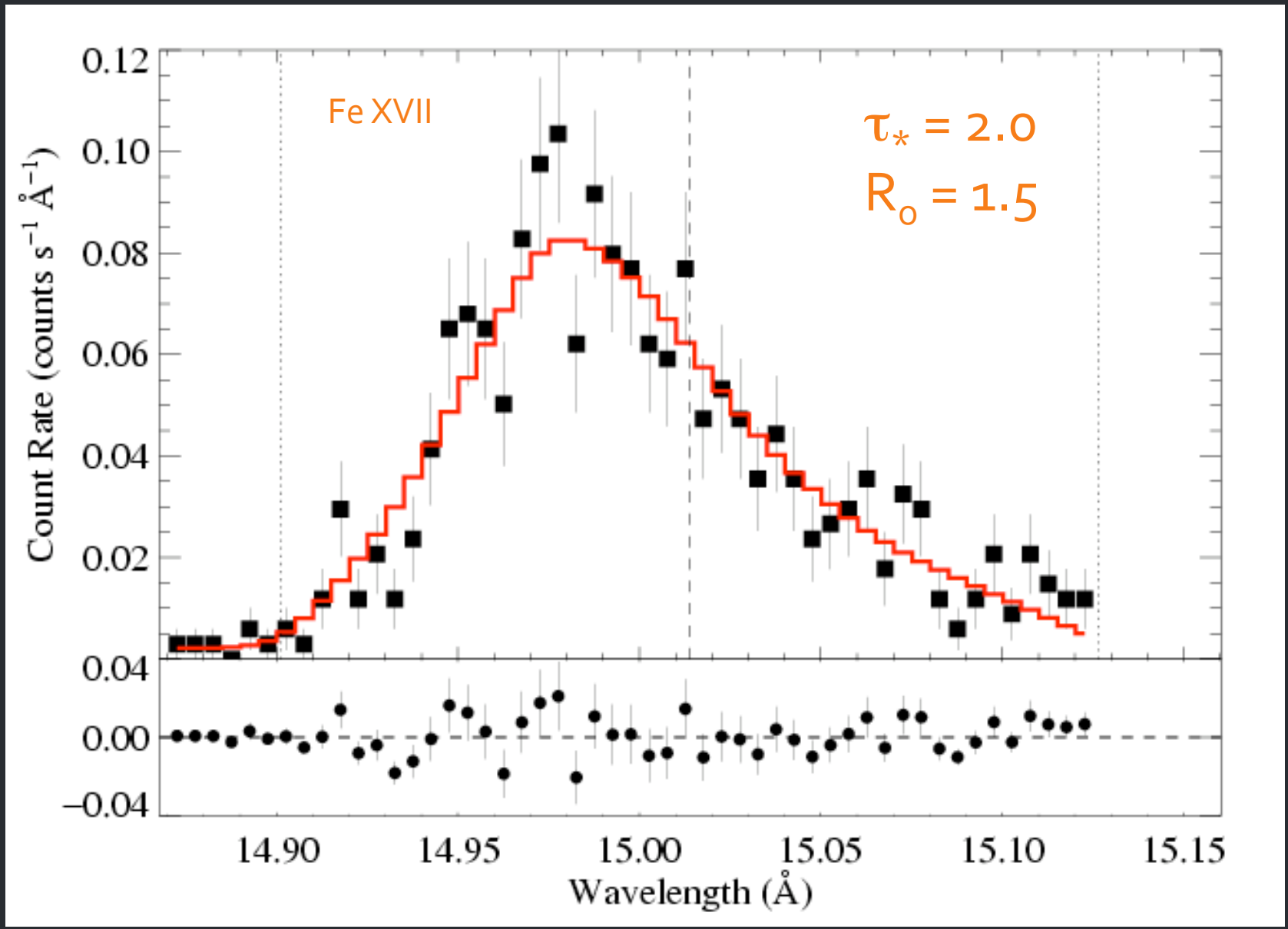

…and place confidence limits on these fitted parameter values

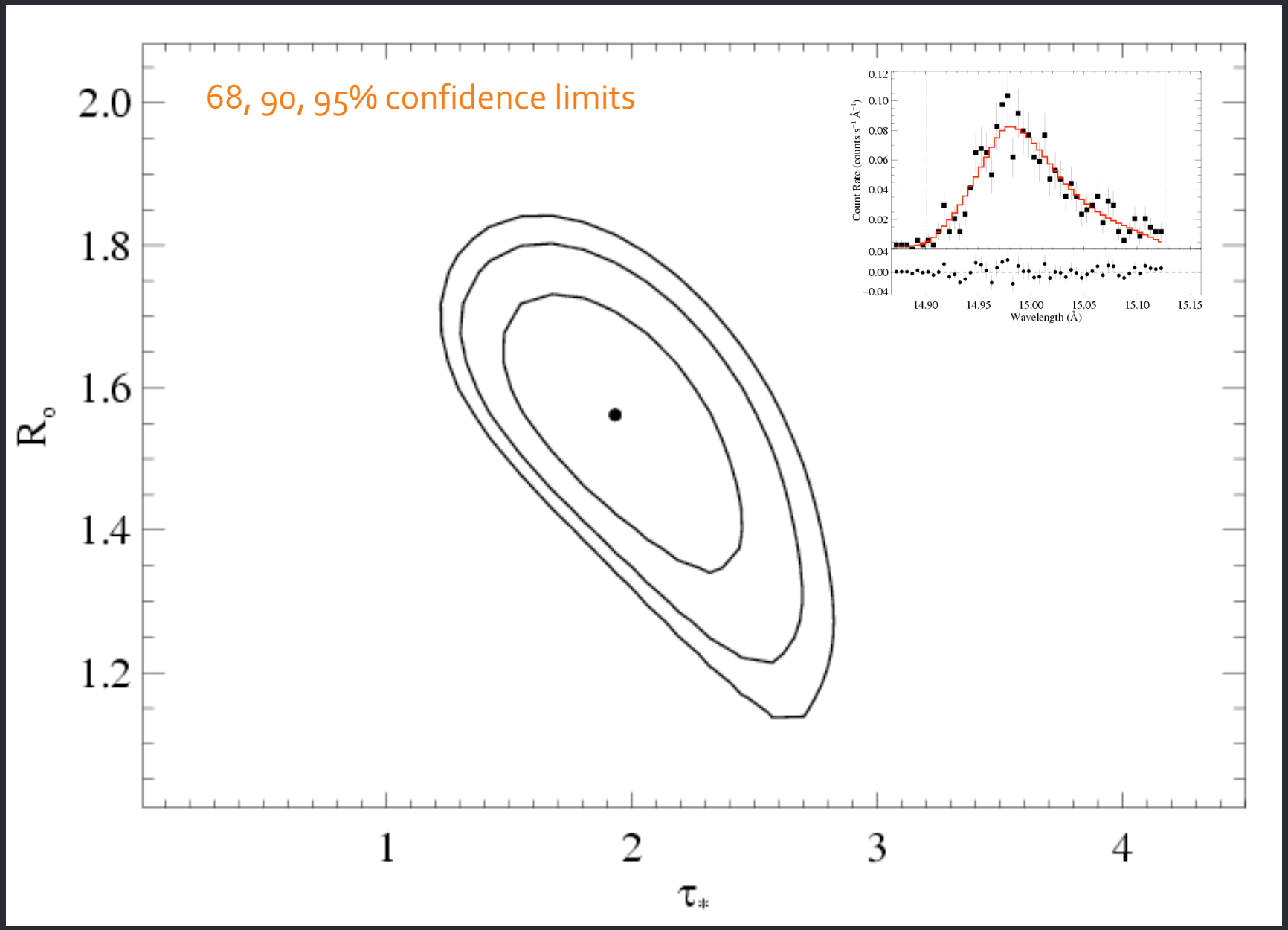

ζ Pup: three emission lines

Mg Lyα: 8.42 Å

Ne Lyα: 12.13 Å

O Lyα: 18.97 Å

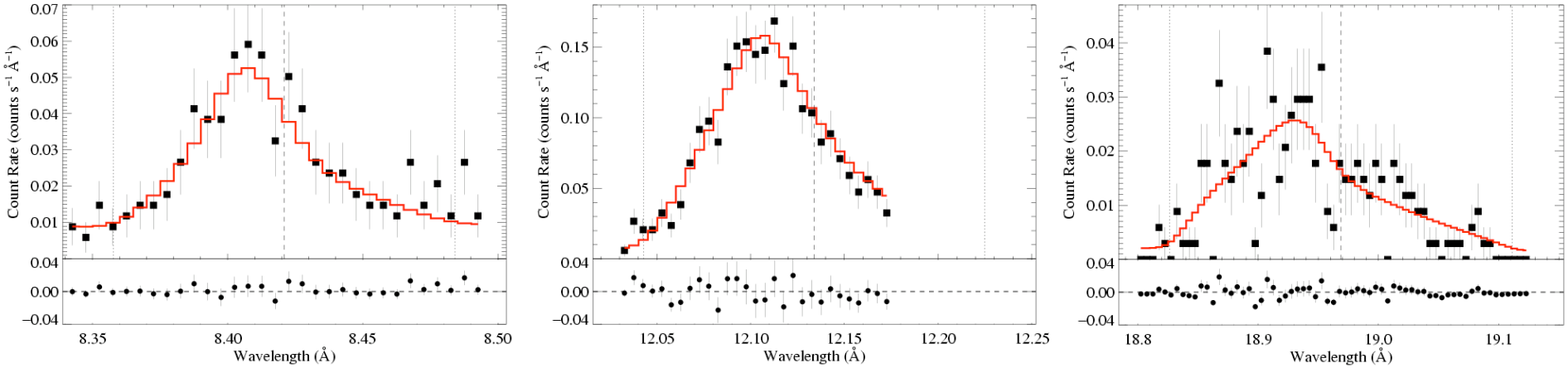

$\tau_* = 1$

$\tau_* = 2$

$\tau_* = 3$

Recall:

$$\tau_* \equiv \frac{\kappa \dot{M}}{4\pi R_* v_\infty}$$

atomic opacity of the wind

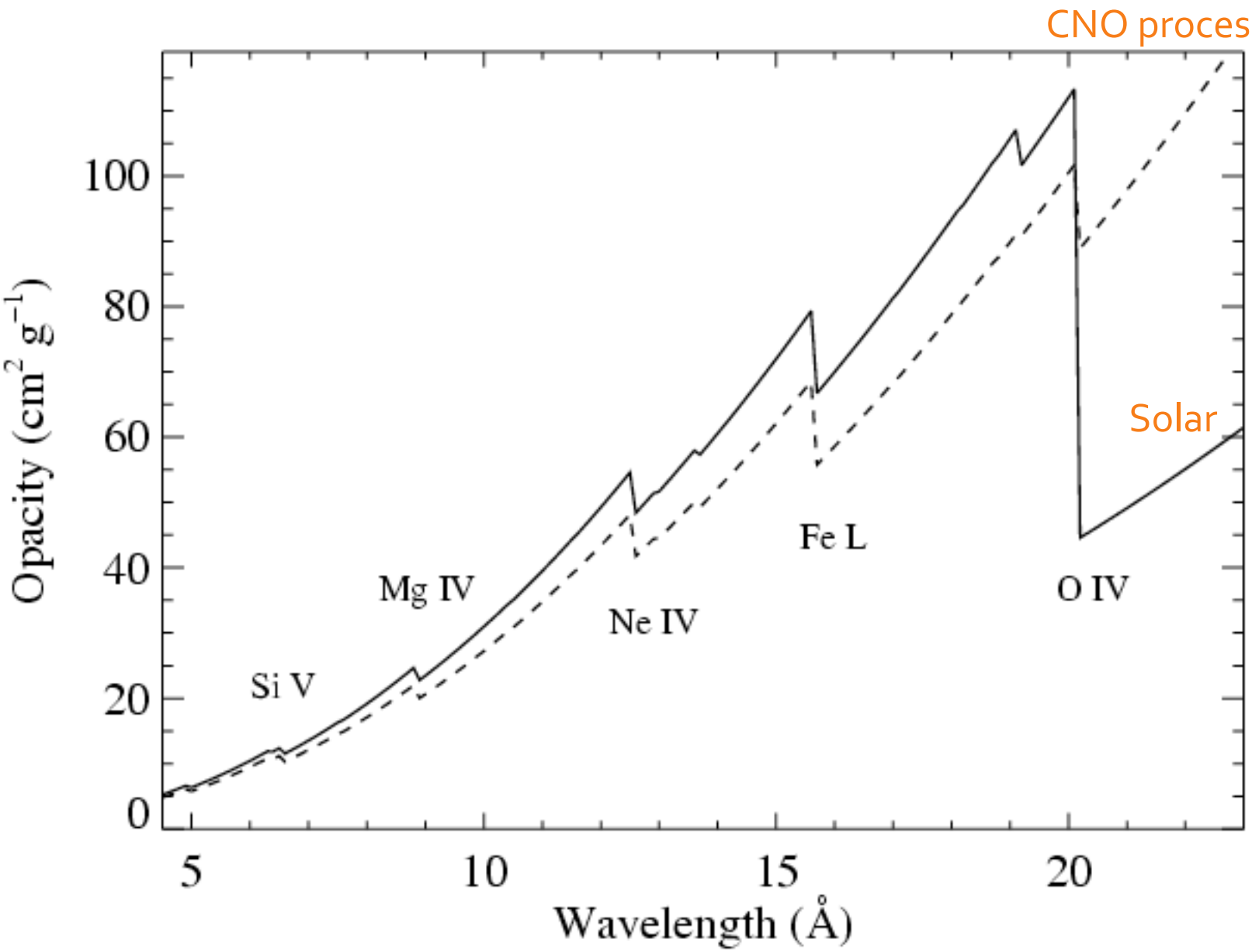

Results from the 3 line fits shown previously

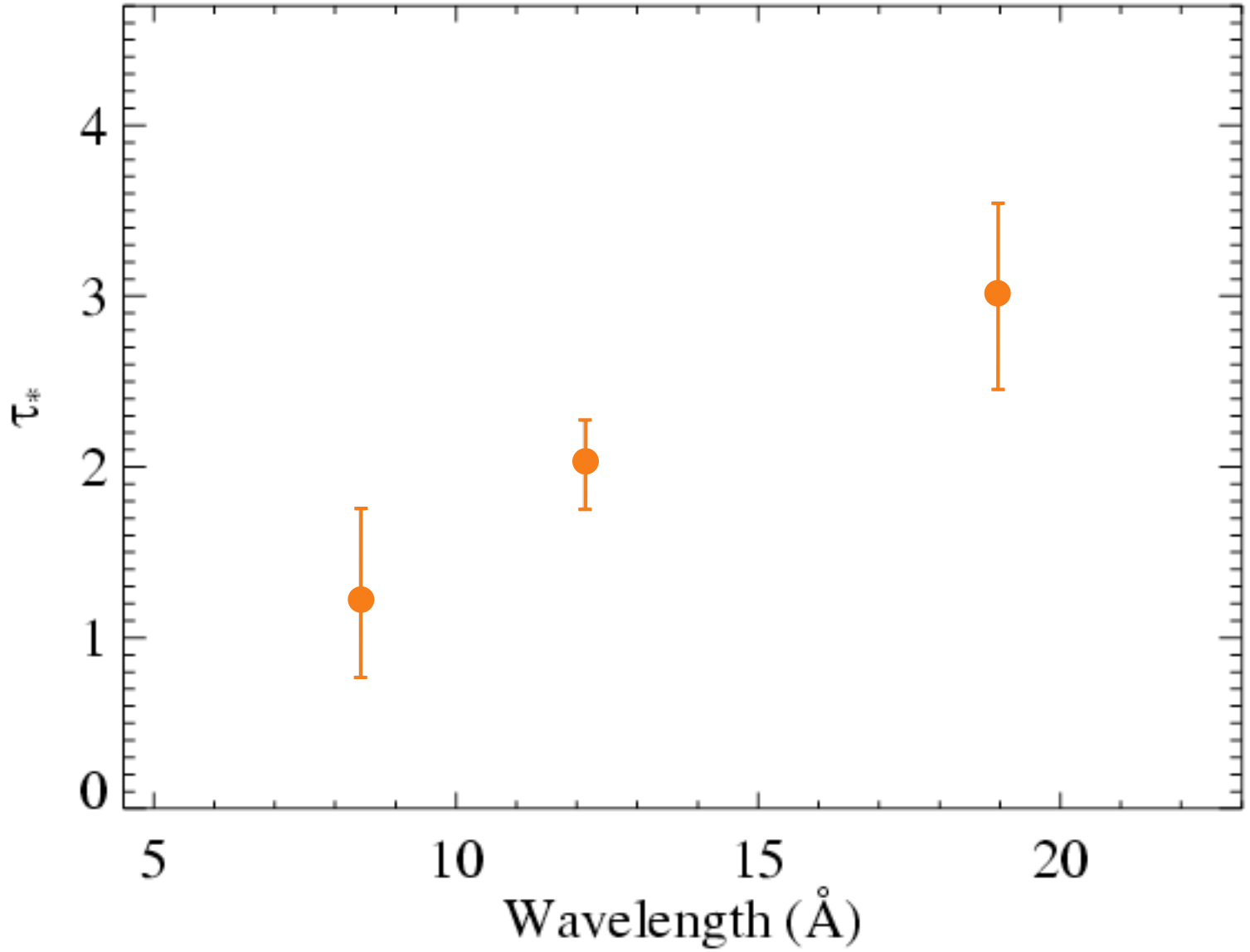

Fits to 16 lines in the *Chandra* spectrum of ζ Pup

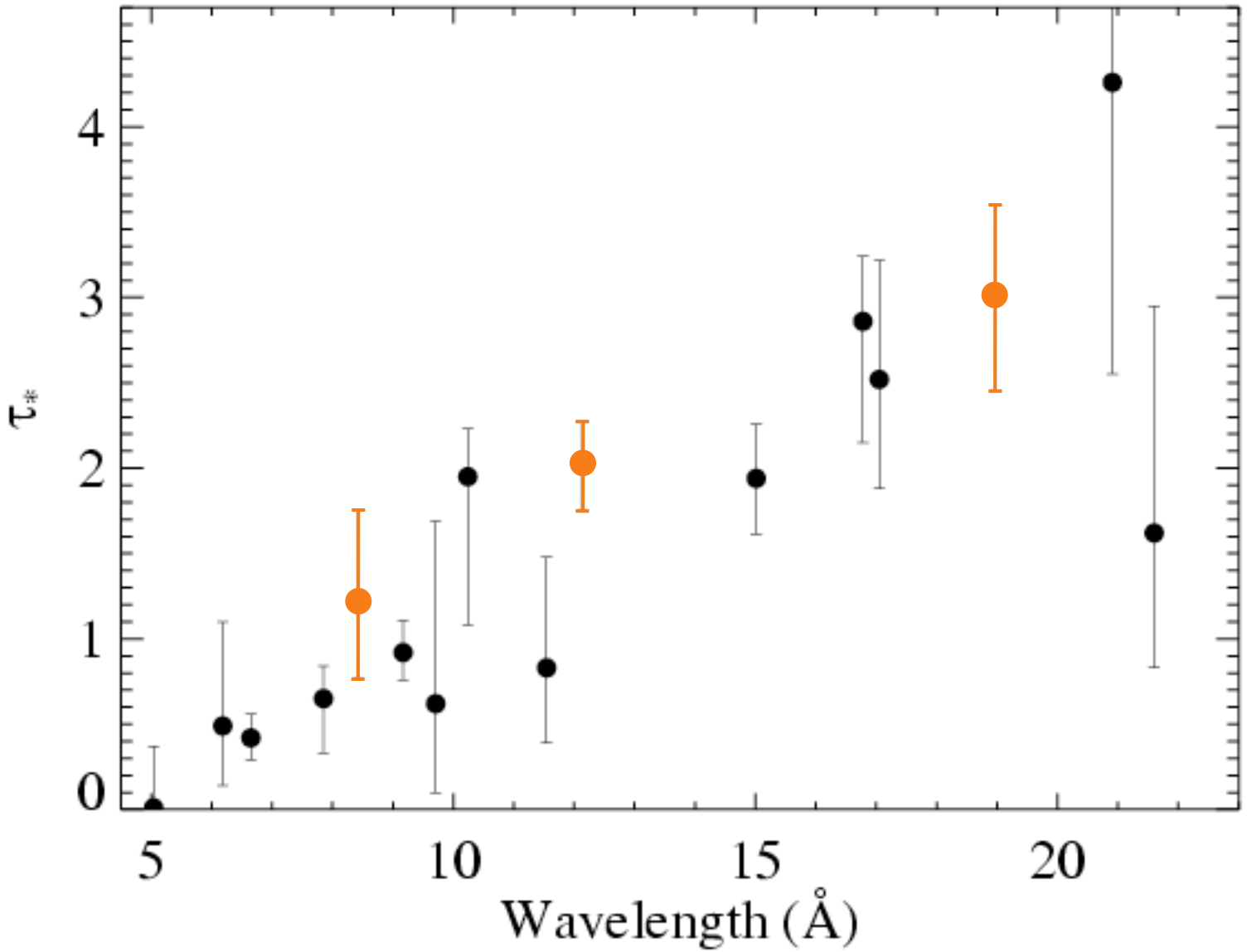

Fits to 16 lines in the *Chandra* spectrum of ζ Pup

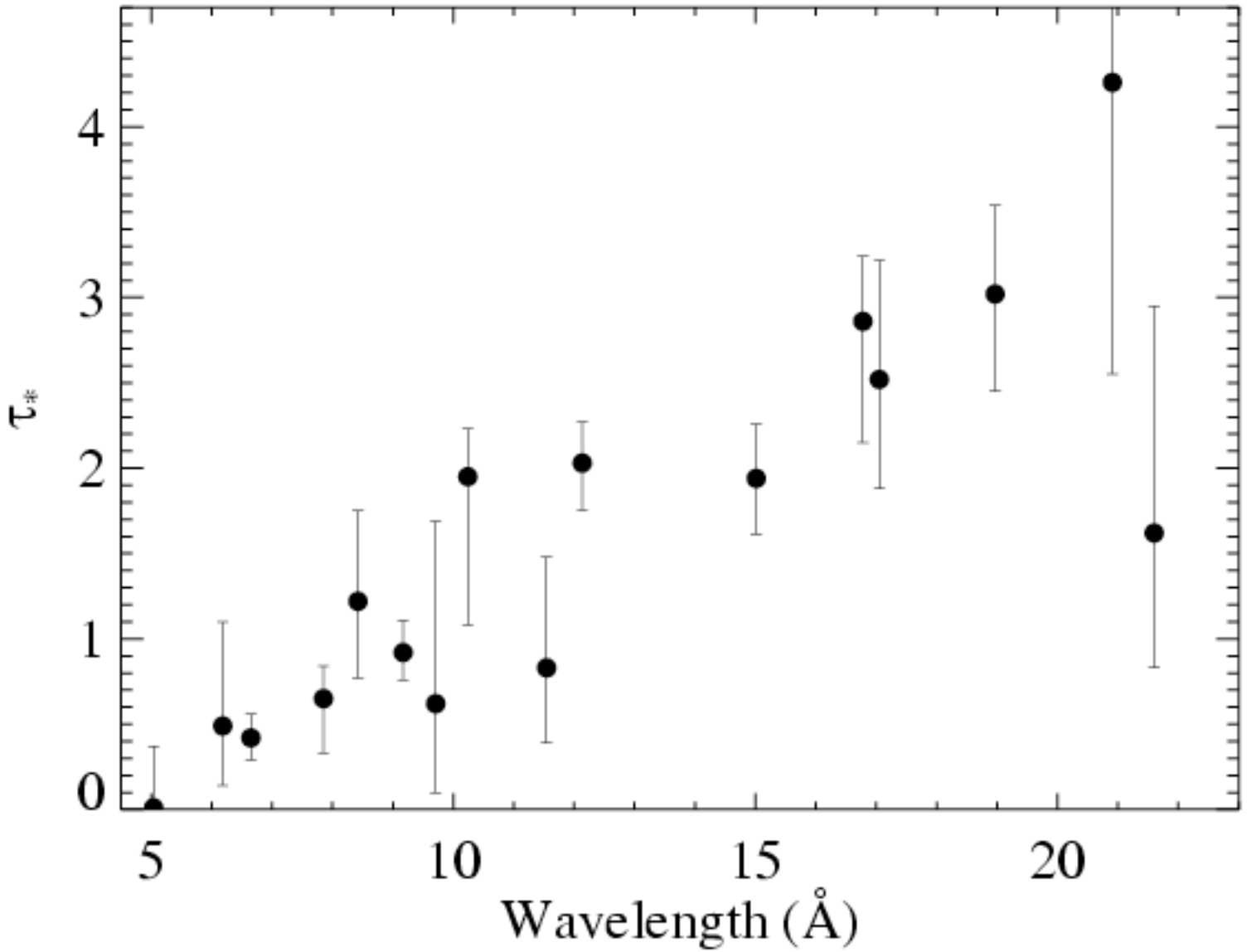

Fits to 16 lines in the *Chandra* spectrum of ζ Pup

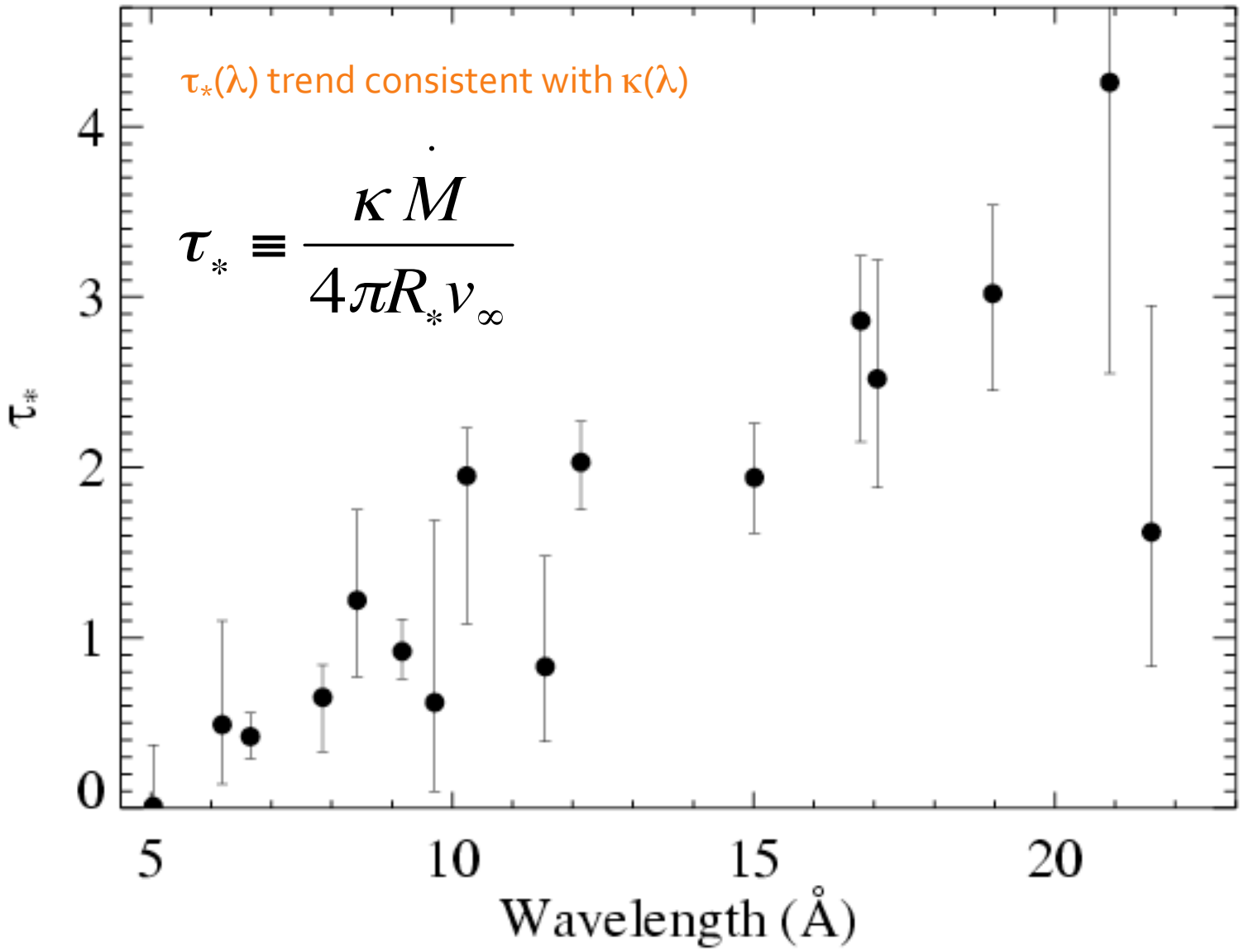

Fits to 16 lines in the *Chandra* spectrum of ζ Pup

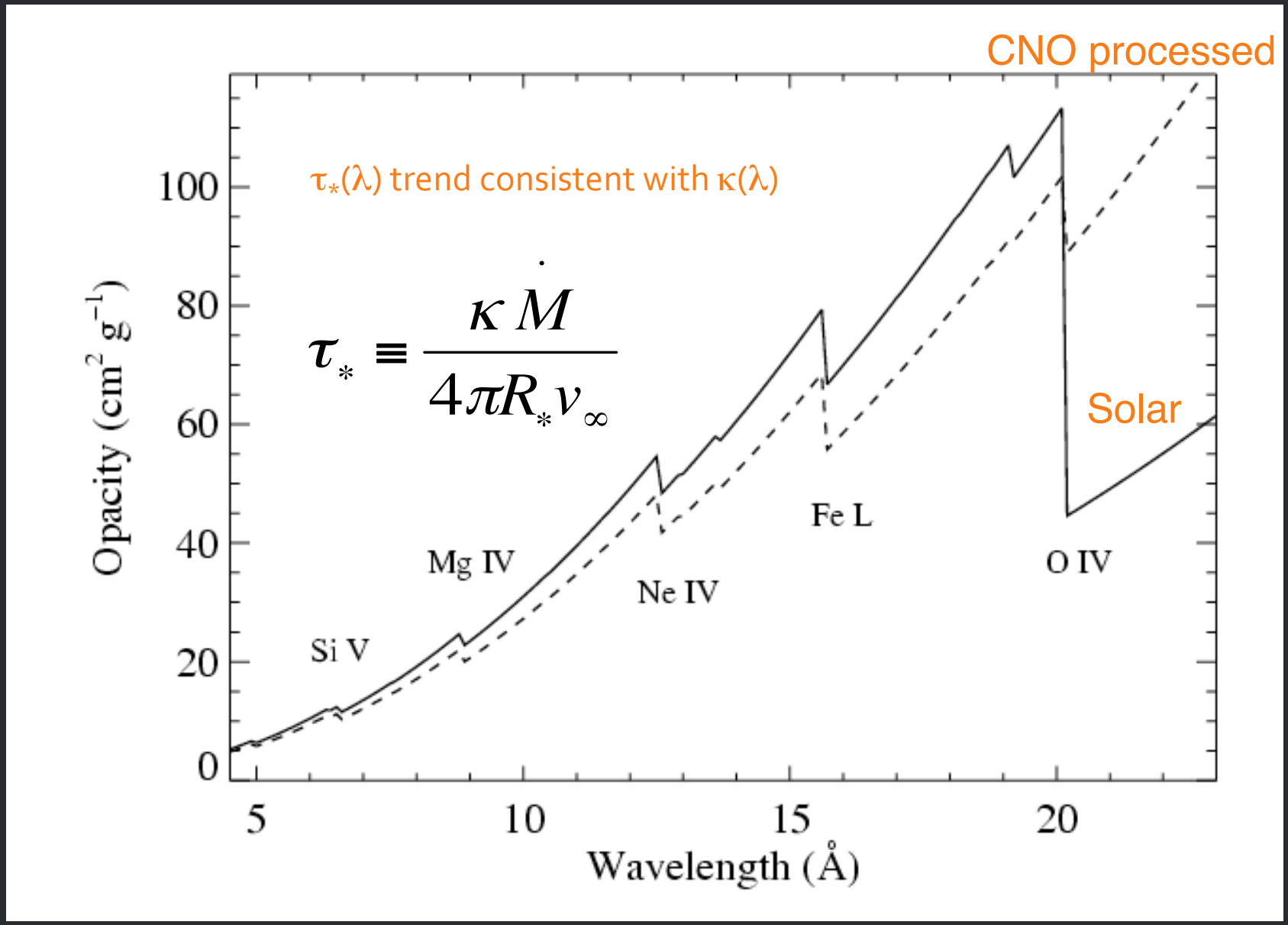

$$\tau_* \equiv \frac{\kappa \dot{M}}{4\pi R_* v_\infty}$$

- $\dot{M}$ becomes the free parameter of the fit to the $\tau_*(\lambda)$ trend

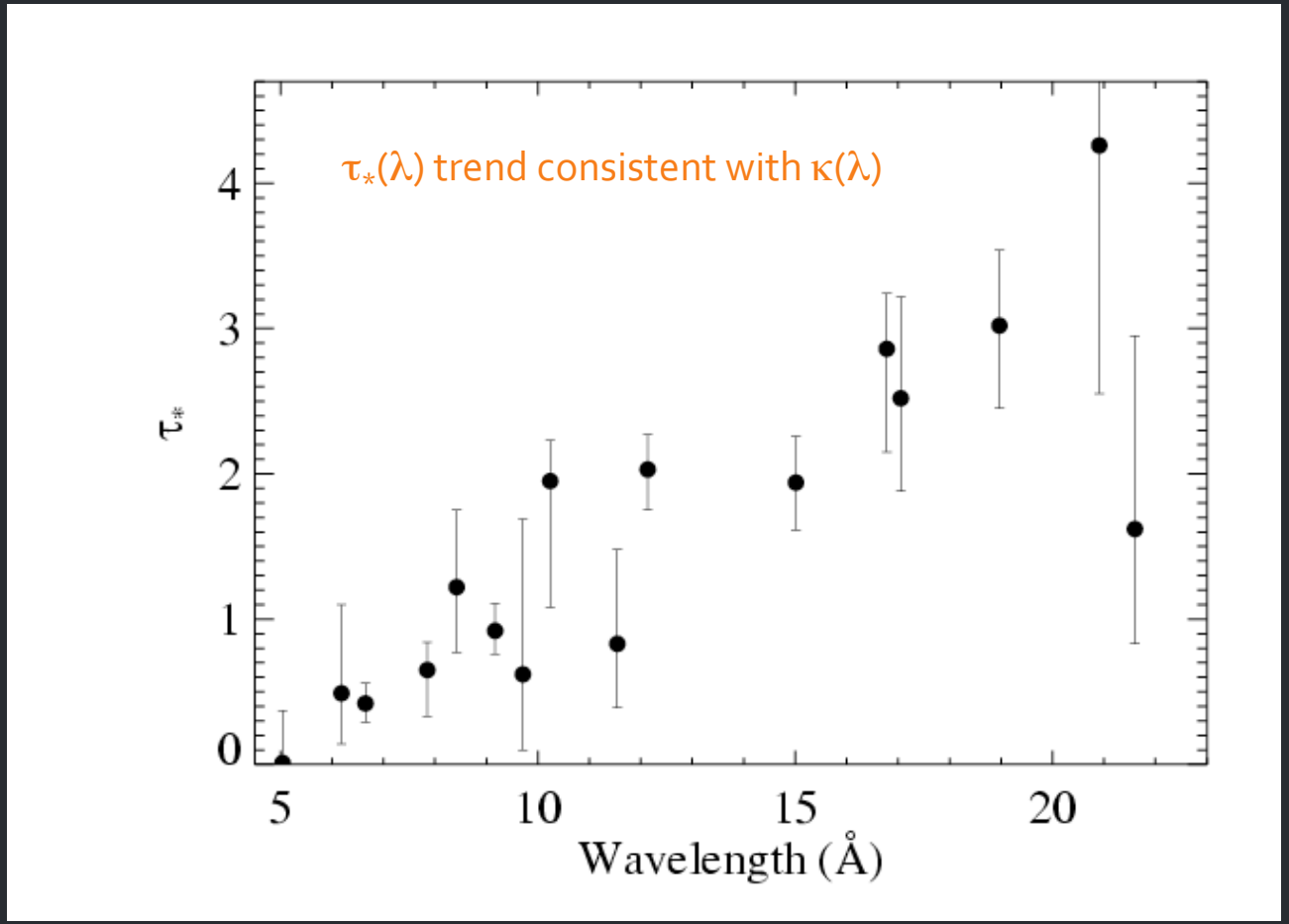

$$\tau_* \equiv \frac{\kappa \dot{M}}{4\pi R_* v_\infty}$$

- $\dot{M}$ becomes the free parameter of the fit to the $\tau_*(\lambda)$ trend

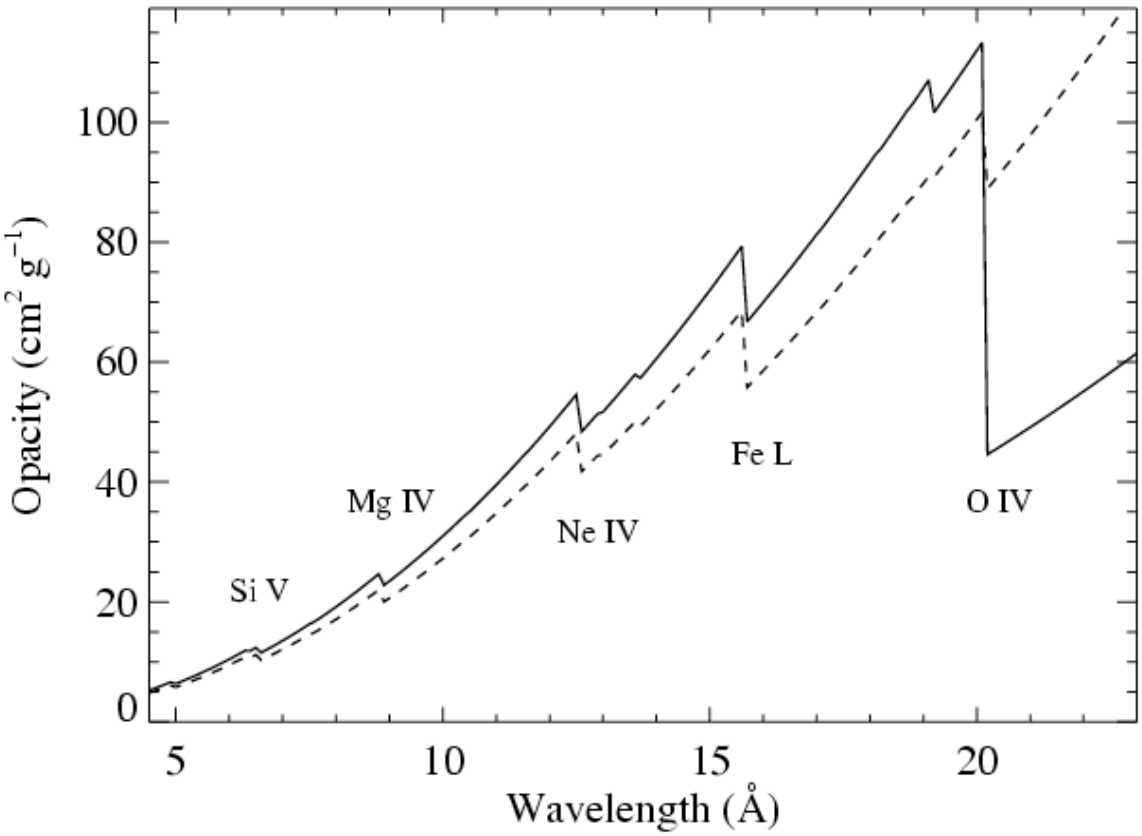

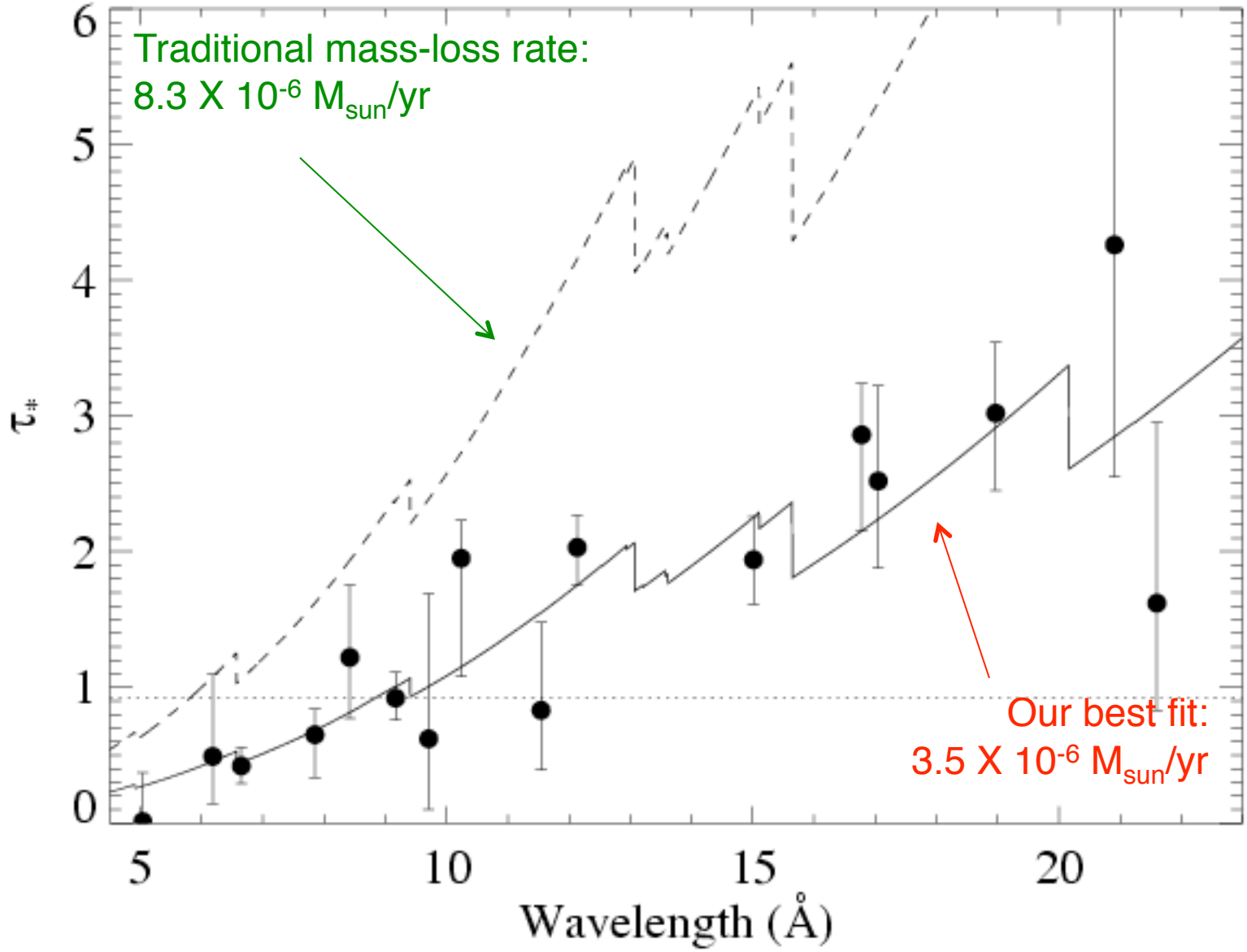
Traditional mass-loss rate:
8.3 X 10-6 Msun/yr
Our best fit:
3.5 X 10-6 Msun/yr
τ#
Wavelength (Å)
0
1
2
3
4
5
6
5
10
15
20

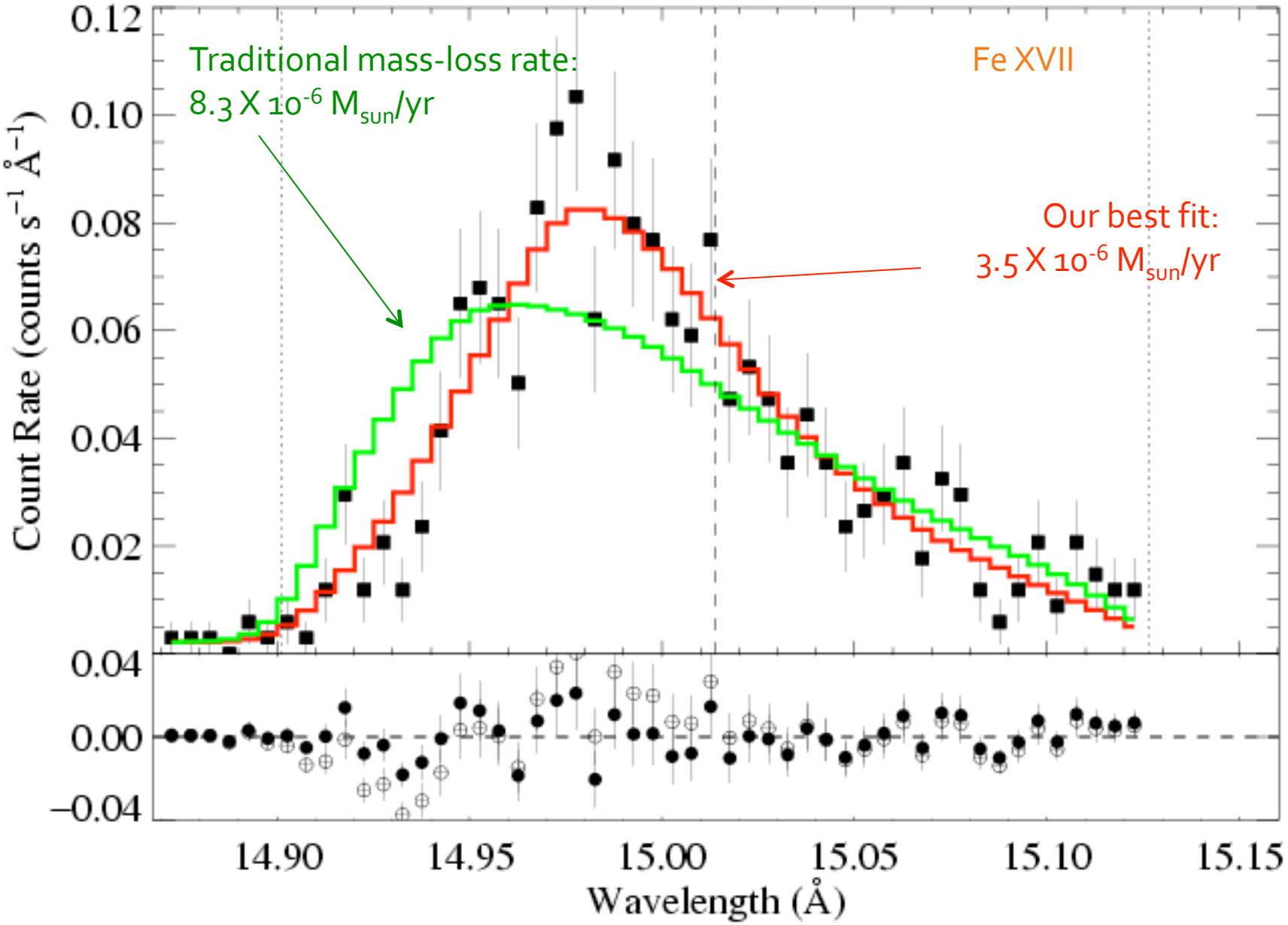
Traditional mass-loss rate:
8.3 X 10-6 Msun/yr
Fe XVII
Our best fit:
3.5 X 10-6 Msun/yr
Count Rate (counts s−1 Å−1)
0.12
0.10
0.08
0.06
0.04
0.02
0.04
0.00
−0.04
14.90
14.95
15.00
15.05
15.10
15.15
Wavelength (Å)

ζ Ori: O9.5

ε Ori: Bo

ζ Ori (09.7 I): O Lyα 18.97 Å

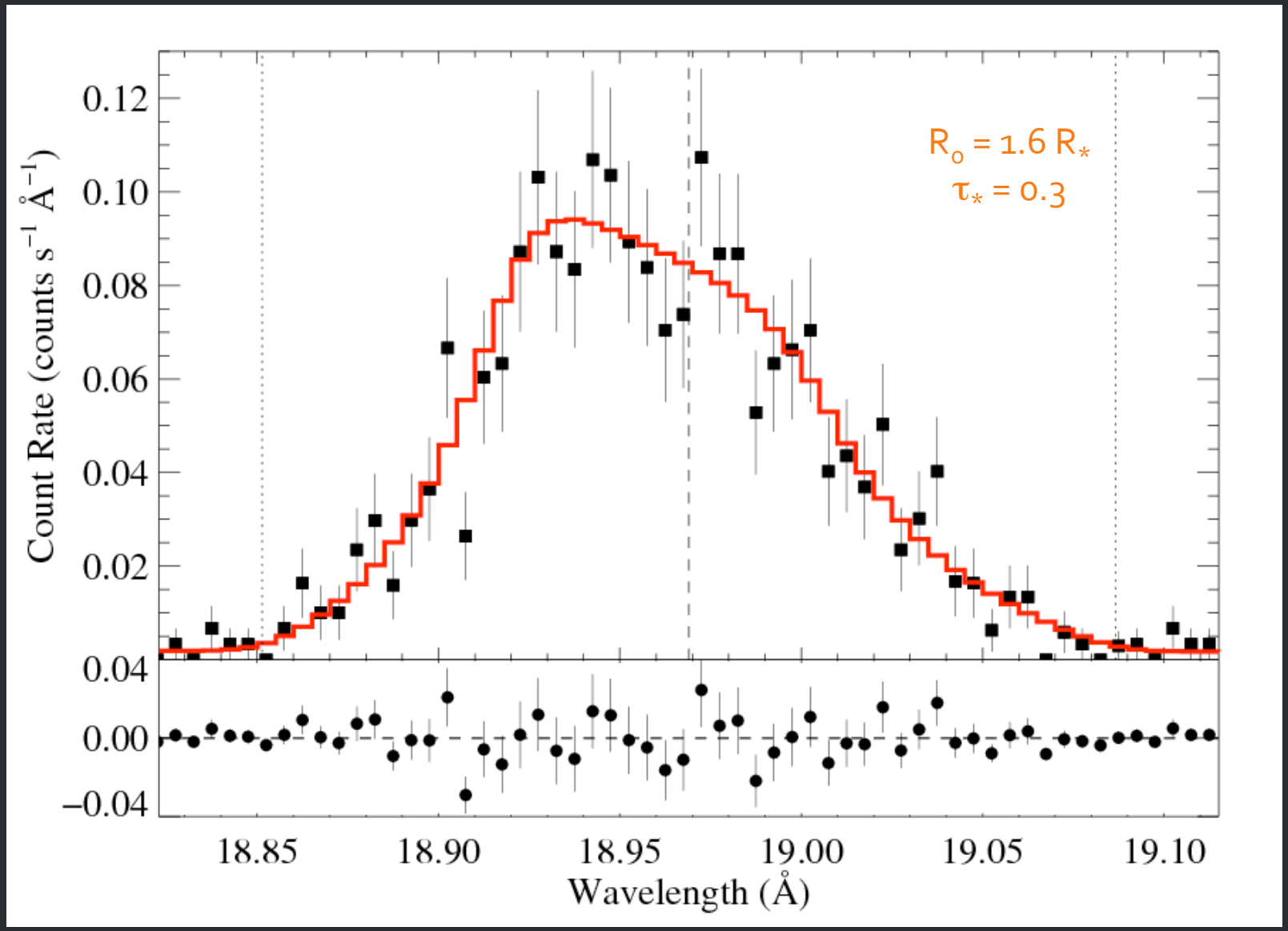

τ_* quite low: is *resonance scattering* affecting this line?

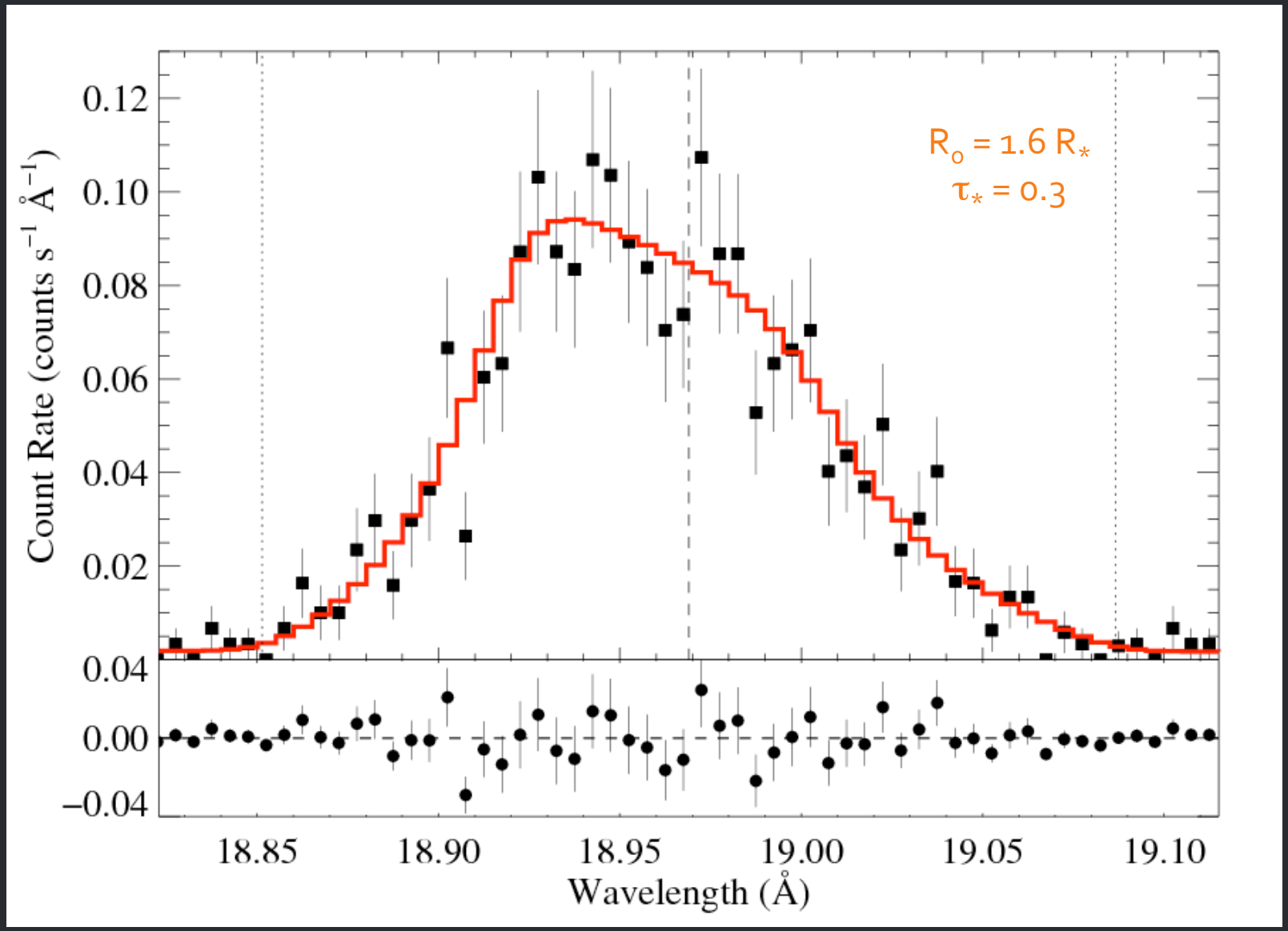

ε Ori (Bo Ia): Ne Lyα 12.13 Å

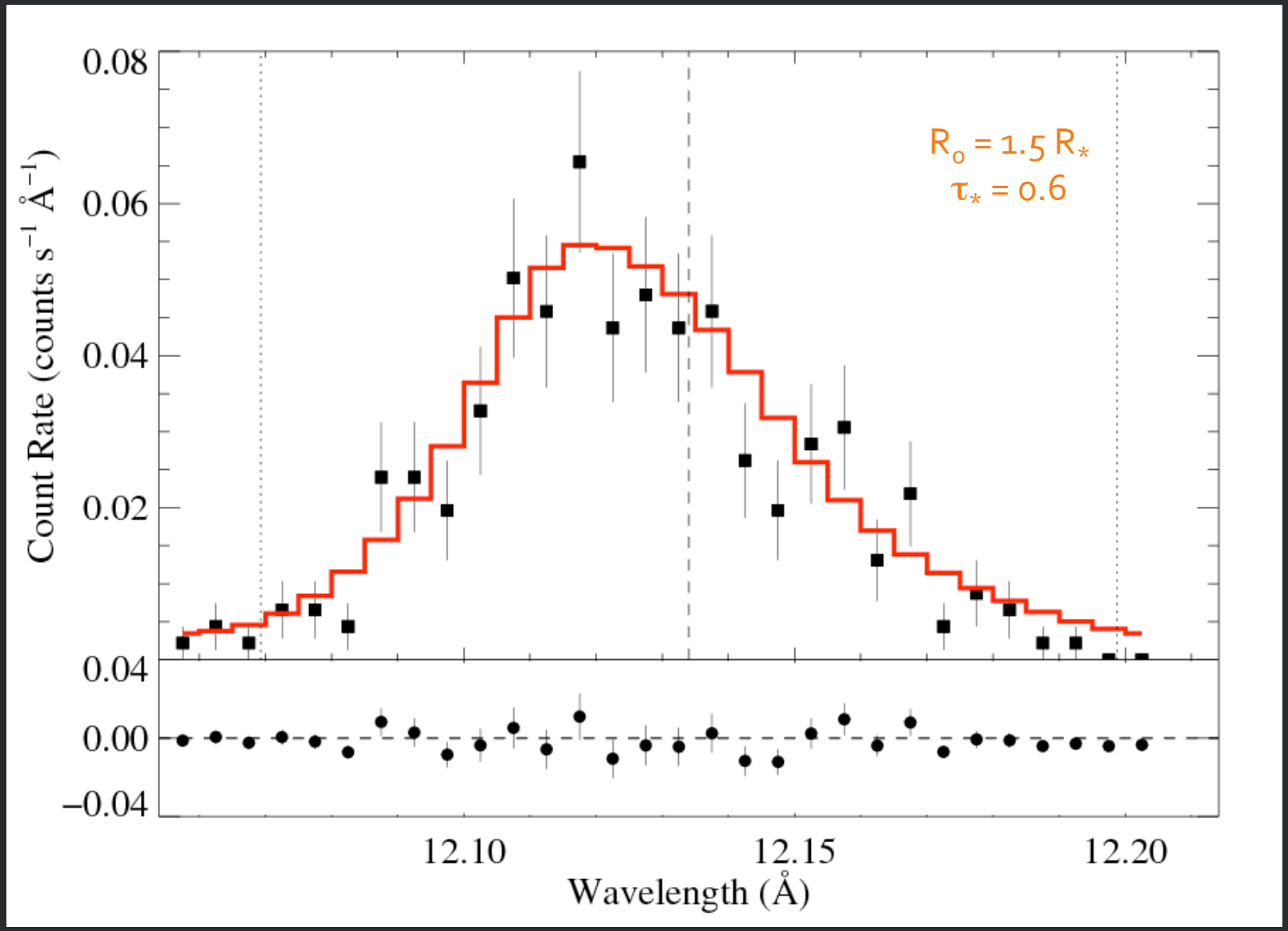

M-dot ~ 2 x 10^{-5} M_{sun}/yr from **unclumped** Hα

V_{inf} ~ 3200 km/s

HD 93129Aab (O2 If*): Mg XII Lyα 8.42 Å

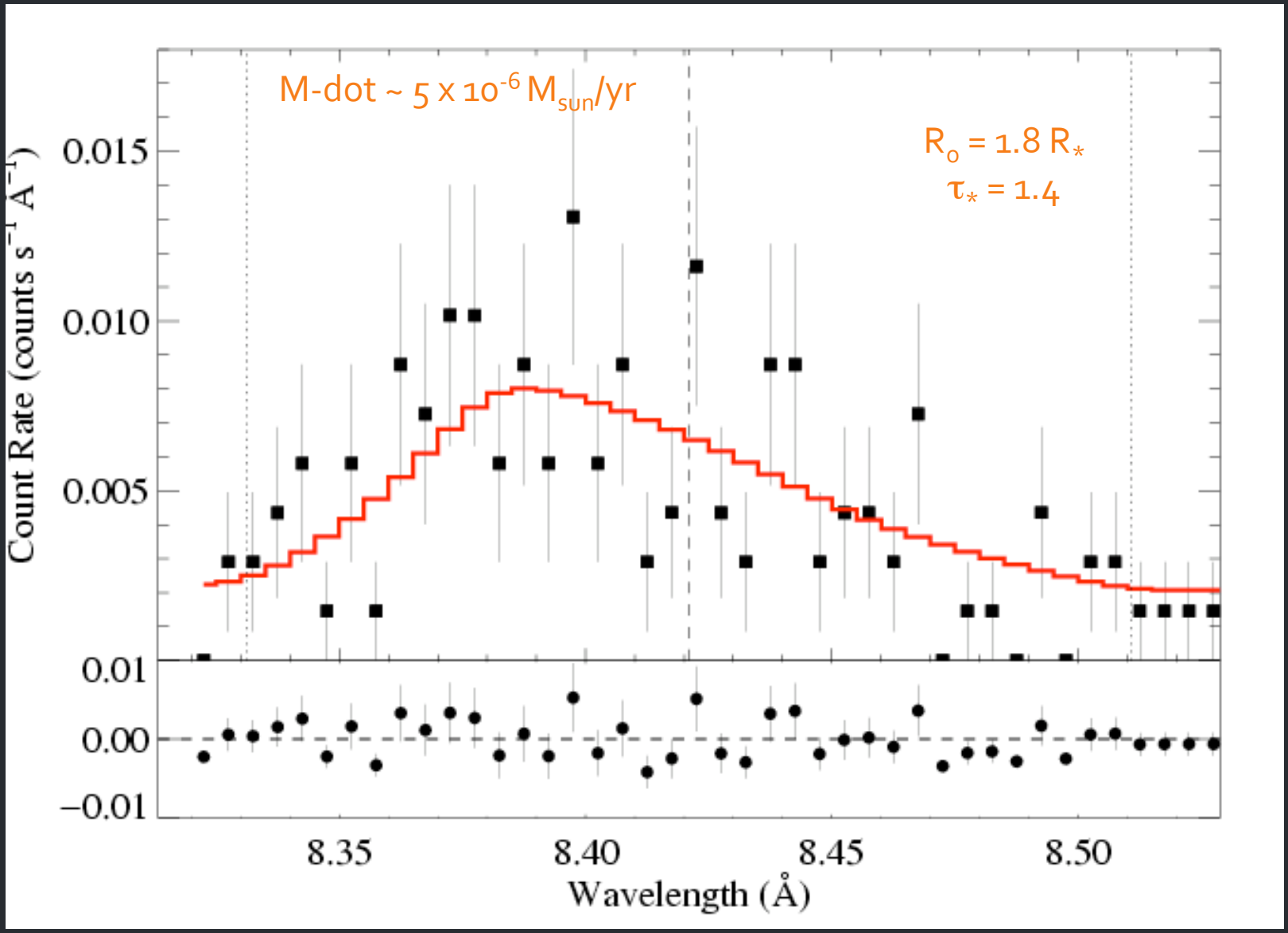

HD93129A – O2 If*

Most massive, luminous O star ($10^{6.4}$ L_{sun})

Strongest wind of any O star

(2×10^{-5} M_{sun}/yr; v_{inf} = 3200 km/s)

Its X-ray spectrum is hard

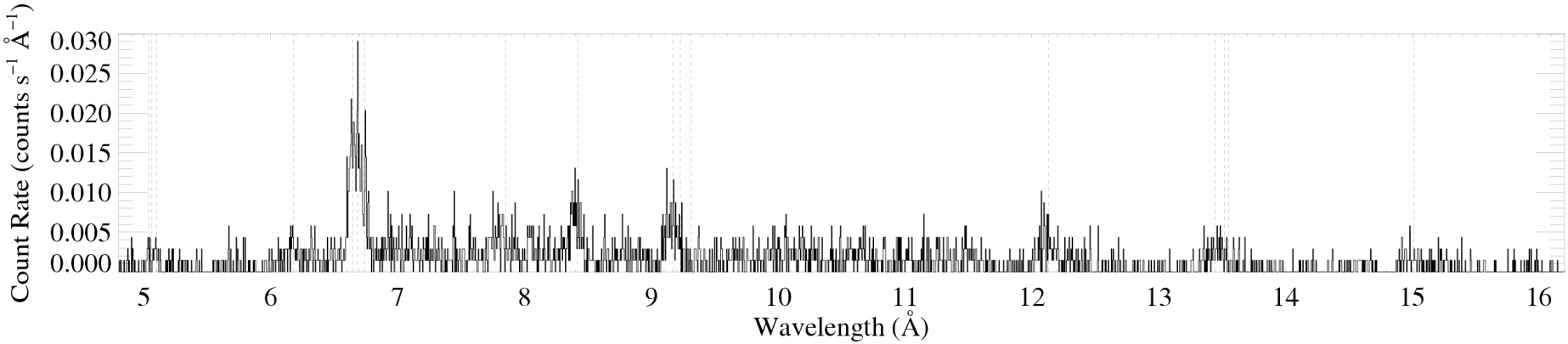

low H/He

high H/He

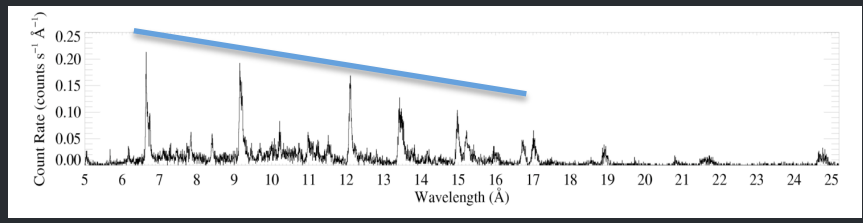

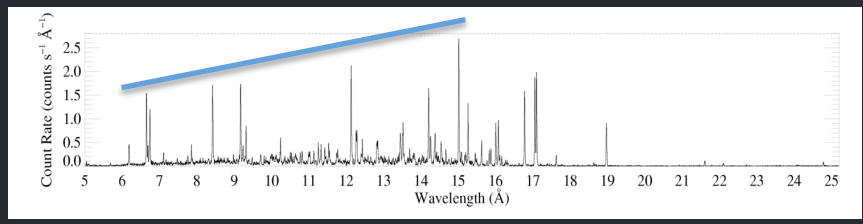

Its X-ray spectrum is hard

Si Mg

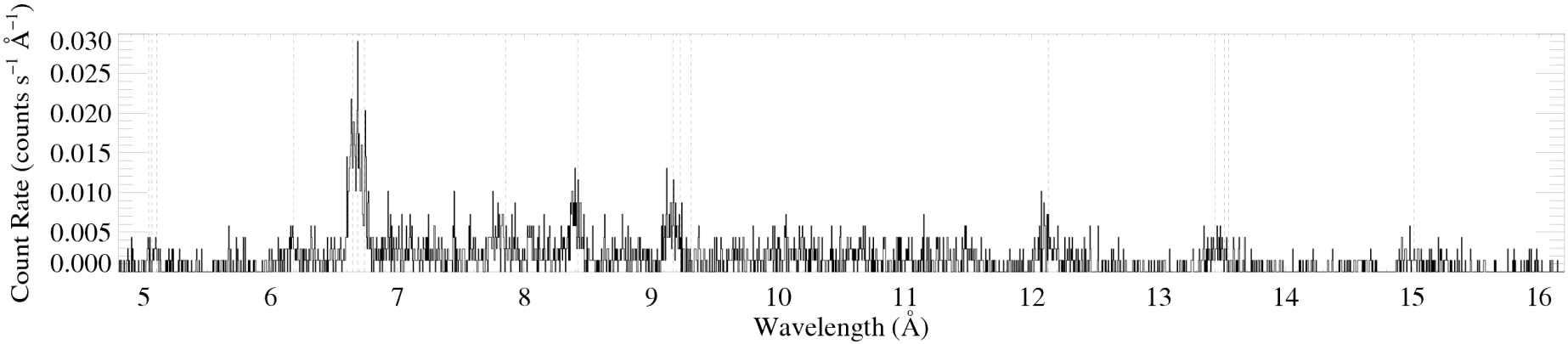

low H/He high H/He

But very little plasma with kT > 8 million K

Low-resolution *Chandra* CCD spectrum of HD93129A

Fit: thermal emission with wind + ISM absorption plus a second thermal component with just ISM

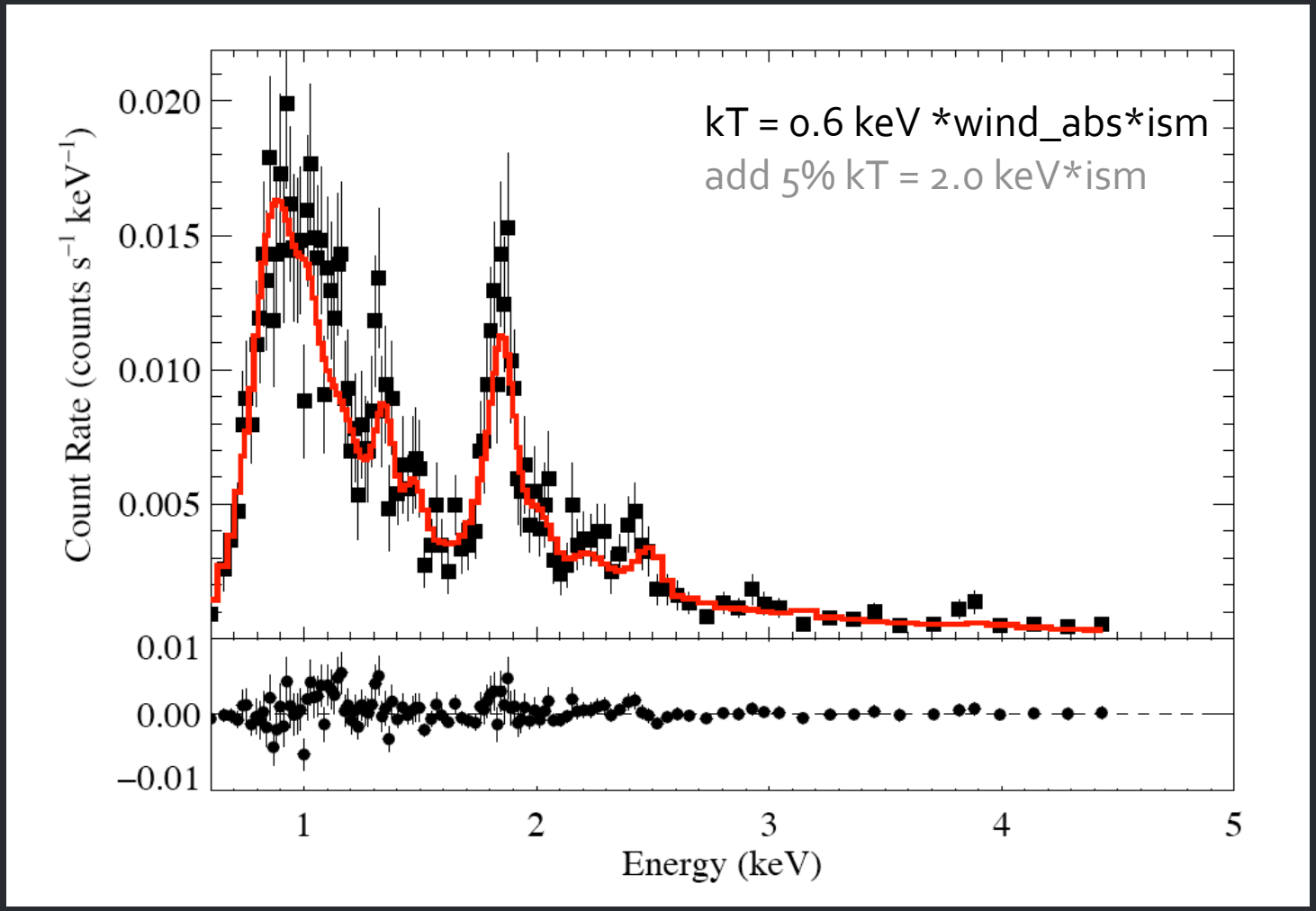

τ_*/κ = 0.03 (corresp. ~ 5 x 10^{-6} M_{sun}/yr)

Typical of O stars like ζ Pup

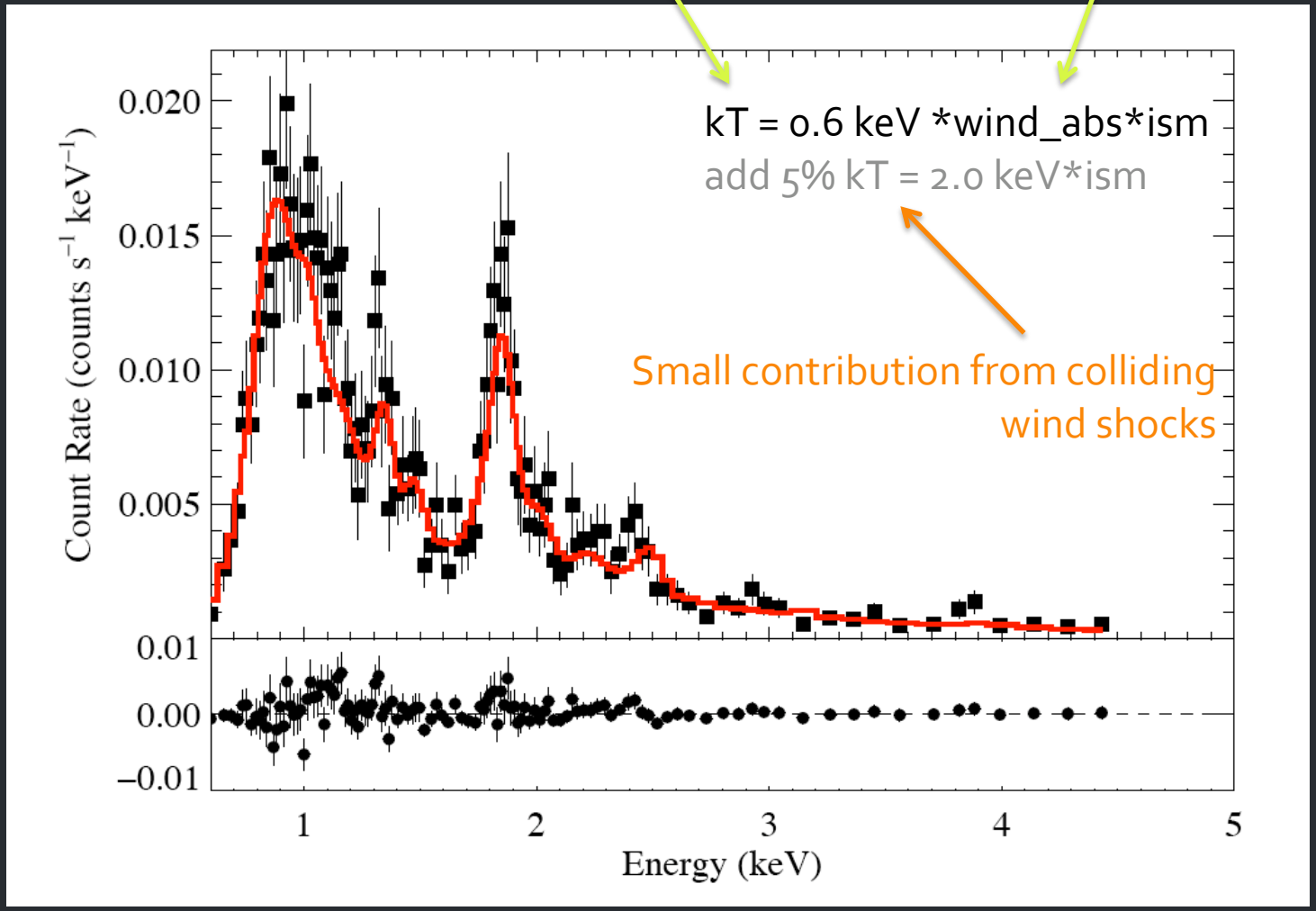

What about broadband effects?

The X-ray opacity changes across the Chandra bandbass – this should affect the overall X-ray SED: soft-X-ray absorption in O star winds should *harden* the emergent X-rays

Emission measure and optical depth

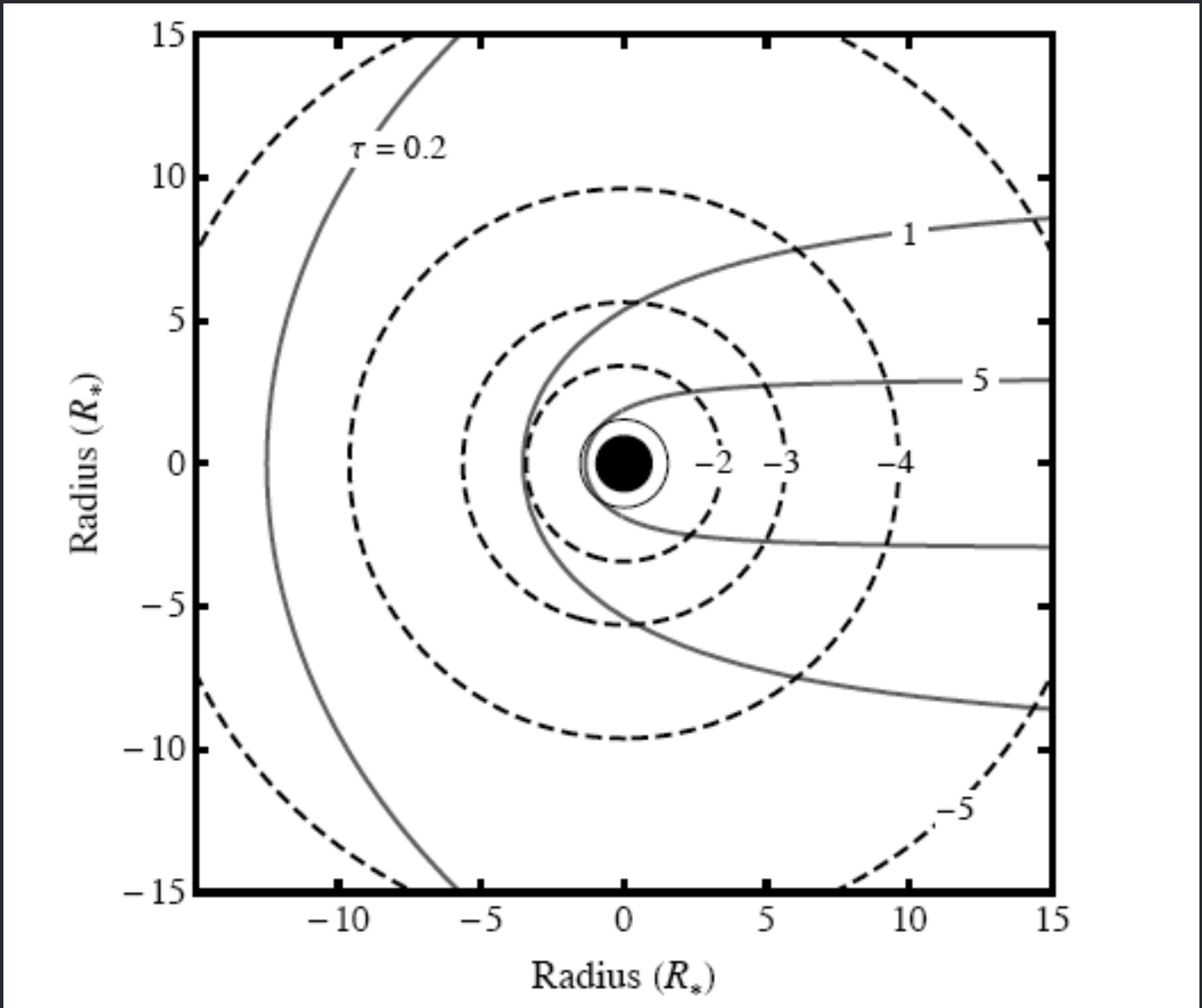

Emergent X-ray flux

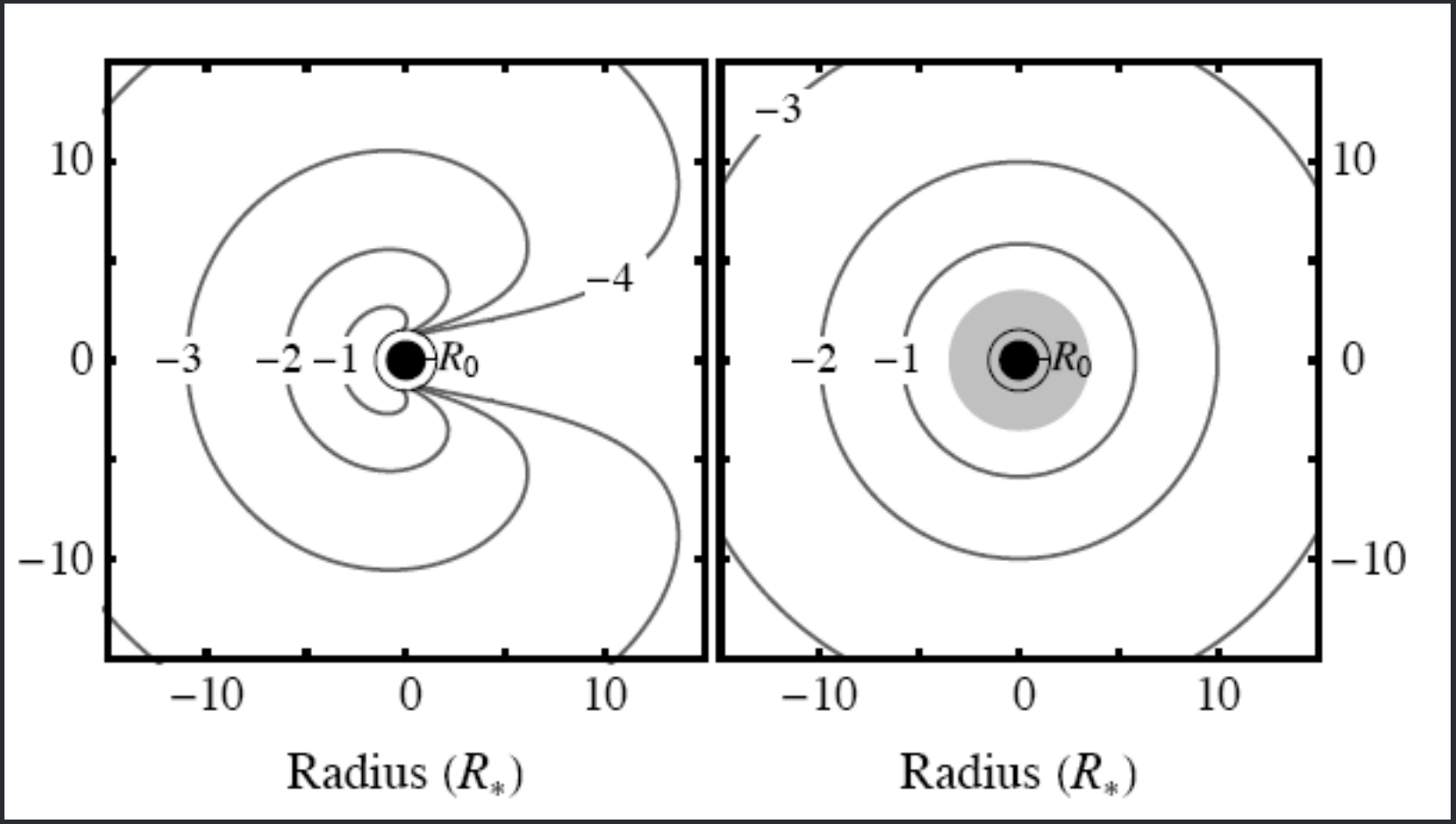

exact

exospheric

Transmission

$$L_\lambda = 4\pi \int dV\, \eta_\lambda(r)\, e^{-\tau(r,\mu,\lambda)}$$

$$T(\tau_*) = \frac{\int dV\, \rho^2\, e^{-\tau}}{\int dV\, \rho^2}$$

Σ_* is the free parameter

Once you assume a run of opacity vs. wavelength, $\kappa(\lambda)$

$$\tau_*(\lambda) = \kappa_\lambda \Sigma_* \ ,$$

$$\Sigma_* \equiv \frac{\dot{M}}{4\pi R_* v_\infty}$$

exponential absorption (from a slab) is inaccurate

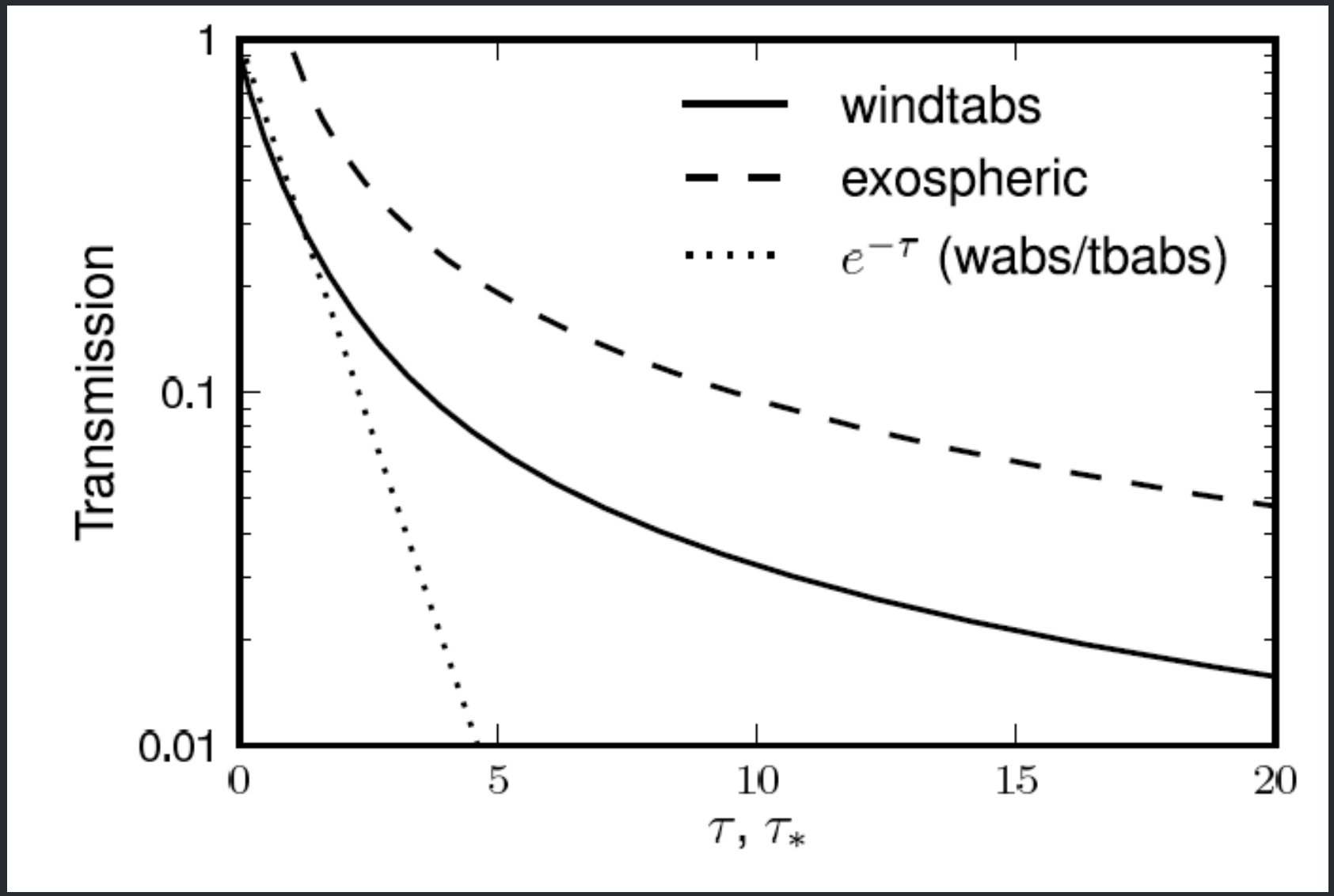

Wind opacity

X-ray bandpass

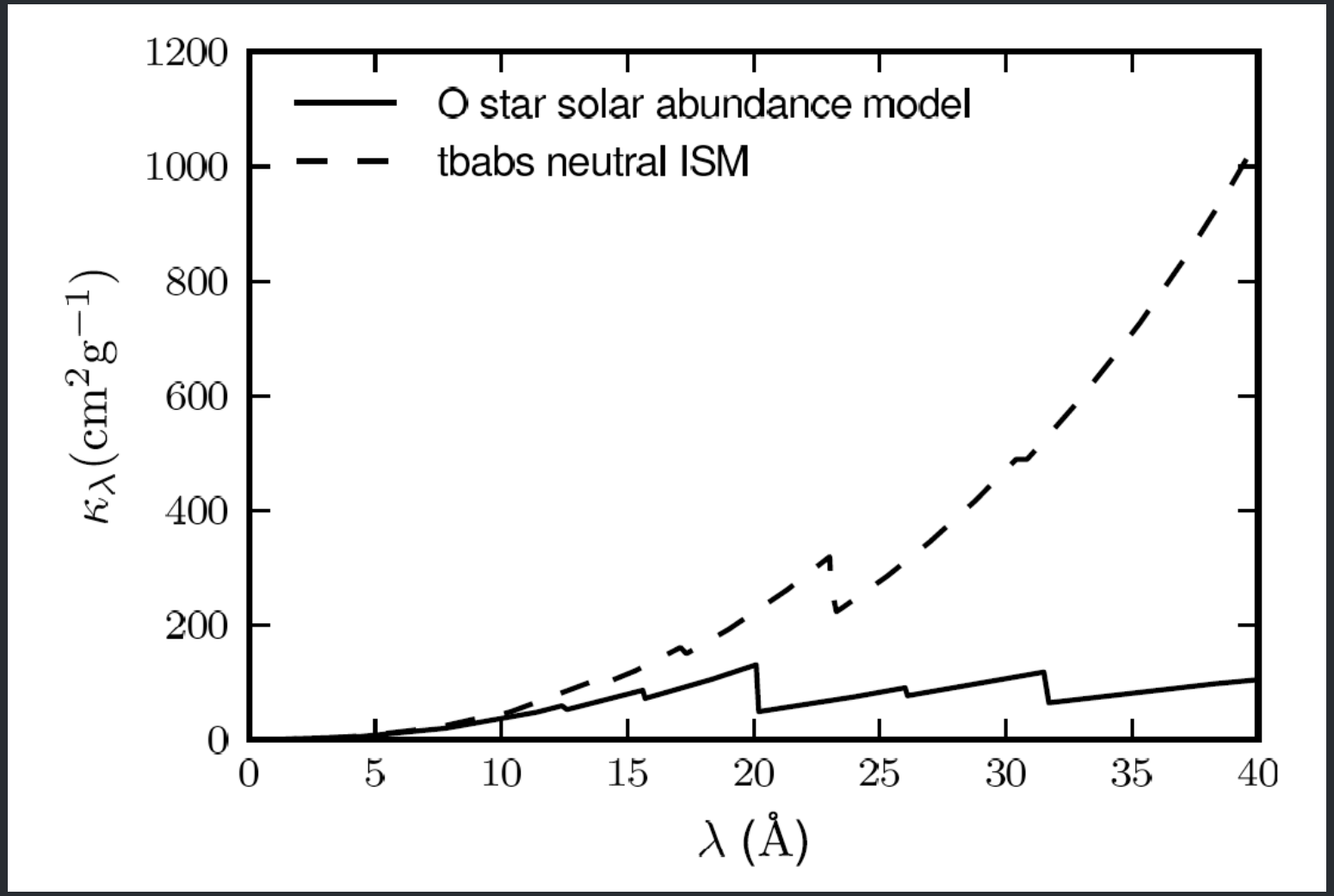

Combining opacity and transmission models

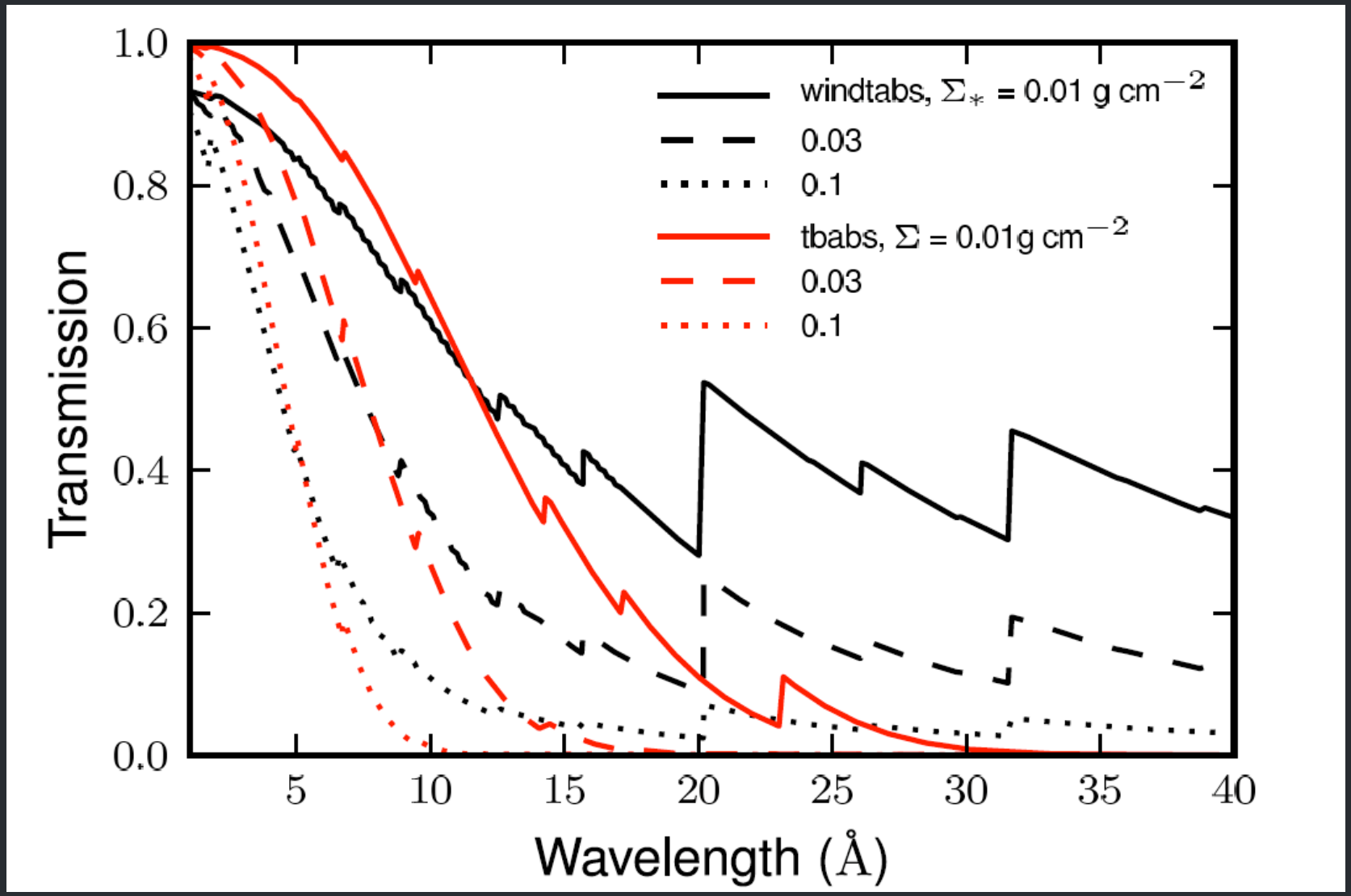

Broadband trend is mostly due to absorption

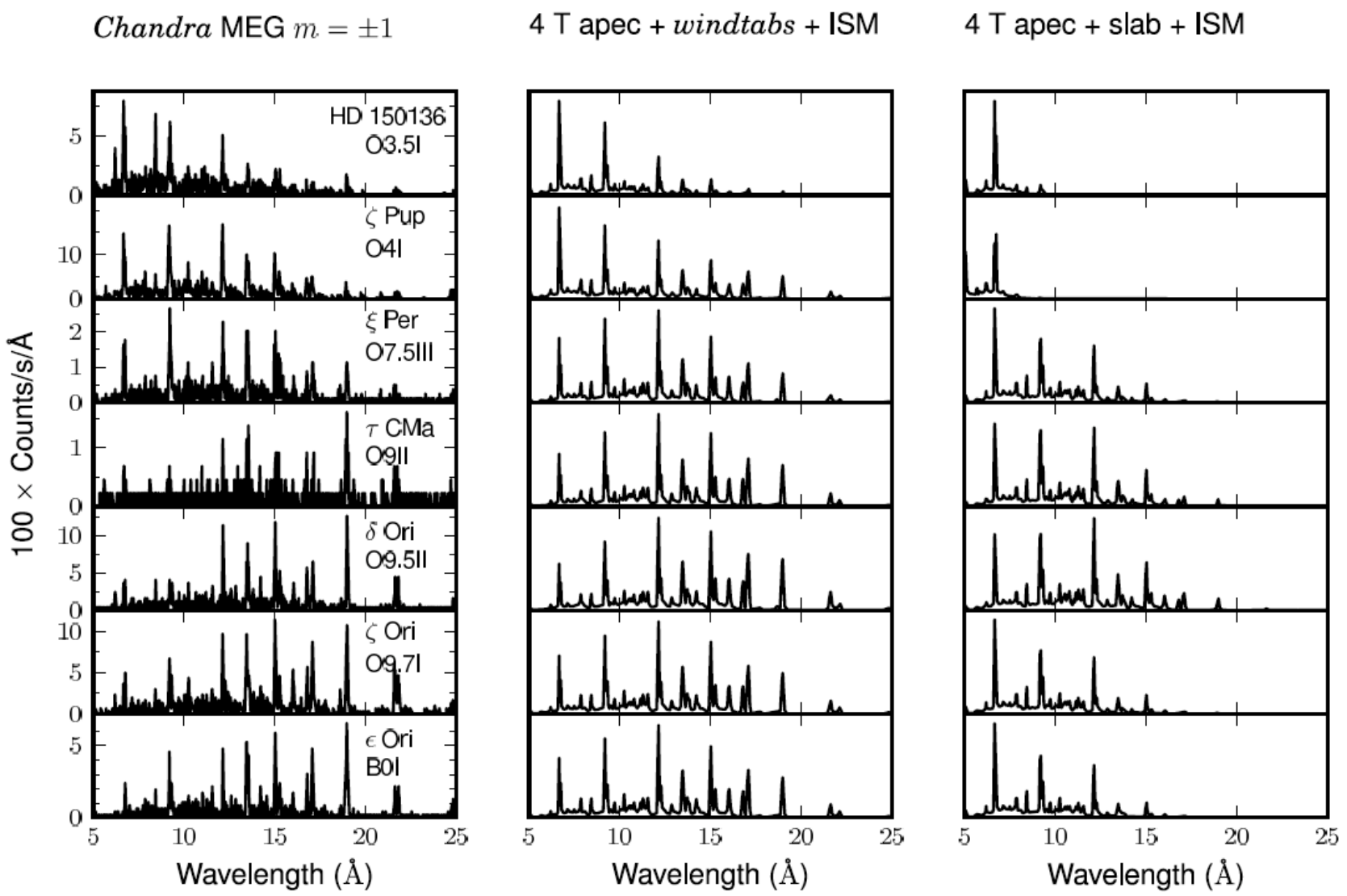

Although line ratios need to be analyzed too

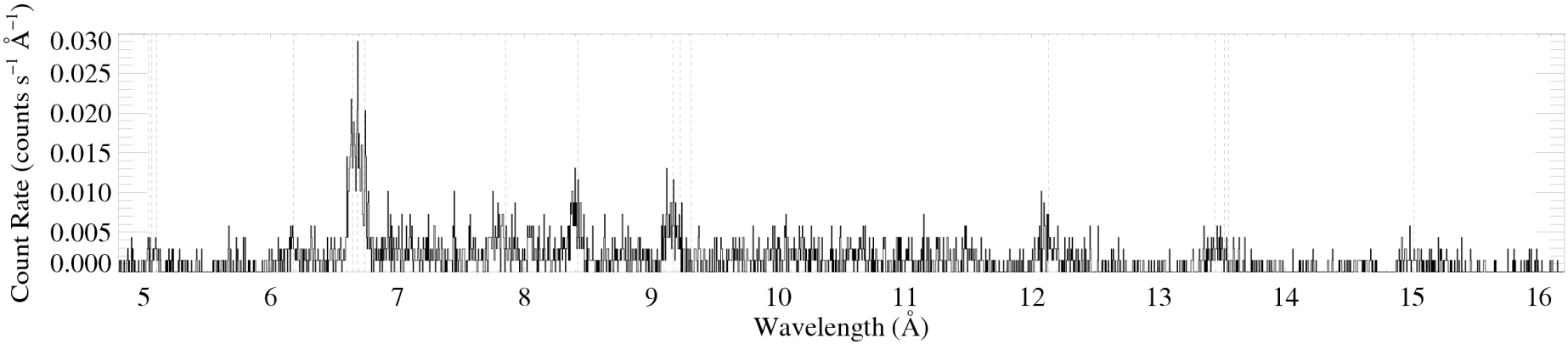

low H/He

high H/He

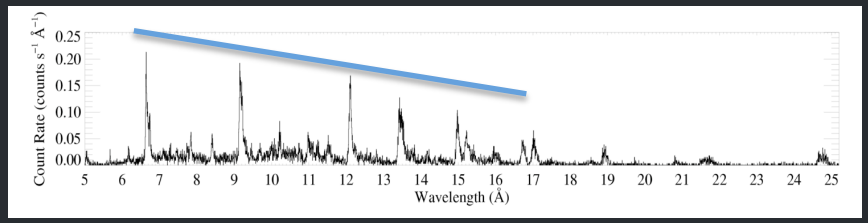

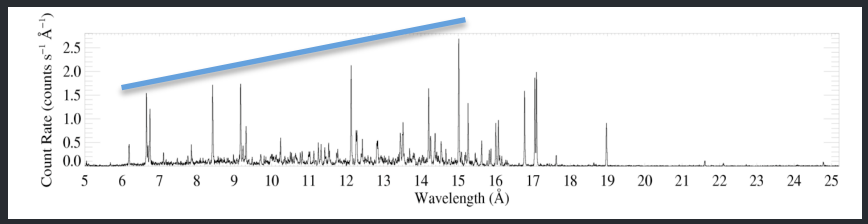

Conclusions

- Wind absorption has an important effect on the X-rays we observe from single O stars
- Resolved line profiles show widths consistent with shock onset radii of ~1.5 R_*
- And shapes indicative of wind absorption – though with low mass-loss rates
- Initial results on broadband X-ray spectra indicate that wind absorption is significant there, too

Additional Slides

Clumping and porosity

Multi-wavelength evidence for lower mass-loss rates 2005 onward

The Astrophysical Journal, 637:1025–1039, 2006 February 1

THE DISCORDANCE OF MASS-LOSS ESTIMATES FOR GALACTIC O-TYPE STARS

A. W. Fullerton[1]
Department of Physics and Astronomy, University of Victoria, P.O. Box 3055, Victoria, BC V8W 3P6, Canada; awf@pha.jhu.edu

D. L. Massa
SGT, Inc., NASA Goddard Space Flight Center, Code 681.0, Greenbelt, MD 20771; massa@taotaomona.gsfc.nasa.gov

AND

R. K. Prinja
Department of Physics and Astronomy, University College London, Gower Street, London WC1E 6BT, UK; rkp@star.ucl.ac.uk
Received 2005 June 10; accepted 2005 October 4

ABSTRACT

We have determined accurate values of the product of the mass-loss rate and the ion fraction of P^{+4}, $\dot{M}q(P^{+4})$, for a sample of 40 Galactic O-type stars by fitting stellar wind profiles to observations of the P v resonance doublet obtained with *FUSE*, *ORFEUS* BEFS, and *Copernicus*. When P^{+4} is the dominant ion in the wind [i.e., $0.5 \lesssim q(P^{+4}) \leq 1$], $\dot{M}q(P^{+4})$ approximates the mass-loss rate to within a factor of $\lesssim 2$. Theory predicts that P^{+4} is the dominant ion in the winds of O7–O9.7 stars, although an empirical estimator suggests that the range O4–O7 may be more appropriate. However, we find that the mass-loss rates obtained from P v wind profiles are systematically smaller than those obtained from fits to Hα emission profiles or radio free-free emission by median factors of $\sim$130 (if P^{+4} is dominant between O7 and O9.7) or $\sim$20 (if P^{+4} is dominant between O4 and O7). These discordant measurements can be reconciled if the winds of O stars in the relevant temperature range are strongly clumped on small spatial scales. We use a simplified two-component model to investigate the volume filling factors of the denser regions. This clumping implies that mass-loss rates determined from "ρ^2" diagnostics have been systematically overestimated by factors of 10 or more, at least for a subset of O stars. Reductions in the mass-loss rates of this size have important implications for the evolution of massive stars and quantitative estimates of the feedback that hot-star winds provide to their interstellar environments.

Subject headings: stars: early-type — stars: mass loss — stars: winds, outflows

ζ Pup mass-loss rate < 4.2 x 10^{-6} M_{sun}/yr

Bright OB stars in the Galaxy

III. Constraints on the radial stratification of the clumping factor in hot star winds from a combined H_α, IR and radio analysis⋆

J. Puls[1], N. Markova[2], S. Scuderi[3], C. Stanghellini[4], O. G. Taranova[5], A. W. Burnley[6] and I. D. Howarth[6]

[1] Universitäts-Sternwarte München, Scheinerstr. 1, D-81679 München, Germany, e-mail: uh101aw@usm.uni-muenchen.de
[2] Institute of Astronomy, Bulgarian National Astronomical Observatory, P.O. Box 136, 4700 Smoljan, Bulgaria, e-mail: nmarkova@astro.bas.bg
[3] INAF - Osservatorio Astrofisico di Catania, Via S. Sofia 78, I-95123 Catania, Italy, e-mail: scuderi@oact.inaf.it
[4] INAF - Istituto di Radioastronomia, Via P. Gobetti 101, I-40129 Bologna, Italy, e-mail: c.stanghellini@ira.inaf.it
[5] Sternberg Astronomical Institute, Universitetski pr. 13, Moscow, 119992, Russia, e-mail: taranova@sai.msu.ru
[6] Department of Physics and Astronomy, University College London, Gower Street, London WC1E 6BT, UK, e-mail: awxb@star.ucl.ac.uk, idh@star.ucl.ac.uk

Received; accepted

Abstract. Recent results strongly challenge the canonical picture of massive star winds: various evidence indicates that currently accepted mass-loss rates, $\dot{M}$, may need to be revised downwards, by factors extending to one magnitude or even more. This is because the most commonly used mass-loss diagnostics are affected by "clumping" (small-scale density inhomogeneities), influencing our interpretation of observed spectra and fluxes.

Such downward revisions would have dramatic consequences for the evolution of, and feedback from, massive stars, and thus robust determinations of the clumping properties and mass-loss rates are urgently needed. We present a first attempt concerning this objective, by means of constraining the radial stratification of the so-called clumping factor.

To this end, we have analyzed a sample of 19 Galactic O-type supergiants/giants, by combining our own and archival data for H_α, IR, mm and radio fluxes, and using approximate methods, calibrated to more sophisticated models. Clumping has been included into our analysis in the "conventional" way, by assuming the inter-clump matter to be void. Because (almost) all our diagnostics depends on the square of density, we cannot derive absolute clumping factors, but only factors normalized to a certain minimum.

This minimum was usually found to be located in the outermost, radio-emitting region, i.e., the radio mass-loss rates are the lowest ones, compared to $\dot{M}$ derived from H_α and the IR. The radio rates agree well with those predicted by theory, but are only upper limits, due to unknown clumping in the outer wind. H_α turned out to be a useful tool to derive the clumping properties inside $r < 3...5\,R_\star$. Our most important result concerns a (physical) difference between denser and thinner winds: for denser winds, the innermost region is more strongly clumped than the outermost one (with a normalized clumping factor of 4.1 ± 1.4), whereas thinner winds have similar clumping properties in the inner and outer regions.

Our findings are compared with theoretical predictions, and the implications are discussed in detail, by assuming different scenarios regarding the still unknown clumping properties of the outer wind.

"Clumping" – or micro-clumping: affects density-squared diagnostics; independent of clump size, just depends on clump density contrast (or filling factor, f)

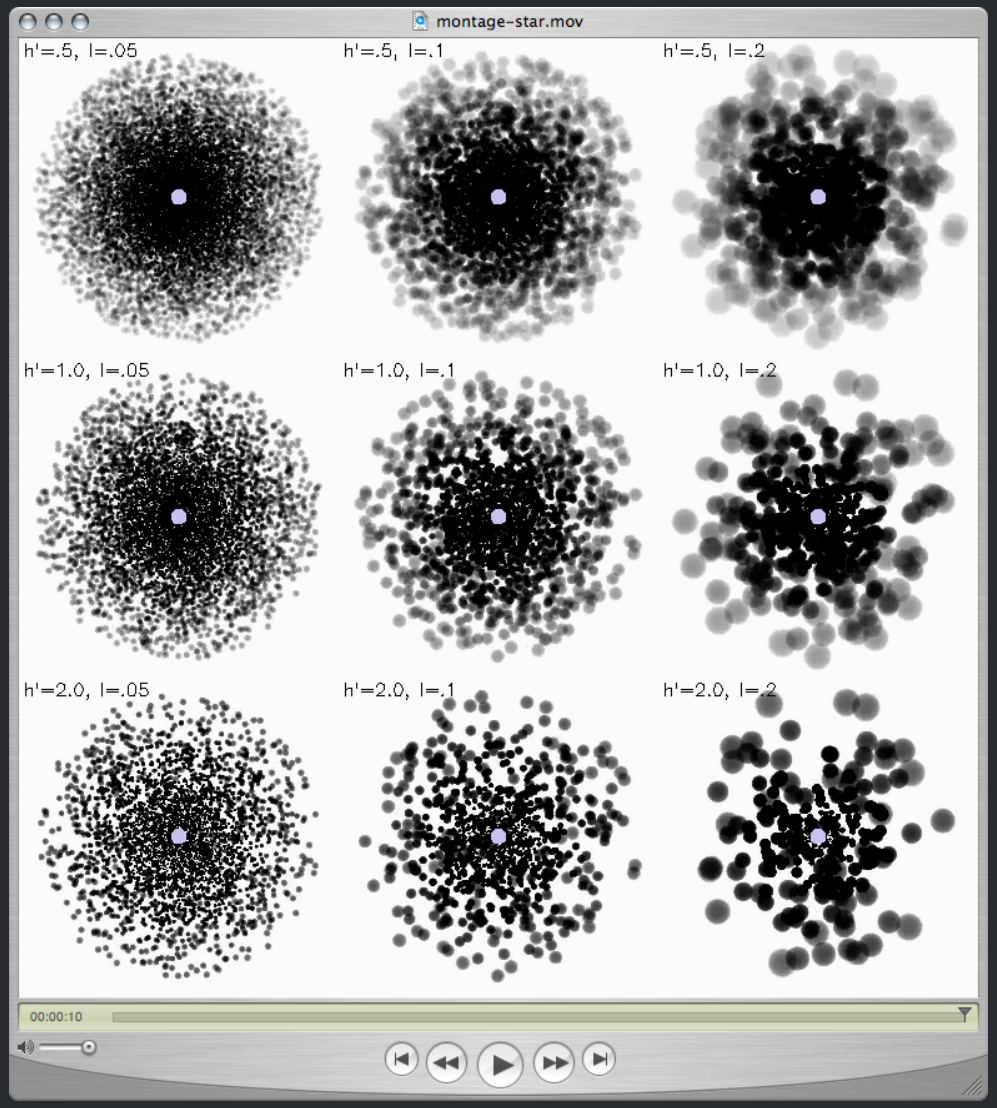

visualization: R. Townsend

But **porosity** is associated with optically thick clumps, it acts to reduce the effective opacity of the wind; it *does* depend on the size scale of the clumps

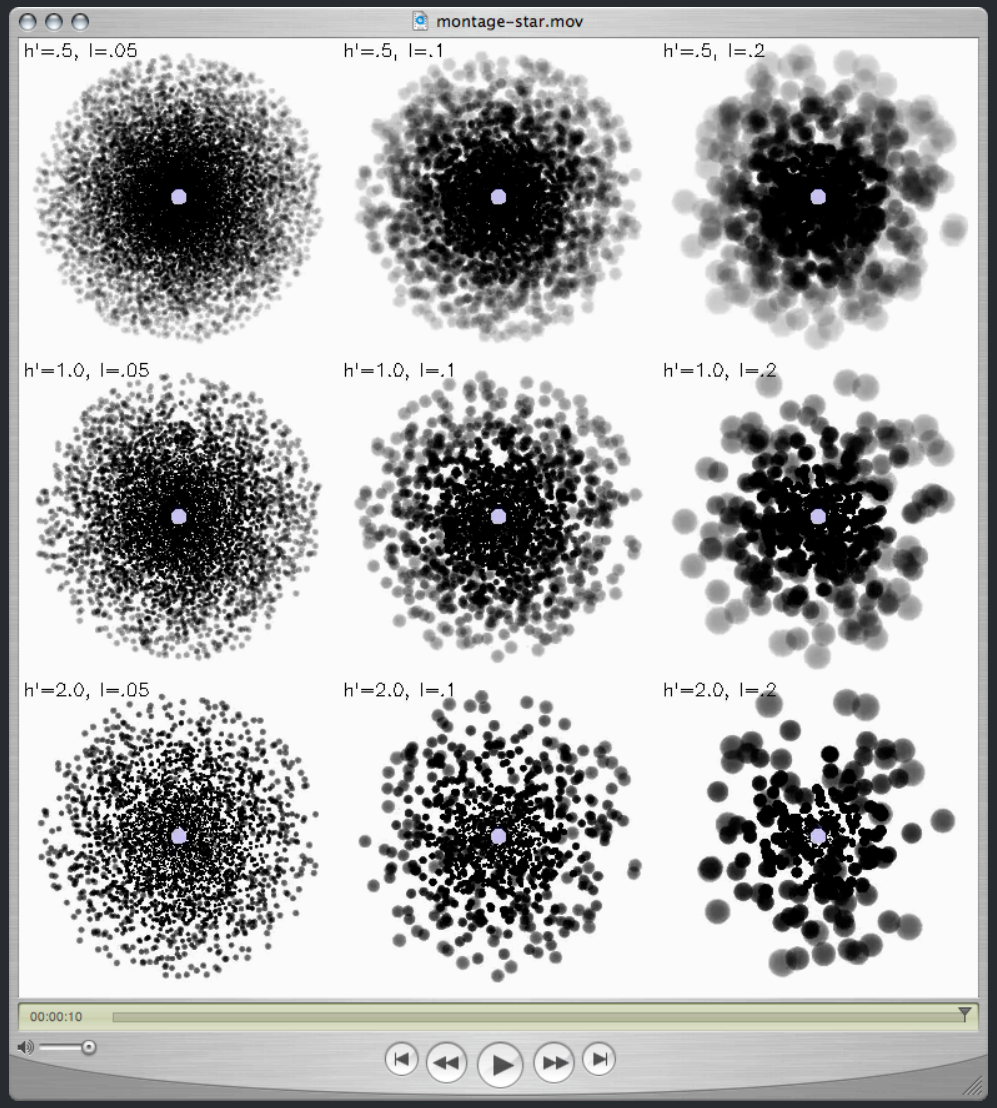

The key parameter is the **porosity length,**

$h = (L^3/\ell^2) = \ell/f$

$f = \ell^3/L^3$

Clump size increasing →

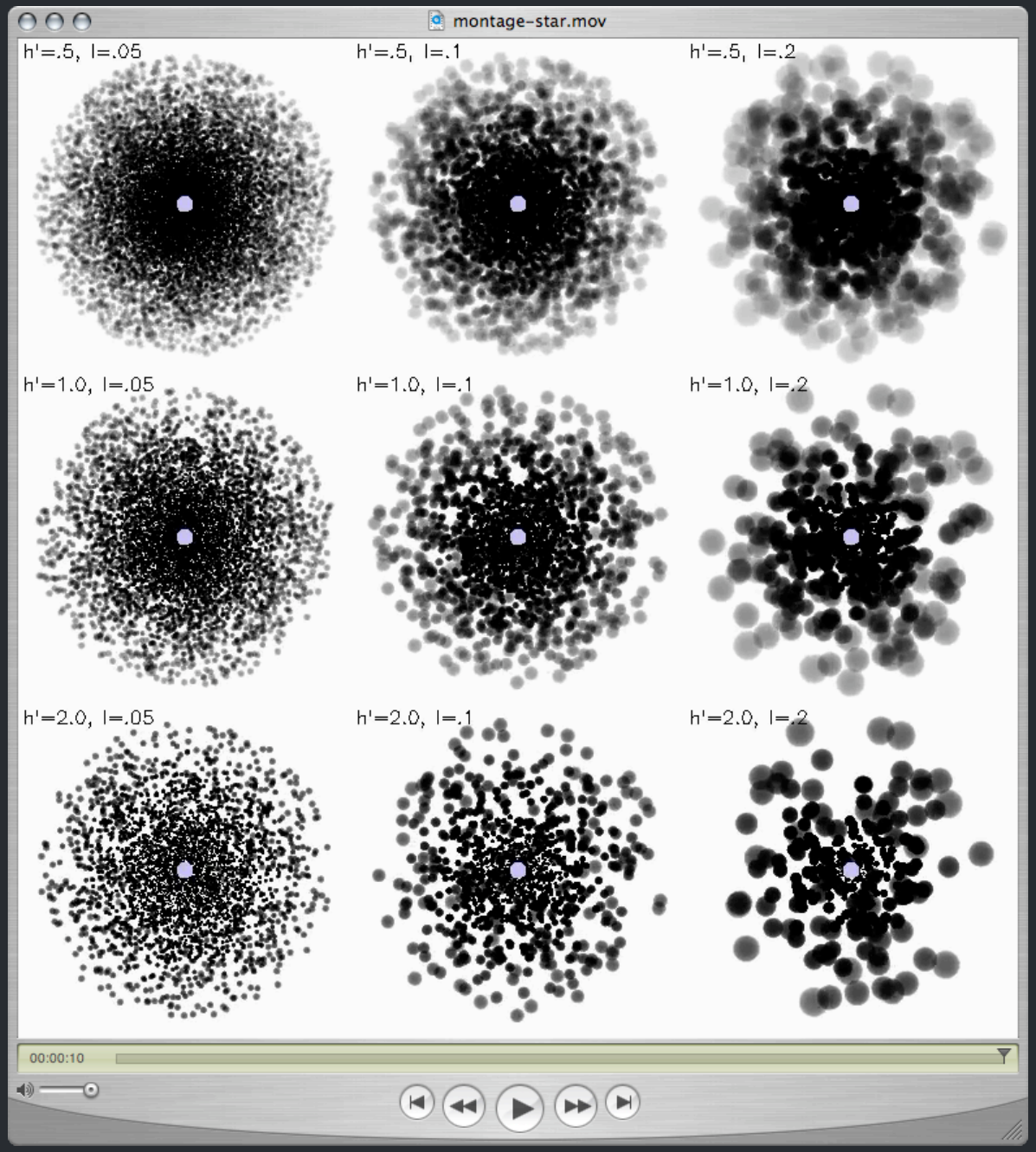

Porosity length increasing →

The porosity length, *h*:

clump size

$$h = \ell / f$$

clump filling factor (<1)

Porosity only affects line profiles if the porosity length (*h*) exceeds the stellar radius

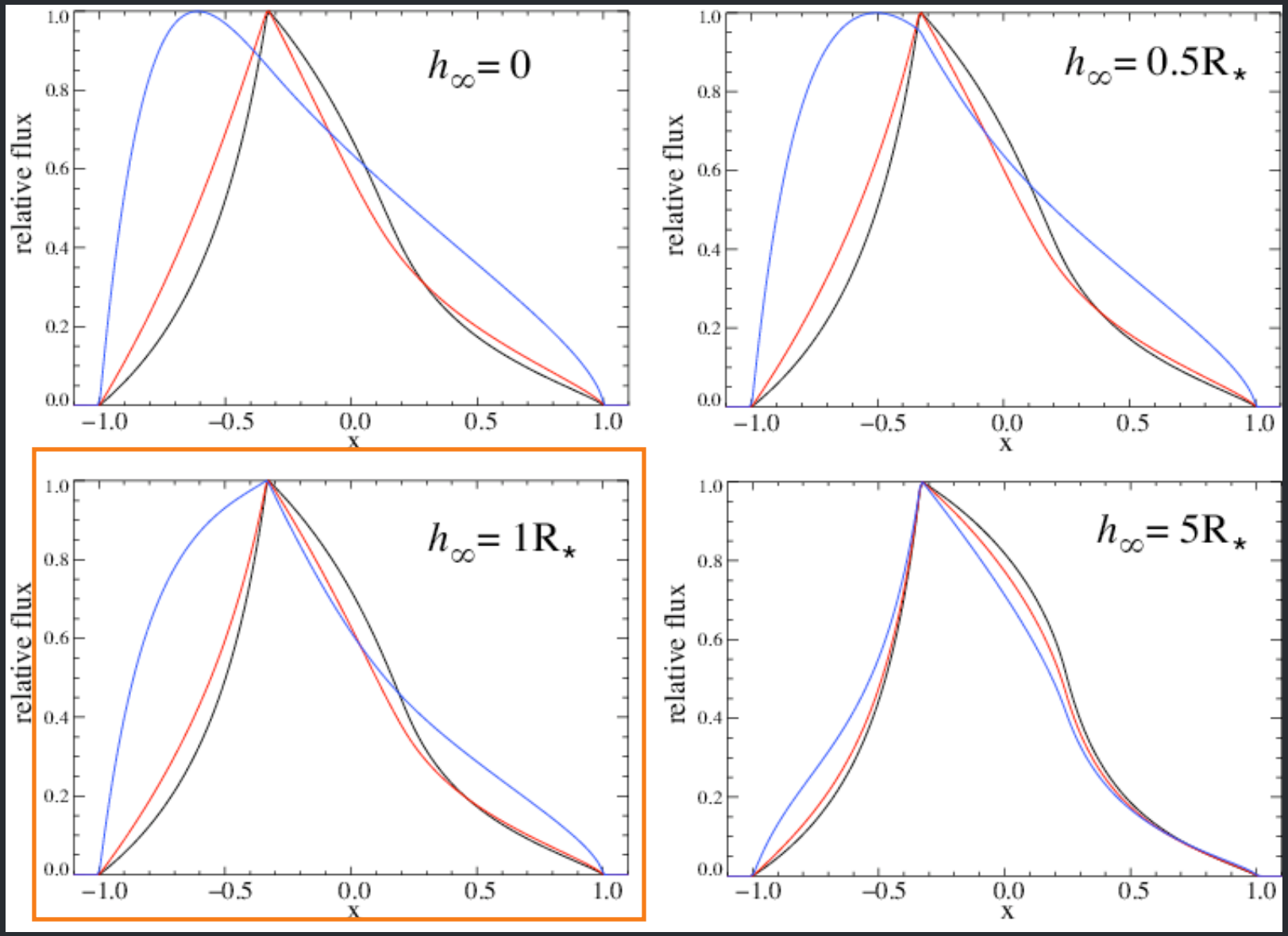

The clumping in 2-D simulations (density shown below) is on quite *small scales*

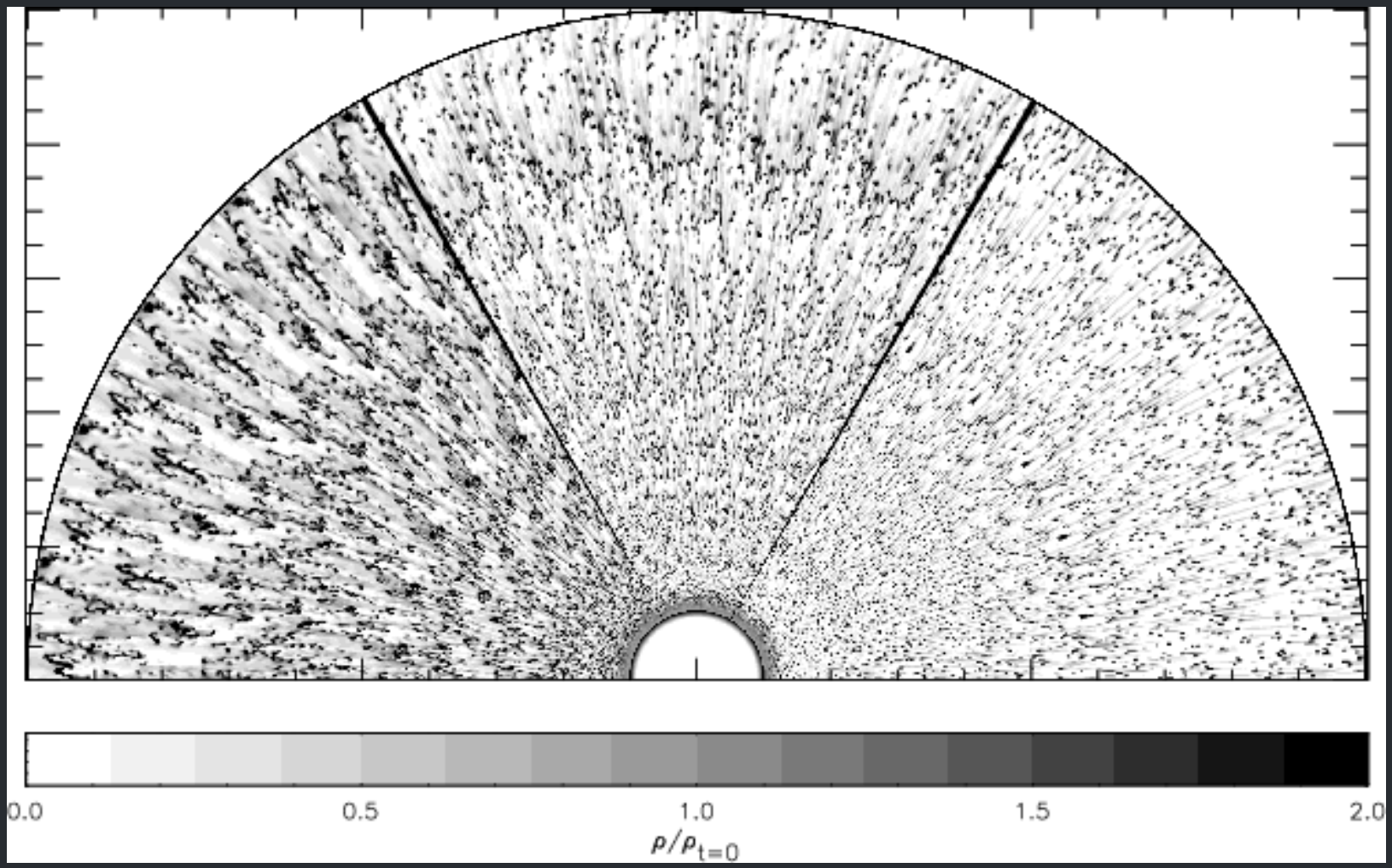

Dessart & Owocki 2003, *A&A*, 406, L1

No expectation of porosity from simulations

Natural explanation of line profiles without invoking porosity

Finally, to have porosity, you need clumping in the first place, and once you have clumping…you have your factor ~3 reduction in the mass-loss rate

No expectation of porosity from simulations

Natural explanation of line profiles without invoking porosity

Finally, to have porosity, you need clumping in the first place, and once you have clumping…you have your factor ~3 reduction in the mass-loss rate

No expectation of porosity from simulations

Natural explanation of line profiles without invoking porosity

Finally, to have porosity, you need clumping in the first place, and once you have clumping…you have your factor ~3 reduction in the mass-loss rate
(for ζ Pup, anyway)

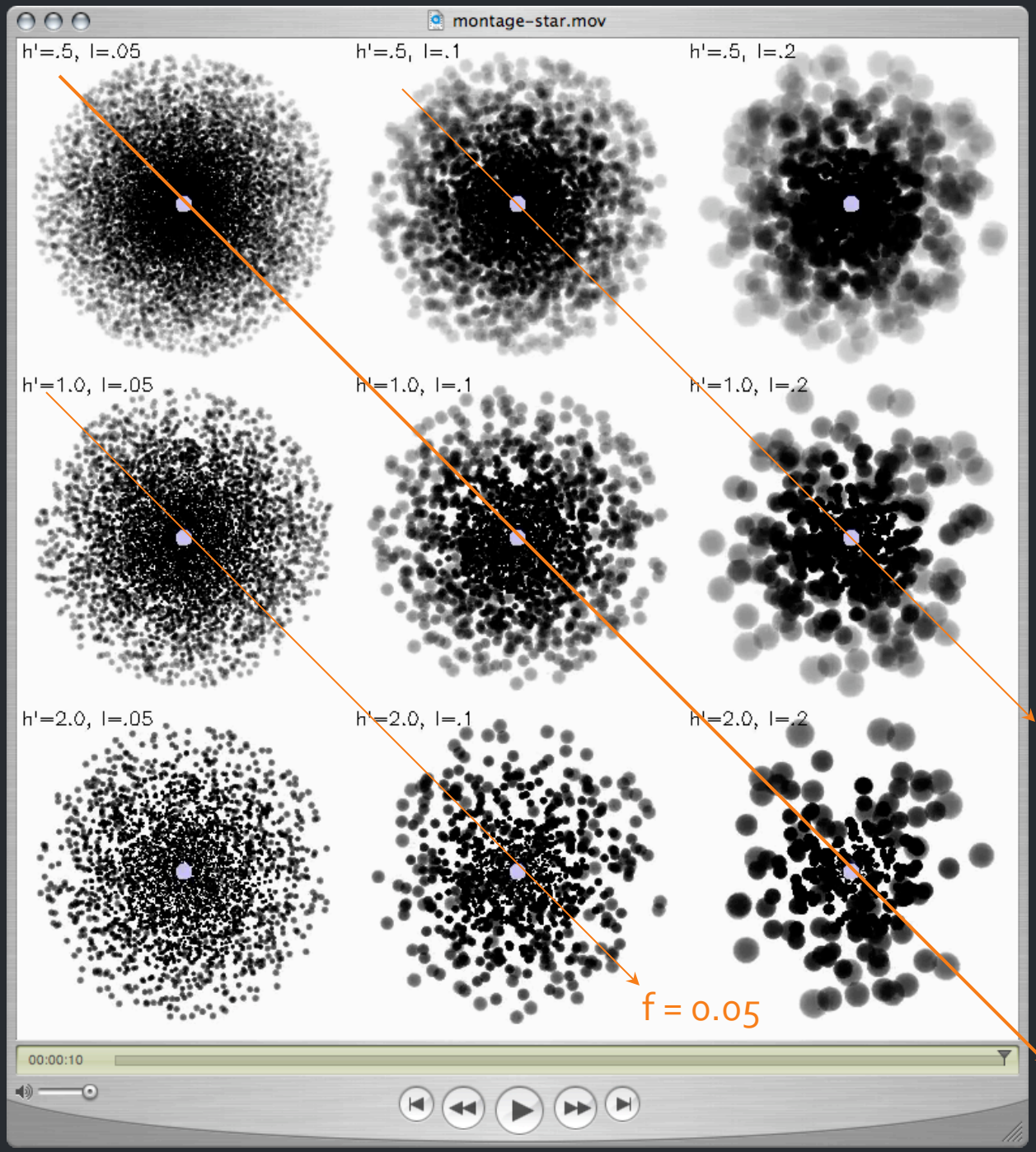

f ~ 0.1 is indicated by Hα, UV, radio free-free analysis

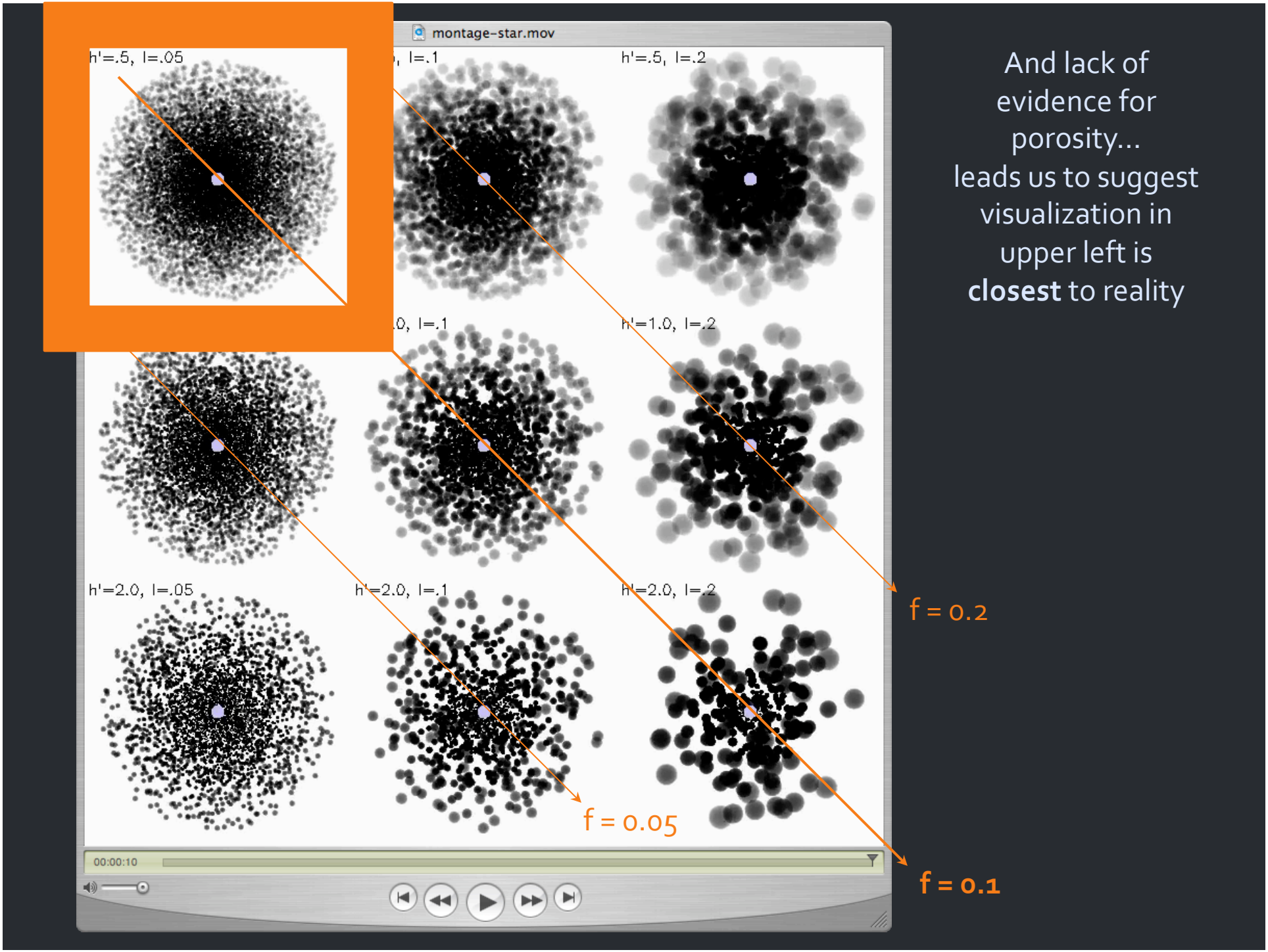

And lack of evidence for porosity… leads us to suggest visualization in upper left is **closest** to reality

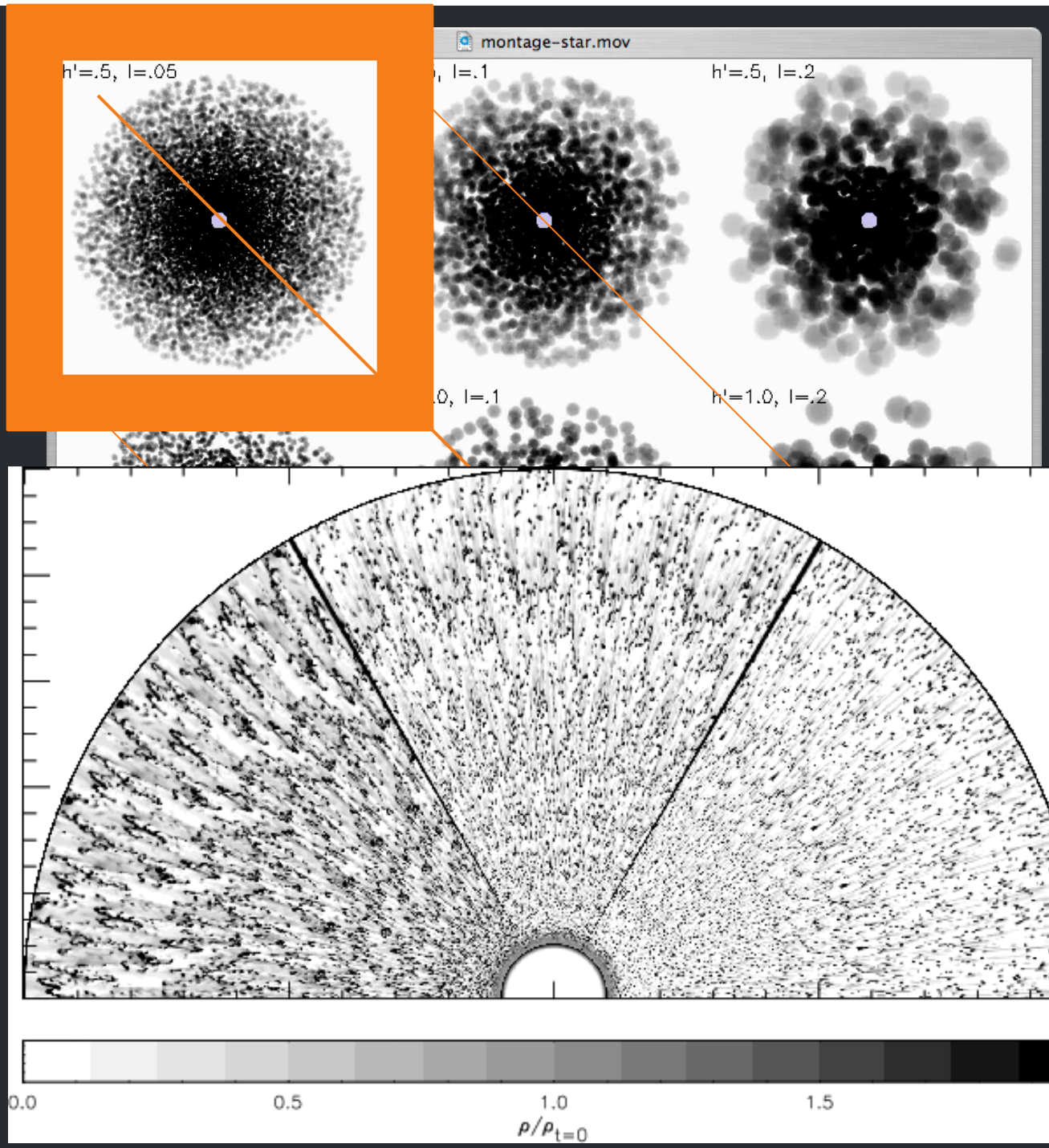

Though simulations suggest **even smaller-scale clumping**

= 0.2

= 0.1